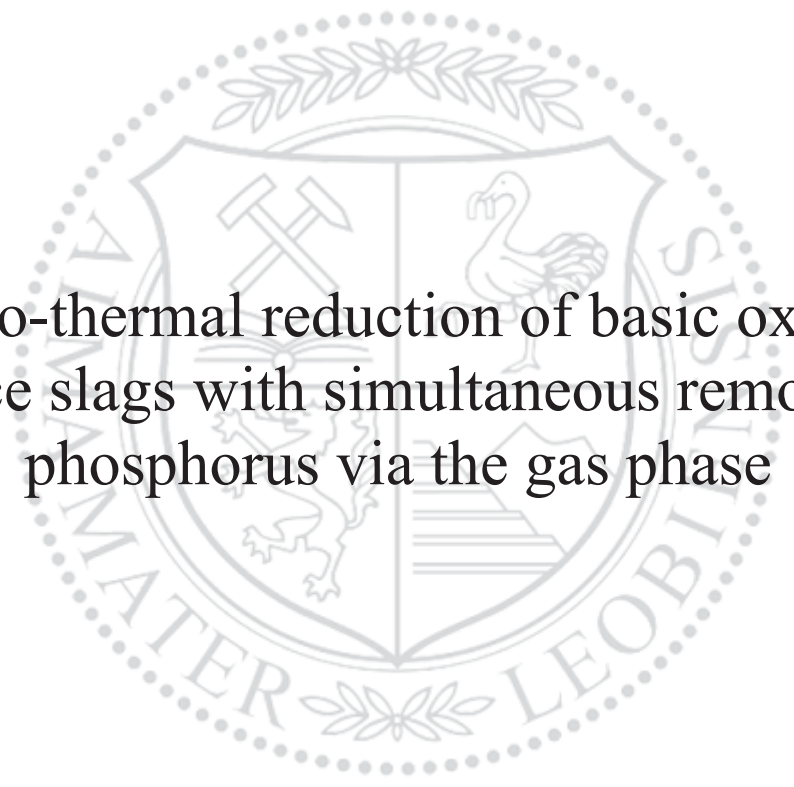




Chair of Thermal Processing Technology

Doctoral Thesis



Carbo-thermal reduction of basic oxygen
furnace slags with simultaneous removal of
phosphorus via the gas phase

Dipl.-Ing. Christoph Ponak, BSc

September 2019



EIDESSTATTLICHE ERKLÄRUNG

Ich erkläre an Eides statt, dass ich diese Arbeit selbständig verfasst, andere als die angegebenen Quellen und Hilfsmittel nicht benutzt, und mich auch sonst keiner unerlaubten Hilfsmittel bedient habe.

Ich erkläre, dass ich die Richtlinien des Senats der Montanuniversität Leoben zu "Gute wissenschaftliche Praxis" gelesen, verstanden und befolgt habe.

Weiters erkläre ich, dass die elektronische und gedruckte Version der eingereichten wissenschaftlichen Abschlussarbeit formal und inhaltlich identisch sind.

Datum 02.09.2019

A handwritten signature in blue ink, appearing to read 'Christoph Ponak', written over a horizontal line.

Unterschrift Verfasser/in
Christoph, Ponak
Matrikelnummer: 01135277

Danksagung

Mein Dank gilt zu allererst meinem Betreuer, Prof. Harald Raupenstrauch. Ihm danke ich nicht nur für die Aufnahme in sein Team, sondern auch für die Begleitung meines wissenschaftlichen Werdegangs von Anfang an. Meine Vorhaben wurden durch ihn auf täglicher Basis ebenso wie in größeren Belangen, wie meinem Auslandsaufenthalt, stets unterstützt. Die darüberhinausgehende soziale Komponente, deren großen Stellenwert ich sehr schätze, bereicherte mich gleichermaßen auf zwischenmenschlicher Ebene.

Auch gilt mein Dank meinem Mentor, Prof. Helmut Antrekowitsch, für den gelieferten Input. Allen inhaltlich Beitragenden möchte ich ebenso an dieser Stelle für ihre Anmerkungen danken, insbesondere Dr. Andreas Schönberg, Dr. Herbert Schmid und Dr. Johannes Rieger. Mein herzlicher Dank gilt auch Prof. Kazuki Morita, Dr. Sakae Shirayama und deren Team an der University of Tokyo, die mich herzlich empfangen haben und mir die Möglichkeit gaben, mich fachlich auch im internationalen Kontext weiterzubilden.

Besonderer, aufrichtiger Dank gilt meinen Kolleginnen und Kollegen. Insbesondere Valentin Mally danke ich für die tatkräftige Unterstützung seit Tag 1. Ohne ihn gäbe es diese Arbeit in ihrem heutigen Umfang nicht. Ebenso danken möchte ich Alexandra Holzer, Stefan Windisch, Felix Breuer und Elias Obererlacher für ihre Beiträge – auf inhaltlicher sowie persönlicher Ebene. Dem Team des TPT gilt mein Dank für die vielen über die Arbeit hinausgehenden, wertvollen Stunden, allen voran Samuel Kainz, Franz Edler und Zlatko Raonic. Meinem guten Freund Anson Ching danke ich aufrichtig für das Korrekturlesen.

So wie es ohne Betreuung, Kolleginnen und Kollegen und den regen Austausch inhaltlich keine Arbeit gäbe, hätte sie ohne die Unterstützung durch meine Partnerin Yasmin Hashw für wesentlich mehr Motivationskämpfe gesorgt. Ihr danke ich für ihr Verständnis für die vielen gearbeiteten Stunden, ihre Unterstützung im Büro sowie außerhalb und ihr offenes Ohr zu jeder Tages- und Nachtzeit.

Zuletzt nur in der Reihenfolge, inhaltlich aber an oberster Stelle, möchte ich meinen Eltern, Susanne und Norbert Ponak, danken. Der erfolgreiche Abschluss dieses Lebensabschnittes ist dem Umstand zu verdanken, dass ich ihn voller bedingungsloser Unterstützung durch meine Familie bewältigen durfte.

Acknowledgement

I want to thank my supervisor Prof. Harald Raupenstrauch for his continuous encouragement. On a professional as well as on a personal level, his support has been highly appreciated.

For valuable input and constructive remarks, I want to thank my mentor Prof. Helmut Antrekowitsch as well as Dr. Andreas Schönberg, Dr. Herbert Schmid and Dr. Johannes Rieger. I am incredibly grateful to Prof. Kazuki Morita, Dr. Sakae Shirayama and their team at the University of Tokyo for allowing me to conduct research as a part of their lab in Japan.

I also thank my dear colleagues Valentin Mally, Alexandra Holzer, Stefan Windisch, Felix Breuer and Elias Obererlacher for their input and friendship. The whole team of our chair I thank for the valuable time reaching far beyond working hours, especially Samuel Kainz, Franz Edler and Zlatko Raonic. I also want to express my gratitude for the proofreading done by my dear friend Anson Ching.

For motivational support inside and outside of the office I want to warmly thank my partner Yasmin Hashw. I thank her for her understanding of long working hours, her support and her sympathetic ear.

Last but not least, I am enormously grateful to my parents Susanne and Norbert Ponak. My path leading to the conclusion of this chapter in life was as smooth as it was only because of their unconditional support.

Förderung/Funding

The author gratefully acknowledges the funding support of K1-MET GmbH. The research programme of the K1-MET competence center is supported by COMET. COMET is funded by the Federal Ministry for Transport, Innovation and Technology, the Federal Ministry for Digital and Economic Affairs, the provinces of Upper Austria, Tyrol and Styria as well as the SFG. The research project itself is mainly financed by voestalpine Stahl GmbH, voestalpine Stahl Donawitz GmbH, Primetals Technologies Austria GmbH and SCHOLZ Austria GmbH.

Die vorliegende Arbeit wird im Rahmen des österreichischen Kompetenzzentren-Programms COMET K1-MET mit Mitteln des BMVIT, BMDW, der Länder Oberösterreich, Steiermark und Tirol gefördert und zusätzlich von den Industriepartnern Primetals Technologies Austria GmbH, SCHOLZ Austria GmbH, voestalpine Stahl GmbH und voestalpine Stahl Donawitz GmbH mitfinanziert.

Kurzfassung

Die weltweit produzierte Stahlmenge ist aktuell auf einem Höchststand. Für die Wettbewerbsfähigkeit von Stahlherstellern ist Ressourceneffizienz ein Schlüsselfaktor. Im Zuge der Stahlherstellung auf der Hochofen-Konverter-Route entstehen riesige Mengen an Stahlwerksschlacken. Etwa ein Viertel dieses Kuppelprodukts der Stahlherstellung besteht aus wertvollen Elementen wie Eisen, Chrom, Mangan und Phosphor in Form von Oxiden und Phosphaten. Werden diese carbo-thermisch vollständig reduziert – was einen Aufbereitungsansatz darstellt, dem momentan viel Forschungsaufwand gewidmet wird – reichert sich Phosphor im gewonnenen Metallprodukt an. Da Phosphor auf der genannten Stahlherstellungsrouten nur im Sauerstoffkonverter entfernt werden kann und dessen Leistung in dieser Hinsicht limitiert ist, ist ein stahlwerksinterner Wiedereinsatz der Legierung aus der Reduktion nicht möglich, ohne die Rohstahlqualität negativ zu beeinflussen.

Im Zuge dieser Arbeit wird ein neuartiges Reaktorkonzept namens InduRed angewendet, um Phosphor während der Reduktion über die Gasphase zu entfernen. Dadurch konnten nach entsprechender Schlackenmodifikation Entfernungsraten von bis zu ca. 83% erreicht werden. Das Schlackenprodukt ist weitgehend frei von Eisen, Chrom und Phosphor.

Zusätzlich wird der Einsatz dieses Reaktorkonzepts als Schritt in einer alternativen Verfahrensrouten untersucht. Der zuvor erwähnte Reduktionsschritt soll dazu in einem Standardaggregat durchgeführt werden, sodass sich Phosphor vollständig im Metallprodukt anreichert. Die entstehende Legierung soll anschließend in einem zusätzlichen Konverter so behandelt werden, dass sich vorrangig Chrom und Phosphor in der Schlacke anreichern. Diese Schlacke soll dann im genannten Reaktor reduziert werden, um eine weitestgehend phosphorfremde Metalllegierung zu produzieren. Im Zuge dieser Arbeit wurden solche Schlacken synthetisch hergestellt und carbo-thermisch nach dem Stand der Technik sowie im InduRed-Reaktor reduziert. Die Schlackenzusammensetzung basiert auf theoretischen Überlegungen und enthält auch hohe Mangananteile. Im InduRed-Reaktor konnten verglichen mit dem Stand der Technik und des Wissens weit höhere Phosphorentfernungsraten von bis zu 42% erzielt werden. Es wurde dennoch ein Einfluss hoher Chrom- und Mangangehalte auf die Phosphorentfernung festgestellt.

Abstract

Steel production is at an all-time high. Resource efficiency is a key factor for production in order to operate competitively in the steelmaking sector. In the course of the blast furnace-basic oxygen furnace steelmaking route, immense amounts of basic oxygen furnace slag are produced. Roughly a quarter of this co-product of steel production consists of valuable elements – namely iron, chromium, manganese and phosphorus – in the form of oxides and phosphates. If fully recovered by carbo-thermal reduction – one of the treatment approaches currently addressed by a number of research activities – phosphorus accumulates in the obtained metal product. Since phosphorus can only be removed from the mentioned process route in the basic oxygen furnace and its performance in this regard is limited, the internal recycling of the iron alloy produced by reduction is not feasible without negatively affecting the crude steel quality.

In the course of this thesis, a novel reactor concept called InduRed is applied in order to remove phosphorus via the gas phase during reduction. Thereby, high phosphorus gasification rates of up to roughly 83% could be achieved after respective slag modification. The slag product contains virtually no iron, chromium or phosphorus.

Additionally, the InduRed reactor concept is also applied as a step in an alternate process route. The initial slag reduction step described above can be conducted in a standard reduction unit so that the phosphorus is fully accumulated in the metal product. This alloy is subsequently treated in an additional refining step, so that mainly chromium and phosphorus are oxidised. The product slag obtained by this step can finally be reduced in the novel reactor in order to produce a low-phosphorus metal product. In the course of this thesis, such slags were produced synthetically and reduced by standard carbo-thermal reduction as well as in the InduRed reactor. The slag composition is based on theoretical assumptions and contains high manganese amounts as well. The gasification rates were much higher after reduction in the InduRed reactor compared to reduction according to the state of the art and the state of knowledge, reaching roughly 42%. An influence of high chromium and manganese amounts, however, was detected.

Table of contents

Table of contents	I
List of abbreviations, formulae and symbols	III
List of illustrations	VI
List of tables	X
1 Challenge and objective outline	1
1.1 Statement of task, background and research relevance.....	1
1.2 Hypotheses.....	4
1.3 Methodology	5
2 Theoretical and practical fundamentals	6
2.1 Literature research and theoretical fundamentals	7
2.1.1 Steelmaking process and slag production.....	7
2.1.1.1 Steel production and potential of BOFS recycling.....	7
2.1.1.2 Steelmaking slag	9
2.1.2 State of the art in BOFS treatment and utilisation	14
2.1.2.1 Mechanical processing of BOFS	15
2.1.2.2 Pyrometallurgical processing of BOFS.....	16
2.1.2.3 Other treatment processes and applications of BOFS	18
2.1.3 State of knowledge in BOFS reduction with simultaneous phosphorus gasification .	19
2.1.4 InduRed reactor and process	20
2.1.5 Thermodynamics and kinetics of BOFS reduction	25
2.1.5.1 Reduction reactions and iron phosphide formation	26

2.1.5.2	Activity of Fe(O) and P ₂ O ₅ in metal and slag phases and thoughts on kinetics	32
2.1.6	Chromium- and phosphorus-rich slags	34
2.2	Practical fundamentals – construction of a lab-scale plant	36
3	Original scientific work	40
3.1	Theoretical work	40
3.1.1	Temperature requirements and carbon consumption	40
3.1.2	Reaction schematics	45
3.2	Preliminary experiments	49
3.2.1	Objectives	50
3.2.2	Methodology	50
3.2.3	Experiment execution	52
3.2.3.1	Smelting experiments	53
3.2.3.2	Reduction experiments	54
3.2.4	Results	55
3.2.5	Research prospects	62
3.3	Improvement of the metal quality	67
3.3.1	Process alteration	67
3.3.2	Determination of a potential phosphate slag composition	68
3.4	Treatment of chromium- and phosphorus-rich slags	71
3.4.1	Objectives	71
3.4.2	Methodology	71
3.4.3	Experiment execution	73
3.4.4	Results	74
3.4.5	Research prospects	83
4	Conclusions	84
4.1	Summary	84
4.2	Assessment of hypotheses and results	85
5	Research prospects	88
5.1	Slag quality	88
5.2	Metal quality	88
5.3	Process and scale-up	89
6	Bibliography	90

List of abbreviations, formulae and symbols

General abbreviations

BF	blast furnace
BOF	basic oxygen furnace
BOFS	basic oxygen furnace slag
EAF	electric arc furnace
EU	European Union
ICP-MS	inductively coupled plasma mass spectrometry
LD	Linz-Donawitz
m.-%	mass percent
QS	quartz sand
RD	reduction degree
SS _{prel}	synthetic slag for preliminary experiments
TC	thermocouple
UTokyo	University of Tokyo
XRD	X-ray diffractometry

Chemical formulae

$3 \text{CaO} \cdot \text{P}_2\text{O}_5$	tricalcium phosphate
$3 \text{FeO} \cdot \text{P}_2\text{O}_5$	iron (II) phosphate
C_3P	tricalcium phosphide
$\text{Ca}_3(\text{PO}_4)_2$	tricalcium phosphate
CaCO_3	calcium carbonate
Cr_xP_y	chromium phosphide
C_xS	(di-/tri-)calcium silicate
e^-	electron
Fe_3P	iron (II) phosphide
$\text{Fe}_3(\text{PO}_4)_2$	iron (II) phosphate
$\text{Fe}_x\text{P}_{(2)y}$	iron phosphide
H_3PO_4	phosphoric acid
Me	metal

Formula symbols

a	activity	[-]
B1	basicity in Equation (2-15)	[-]
$B_{2/3/4}$	basicity	[-]
f	frequency	[Hz]
K	equilibrium constant	[-]
N	mole fraction in Equation (2-43)	[-]
p	partial pressure	[bar]
P	power	[W]
R	universal gas constant	[Jmol ⁻¹ K ⁻¹]
T	temperature	[K]
x	mole fraction	[-]

γ	activity coefficient	[-]
$\gamma^{(H)}$	activity coefficient in diluted solutions (Henry)	[-]
$\Delta G_{\text{EQU}}^{\ominus}$	free molar enthalpy (equilibrium)	[kJmol ⁻¹]
$\Delta G_{\text{TD}}^{\ominus}$	free molar enthalpy (thermodynamics)	[kJmol ⁻¹]
ΔH^{\ominus}	molar enthalpy	[kJmol ⁻¹]
ΔS^{\ominus}	molar entropy	[kJmol ⁻¹ K ⁻¹]
ε_i^j	influence parameter (influence of j on i)	[-]

Aggregate state and phase indication

(g)	gaseous state
(l)	liquid state
(s)	solid state
()	slag phase
[]	molten bath (dissolved in liquid metal phase)
{ }	gas phase

List of illustrations

Figure 1: World crude steel production by region from 1950 to 2018 [1]	2
Figure 2: Process routes of steelmaking [14]	8
Figure 3: Relation between basicity and viscosity of slags [17]	13
Figure 4: CaO-FeO _n -SiO ₂ phase diagram [23]	14
Figure 5: InduRed reactor [49]	21
Figure 6: InduRed pilot-scale plant and its main components (1: reactor, 2: combustion chamber, 3: gas scrubber).....	22
Figure 7: InduRed process flow chart and research areas covered by this thesis	23
Figure 8: Development of the reactor bottom design in the InduRed pilot-scale plant (a: tapping holes, b1: internal inductive heating by graphite pieces, b2: slits for larger tapping area, c: graphite frustum)	24
Figure 9: Goods balance of the steelmaking process including the proposed InduRed process	24
Figure 10: Blast furnace model [55]	26
Figure 11: Richardson-Ellingham diagram [17]	29
Figure 12: Baur-Glaessner diagram [59]	30
Figure 13: CaO-FeO _x -P ₂ O ₅ phase diagram [23]	35
Figure 14: Schematic setup of the lab-scale plant InduMelt	36
Figure 15: Realistic illustration of the InduMelt plant and its main components	36

Figure 16: Experimental setups for smelting and reduction in the lab-scale InduMelt plant [49].....	38
Figure 17: Power input in different susceptor geometries investigated in the InduMelt plant in cooperation with Elias Obererlacher (Chair of Thermal Processing Technology)	38
Figure 18: Power input in thin susceptor rings investigated in the InduMelt plant in cooperation with Elias Obererlacher (Chair of Thermal Processing Technology).....	39
Figure 19: Richardson-Ellingham diagram drawn with data retrieved from HSC [65]	41
Figure 20: Rist diagram for C_3P and FeO reduction and its relation to the Baur-Glaessner diagram (adapted from [17, 60])	43
Figure 21: Extended Rist diagram for the reduction of basic oxygen furnace slags (adapted from [17, 60]).....	44
Figure 22: Metal layer formed on graphite cubes during the reduction of basic oxygen furnace slags in the InduMelt plant	45
Figure 23: Schematics of reduction reactions and phosphide formation during the treatment of basic oxygen furnace slags in the InduRed reactor	46
Figure 24: Equilibrium composition during the direct reduction of C_3P [65]	47
Figure 25: Equilibrium composition during the direct reduction of C_3P with simultaneous silicate formation [65]	48
Figure 26: $Fe_{2/3}P$ formation as a function of the temperature [65]	49
Figure 27: Fields of conflict between basic oxygen furnace slag processing parameters .	50
Figure 28: InduMelt plant and temperature measurement equipment in operation (1: optical temperature measurement, 2: induction coil with reactor, 3: thermocouples, 4: cooling water distribution, 5: laptop)	51
Figure 29: Overview of conducted experiments during the first experimental campaign [49]	53
Figure 30: InduMelt plant during operation and heated graphite cubes shortly after tapping	55
Figure 31: Experimental sequence for smelting and reduction in the InduMelt plant and images from preliminary experiments	55

Figure 32: Complexity of metal and slag samples after reduction of basic oxygen furnace slags in the InduRed reactor (left: metal spheres on graphite cubes, right: metal on cubes and green, partially reduced product slag).....	57
Figure 33: Reduction degrees for Fe, Cr, P and Mn based on ICP-MS analysis results for experiments 1h, 3m and 3h with basic oxygen furnace slags	59
Figure 34: SEM images of produced slag samples: (a) BOFS+BFS, $B_2=1.5$, smelting step (b) BOFS+QS, $B_2=1.5$, smelting step (c) slag from experiment 1h (1650°C) (d) slag from experiment 3h (1650°C)	60
Figure 35: Input phosphorus distribution for experiments 1h, 3m and 3h conducted in the InduMelt plant with basic oxygen furnace slags	61
Figure 36: Path of the slag composition during the proposed treatment steps in a CaO-FeO _n -SiO ₂ phase diagram [23]	62
Figure 37: Phosphorus balance after implementation of the InduRed process	63
Figure 38: Phosphorus balance with internal recycling of the produced iron alloy	64
Figure 39: Goods balance with internal recycling of the produced iron alloy	64
Figure 40: InduRed reactor in operation and slag/metal products from the first continuous experiment (1: reactor in operation, 2: graphite cubes and slag, 3: metal pieces).....	65
Figure 41: Powder found in the InduRed reactor after the second continuous experimental campaign.....	66
Figure 42: Proposed alteration of the basic oxygen furnace slag treatment process	68
Figure 43: Potential calcium phosphate slag composition after pre-treatment for the reduction in the InduRed plant [23]	70
Figure 44: Furnace setup used for preliminary experiments on Cr- and P-rich slags at UTokyo.....	72
Figure 45: Furnace including equipment used for preliminary experiments with Cr- and P-rich slags at UTokyo (1: power supply and control unit, 2: furnace, 3: ceramics pipe holding the crucible, 4: Ar supply).....	74
Figure 46: Synthetic, Cr- and P-rich slag for standard carbo-thermal reduction	75
Figure 47: Metal and slag product phases after standard carbo-thermal reduction of Cr- and P-rich slag	77

Figure 48: Phosphorus balance using results from the preliminary experiments (standard carbo-thermal reduction of Cr- and P-rich slag)77

Figure 49: Synthetic slag mixture (left) and product after smelting (right) for reduction in the InduMelt plant.....78

Figure 50: Graphite cubes (1) with metal spheres (2) and slag (3) after reduction of synthetic slag in the InduMelt plant.....79

Figure 51: Phosphorus balance using results from the InduMelt reduction experiments with Cr- and P-rich slag80

Figure 52: Goods balance using results from the InduMelt reduction experiments with Cr- and P-rich slag80

Figure 53: Comparison of reduction degrees achieved by standard reduction and reduction in the InduMelt plant81

Figure 54: Comparison of phosphorus distribution achieved by standard reduction and reduction in the InduMelt plant.....81

Figure 55: Calcium phosphate slag composition after reduction of Cr- and P-rich slags [23]82

Figure 56: Path of the calcium phosphate slag during reduction [23]82

List of tables

Table 1: Average basic oxygen furnace slag composition at voestalpine Stahl Linz GmbH in 2014 [5]	12
Table 2: Compositions of blast furnace slag, basic oxygen furnace slag and quartz sand used for preliminary experiments in the InduMelt plant [5]	53
Table 3: Compositions of mixtures produced for preliminary experiments in the InduMelt plant	54
Table 4: Calculated mixture compositions for smelting experiments in the InduMelt plant	56
Table 5: Comparison of calculated, analysed and weighed amount of metal phase obtained in experiment 3h conducted in the InduMelt plant.....	56
Table 6: Product stream masses out of experiments 1h, 3h and 3m conducted in the InduMelt plant.....	57
Table 7: ICP-MS analysis results for the metal phases from the basic oxygen furnace slag reduction experiments conducted in the InduMelt plant	58
Table 8: ICP-MS analysis results for the slag phases from the basic oxygen furnace slag reduction experiments conducted in the InduMelt plant	58
Table 9: Reduction degrees achieved in the course of preliminary experiments with basic oxygen furnace slags	59
Table 10: Phosphorus distribution achieved in the course of preliminary experiments conducted in the InduMelt plant with basic oxygen furnace slags	61

Table 11: Estimated metal composition after reduction of basic oxygen furnace slag in an EAF	69
Table 12: Estimated slag composition after refining the metal product from EAF reduction	69
Table 13: Desired slag composition for the reduction experiments on Cr- and P-rich slags	70
Table 14: Reagent mixture composition for the production of synthetic slags	73
Table 15: Desired and analysed composition of the synthetic slag produced for standard reduction experiments	75
Table 16: ICP-MS analysis results after carbo-thermal reduction of Cr- and P-rich slags	76
Table 17: Reduction degrees achieved by standard carbo-thermal reduction of Cr- and P-rich slag	76
Table 18: Phosphorus distribution after standard carbo-thermal reduction of Cr- and P-rich slag	76
Table 19: Product stream masses after standard carbo-thermal reduction of Cr- and P-rich slag	76
Table 20: ICP-MS analysis results after reduction in the InduMelt plant	78
Table 21: Reduction degrees achieved by reduction of synthetic, Cr- and P-rich slag in the InduMelt plant.....	79
Table 22: Phosphorus distribution after reduction of synthetic, Cr- and P-rich slag in the InduMelt plant.....	79
Table 23: Product stream masses after reduction of synthetic, Cr- and P-rich slag in the InduMelt plant.....	79

1 Challenge and objective outline

Every research effort has a driving force. In the case of steelmaking residues, societal, legal, political, environmental, historical and economic factors are highly intertwined. This opening chapter explains to what field of interest this thesis can be generally ascribed and why the conducted research is relevant to these seemingly conflicting research stimuli.

Out of many related aspects of research, a very specific topic is addressed by the work conducted in the course of this thesis. The underlying hypotheses are therefore described in this chapter.

In order to corroborate or refute the hypotheses, a series of theoretical and experimental tasks were carried out. The methodology applied is explained, so that the structure of this thesis can be understood and navigated easily.

1.1 Statement of task, background and research relevance

Around the globe, iron and steel are produced to an enormous extent. Iron is by far the most important technical metal in terms of quantity. Its applications are manifold, including the most important aspects of human existence in the 21st century, such as construction and mobility. A well-known graphic in the field of ferrous metallurgy is shown in **Figure 1**. [1]

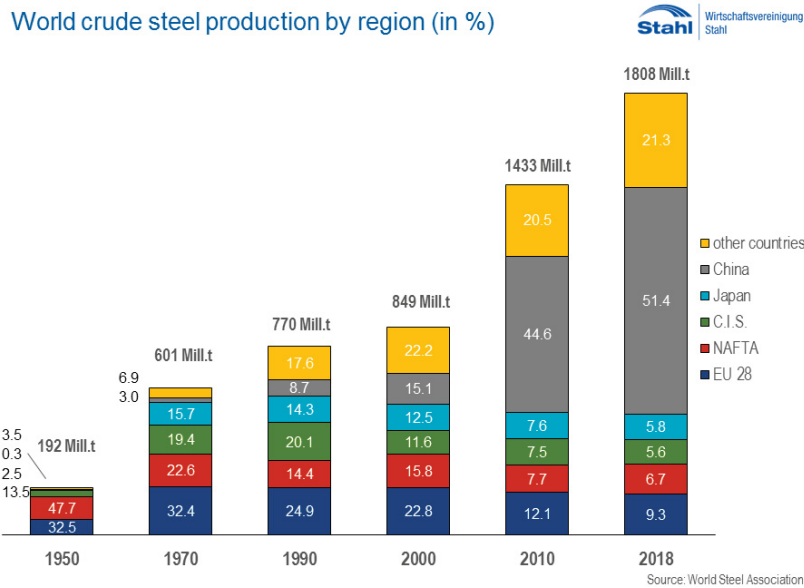


Figure 1: World crude steel production by region from 1950 to 2018 [1]

This supply is, naturally, the answer to a high demand. However, with China being the world's biggest supplier of steel, contestability for other steel-producing regions is an ever-growing issue. Historically, Austria has put a lot of effort into ongoing research activities, it being the birthplace of the Linz-Donawitz process of oxygen steelmaking (LD process). The political and legal framework of the European Union (EU), however, requires a lot of investment regarding environmental protection. High levels of liveability, high worker protection standards and firm restrictions with regard to industrial environmental pollution leave EU companies no choice but to produce high quality products in order to compete on a global scale.

Immensely influential megatrends driving innovation in the steelmaking sector are, with no doubt, environmental awareness and mobility. Predicting and acting according to these megatrends is crucial to contestability in a world facing increasing volatility. [2] If new challenges are foreseen and innovation is triggered, dominance battles will be carried out. Suarez provides fundamental insight into these battles and determines several factors as crucial to technology dominance. They are divided into firm-level and environmental factors, some of which are especially relevant to the phase of innovation this thesis is positioned in: [3]

- a firm's technological superiority (firm-level)
- regulation (environmental)
- regime of appropriability (environmental)
- characteristics of the technological field (environmental, regarding for instance the number of actors and the level of competition) [3]

The dominance process can be divided into five stages: R&D build-up, technical feasibility, creating the market, the decisive battle and post-dominance. The factors named above are all relevant mostly to the first two phases. [3] Therefore, this stage is highly crucial to future contestability from a standpoint of societal challenges and the work conducted shall deliver a small contribution to the bigger picture in that regard.

As is extensively laid out in the fundamentals part of this thesis, the steelmaking route applying a basic oxygen furnace (BOF) as the refining step for hot metal from a blast furnace (BF) is the main route used globally for steel production. [4] Its products, next to exhaust gas, dusts and crude steel, include basic oxygen furnace slag (BOFS). They are not just an unwanted co-product of steelmaking but perform a number of metallurgical tasks. Upon tapping, roughly a quarter of their mass consists of highly valuable elements, namely iron, chromium, manganese and phosphorus. [5] It is the overall objective of a number of research efforts, including that presented in this thesis, to utilise these elements as secondary raw materials.

Phosphorus, including the primary resource phosphate rock, is a critical raw material to the EU. [6] However, to the steelmaking process it is a burden since it causes undesired effects in steel (with the exception of some specific steel qualities) regarding workability in the course of secondary metallurgy treatments. [7] Once phosphorus enters the steelmaking process of the BF-BOF route, it is removed from the hot metal only in the converter refining step (Japanese steelmaking often includes a dephosphorisation step before refining in a BOF, which represents an exception to this statement). [8]

The BOFS treatment approach addressed in this thesis desires the full reduction of the slags in order to recover the valuable metals it contains. If this is done at high temperatures of roughly 1923.15 K, phosphorus compounds are reduced and – as it happens in the BF – the element accumulates in the obtained metal phase. The internal recycling of the metal product of the reduction is, therefore, impossible without impairing the crude steel quality. The reactor concept applied in the course of the conducted experiments provides a possibility to remove the phosphorus in its elementary form via the gas phase.

In Austria, 800,000 tons of BOFS are produced annually. [9] Apart from the potential regarding resource efficiency founded in the desired metal recovery, the legal situation in Austria limits the utilisation of BOFS in road construction – being one of the most important fields of application to date – to a high extent. [10] The occurrence of chromium in the slags causes concerns with respect to elution and groundwater protection. This is in spite of extensive research refuting the theories the chromium-related apprehension is based on. The suitability of chosen, legal thresholds for the determination of environmental impacts of the

BOFS utilisation in road construction, however, is still debatable. [11] Therefore, a more holistic approach is desired.

In conclusion, with steel production being at an all-time high, a declining availability of high-quality, low-phosphorus ores [12] and resource efficiency being an enormously important topic with regard to both contestability and climate protection, the research attention paid to the recycling of steelmaking residues is well-deserved.

1.2 Hypotheses

An essential part of the theoretical fundamentals this thesis is based on is the state of knowledge. It is described in great detail in chapter 2.1.3 of this thesis and it is deliberately separated from the state of the art regarding BOFS treatment. It is, more specifically, focused on the aspect of the removal of phosphorus from BOFS in its elementary form via the gas phase, or phosphorus gasification. Indications for the possibility of phosphorus gasification can be found in respective literature. However, gasification rates are not yet sufficiently high enough to imagine the proposed internal recycling process on an industrial scale. By applying a novel reactor concept, the gasification rate was expected to be increased. This objective is verbalised in the following main hypothesis:

By carbo-thermal reduction of basic oxygen furnace slags in an inductively heated bed of graphite pieces, high phosphorus gasification rates can be achieved.

In order to corroborate or refute this main hypothesis, the following supporting hypotheses are constructed:

1. A modification of BOFS is required in order to retain flowability and to thermodynamically support the phosphorus gasification.
2. The most important modification is the addition of a silica source.
3. Blast furnace slag (BFS) is a suitable silica source for the modification step.
4. High temperatures are required to achieve high phosphorus gasification rates.
5. The iron oxide content of BOFS poses the most influential limitation to the gasification process.
6. Altering the process route in order to produce and treat Cr- and P-rich slags in the presented reactor concept leads to even higher gasification rates.
7. Chromium and manganese phosphide formation does not limit the gasification rates.
8. The applied reactor concept benefits the phosphorus gasification substantially.

These hypotheses are investigated in the course of this thesis. Results are presented so that the assumptions made can be supported or refuted.

1.3 Methodology

The approach to corroborate or refute the hypotheses stated above comprises several theoretical as well as practical steps and work packages.

Firstly, the results of extensive literature research shall portray the area of interest so that the production of BOFS, the state of the art of its treatment as well as the state of knowledge regarding phosphorus gasification during its reduction can be used as a starting point of the conducted research. This scientific approach enables the evaluation of the novelty of the conducted work and the extent to which the state of knowledge can be exceeded.

Secondly, the reactor concept used to achieve the research objectives is neither commercially available nor has it been applied to BOFS elsewhere. It is therefore explained in detail. Additionally, the thermodynamic fundamentals needed to address the desired reduction of BOFS with simultaneous phosphorus removal via the gas phase are presented in the theoretical part of this thesis.

Practical fundamentals include the construction of a new lab-scale furnace in which the required experiments are executed as well as a novel experimental setup and related investigations on heat input.

Subsequently, theoretical work and reaction schematics constitute the first part of the original scientific work conducted in the course of this thesis. Required reduction temperatures as well as carbon demands are derived from theoretical considerations.

The experimental part comprises preliminary experiments on the phosphorus gasification from BOFS. Their execution and the achieved results are described. Research areas that have been worked on, but which are not the main focus of this thesis, are shortly presented.

As a consequence of the preliminary experiments, an alternate process route is derived and theoretically explained. Expected Cr- and P-rich slag compositions are calculated. Such slags, since they are not yet available as a product of existing industrial processes, were synthetically produced and reduced in the applied reactor concept. These experiments are presented along with a comparison of the obtained results with those of standard carbo-thermal reduction.

2 Theoretical and practical fundamentals

The removal of phosphorus from steelmaking slags has attracted an immense amount of research attention over the past couple of years. Main fields of focus include, firstly, the composition of steelmaking slags. In this field, the objective is to evaluate the potential of mechanical, pyrometallurgical and hydrometallurgical processing by understanding the slag structure and – with regard to phosphorus – its occurrence in the slag matrix.

Processing methods and fields of application have developed quickly, as has their number. It becomes apparent, however, that the separation of iron and phosphorus in steelmaking slags is the main objective. Different approaches aim at utilising the mineral fraction and the magnetic, iron-containing fraction or both simultaneously. Mechanical as well as pyrometallurgical processes both have their limitations, which are described in this chapter. Hydrometallurgical processing plays a minor role in basic oxygen furnace slag treatment and is not covered.

In this thesis, one particular processing approach is described in detail. The so-called InduRed process aims at the carbo-thermal reduction of BOFS with simultaneous removal of phosphorus via the gas phase. It is reported in literature that this gasification is possible. The objective of this thesis is to advance the state of knowledge in this regard.

In order to conduct experiments on the behaviour of phosphorus during reduction, a lab-scale plant was constructed. The plant as well as the reactor that is its core component are described in the practical fundamentals part of this thesis.

2.1 Literature research and theoretical fundamentals

The theoretical part of this thesis, firstly, focuses on the formation of steelmaking slag and its composition.

Subsequently, the state of the art in the field of BOFS treatment is described in detail. From a scientific standpoint, it is clearly distinguished from the state of knowledge in the specific field of carbo-thermal reduction of BOFS with a special focus on the behaviour of phosphorus.

Naturally, the proposed treatment process and the reactor concept applied are described as well. This description is followed by thermodynamic fundamentals with regard to the reduction of BOFS.

Since the second part of the experimental section of this thesis focuses on an altered BOFS treatment route, the chromium- and phosphorus-rich slags that form in the course of this route are described. The process flow is described in the last part of this subchapter.

2.1.1 Steelmaking process and slag production

By looking at the enormous amounts of steel being produced world-wide using the BOF technology, the potential of efficient recycling processes can be highlighted. One of the big challenges in developing such a recycling method comes from phosphorus contained in the BOFS. In the following chapter, it is explained why phosphorus poses such a challenge.

Furthermore, the formation of BOFS shall be examined so that its composition and the inclusion of phosphorus can be discussed.

2.1.1.1 Steel production and potential of BOFS recycling

Of all metals used on an industrial scale, iron is by far the one with the highest production volume. Nearly 1.6 Bio. tons of the metal were produced in 2017, with Australia, China and Brazil being the largest producers. [13] The world's steel production was slightly more than 1.7 Bio. tons in the same year and surpassed 1.8 Bio. tons in 2018. China, India and Japan lead the list of the world's largest producers of crude steel in both years. [9]

Steel production can be divided into four main production routes. By far the largest amount of steel is produced via the BF- BOF route, followed by smelting of scrap in electric arc furnaces (EAF). Another route refines metal from smelting reduction processes in a BOF and the fourth route processes direct reduced iron or hot briquetted iron in an EAF. An overview is provided by **Figure 2**. [14]

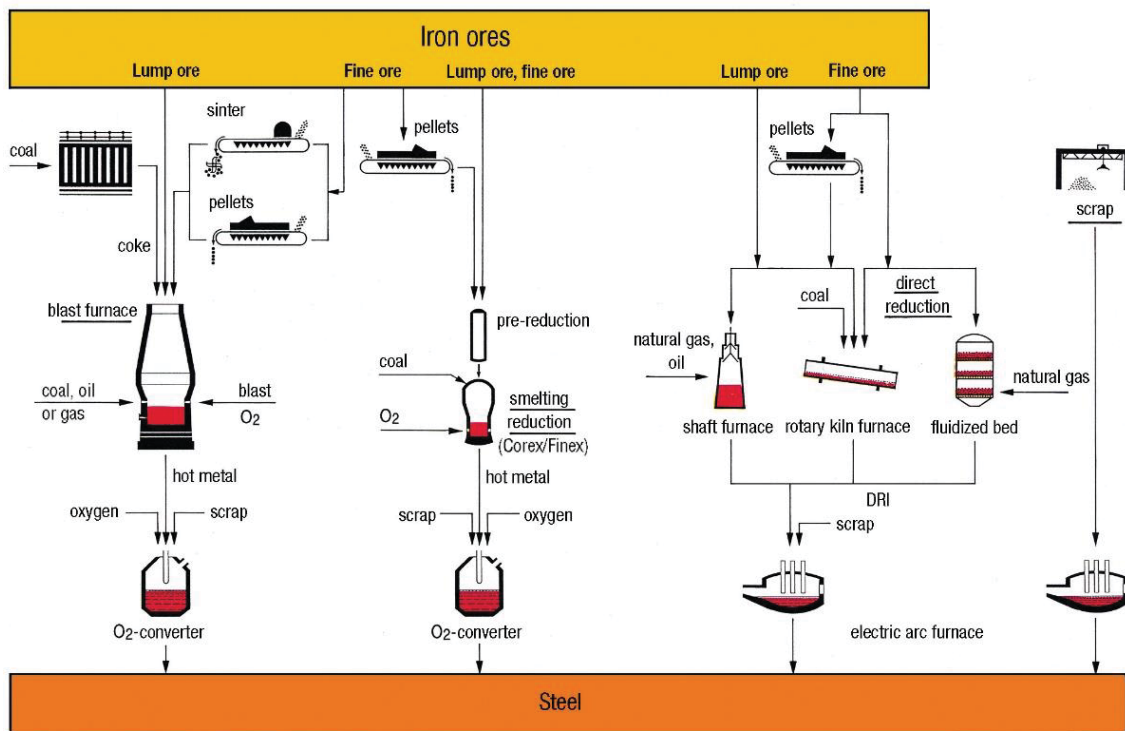


Figure 2: Process routes of steelmaking [14]

This thesis focuses on the BF-BOF route and the slag that is produced in the second step, the refining of hot metal. If not indicated otherwise, steelmaking slag, converter slag, refining slag or Linz-Donawitz slag refer to these basic oxygen furnace slags.

With roughly 71% of the world's crude steel production occurring in a BOF [4] and a BOFS formation rate of 130 kg t^{-1} crude steel [15], about 230 Mio. tons of BOFS are produced globally per year (calculated from stated data from 2018). In Austria alone, the number is roughly 800,000 tons (calculated from stated data from 2018) of BOFS. [9] On average, 30 mass percent (m.-%) of the slags are oxides of valuable metals – mostly iron, manganese and chromium. [5] If fully recovered, the iron amount and value in BOFS reused in the BOF calculated with carbon steel prices of roughly 750 USD t^{-1} [16] accounts for 45 Mio. tons of steel or 34 Bio. USD. This does not take into account the potential value of other metals separately recovered or the remaining mineral fraction and phosphorus products.

In this thesis, phosphorus and its effect on the treatment of BOFS will be discussed and investigated. Therefore, its path into the slags is shortly described. Phosphorus enters the steelmaking process as a part of the ashes of coke and coal as well as the gangue of iron ores. [17] Neither sintering nor pelletising processes operate at temperatures sufficient to alter the occurrence of phosphorus in the raw materials (mostly phosphates) used for iron making. Therefore, the whole amount of phosphorus contained in the ores reaches the BF, where it is

reduced, and – because of its oxygen potential being close to that of iron – accumulates completely in the hot metal in the BF. [18] This leaves the BOF as the aggregate required to remove phosphorus as efficiently as possible, because of the negative effects phosphorus has on the steel quality (during cooling, P displaces C and reduces the ductility, toughness and causes brittleness). [7]

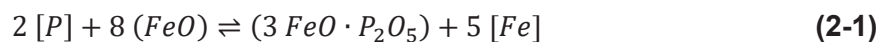
The described challenges have led to the development of two major ways of dealing with the high phosphorus load in the BOF:

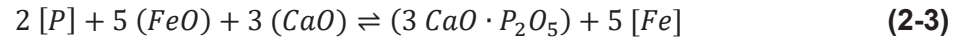
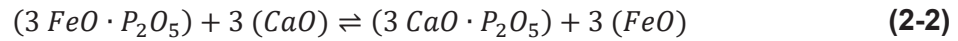
- European route: The BOF has to oxidise and bind the phosphorus contained in the hot metal so that the desired steel quality can be produced. This poses a challenge for the refining step and limits the amount of phosphorus being fed into the BF and, in turn, the amount of internal recycling of refining slag products.
- Japanese route: The hot metal is dephosphorised and, because it is thermodynamically required, desiliconised before its processing in the BOF. This, while relieving the BOF with regard to its dephosphorisation task and producing low BOFS volumes, limits the amount of scrap metal that can be recycled in the steelmaking process due to the cooling of the slag during the two pre-treatment steps as well as the missing silicon providing heat during oxidation. [8]

Since the available amounts of low-phosphorus ores are reported to be declining [12], dephosphorisation is a big issue in the field of BOF technology and related research. The challenge posed by phosphorus also leads to the development of and research on BOFS recycling processes that try to limit the load of phosphorus as well as recycling products that are to be reused in the BF-BOF route.

2.1.1.2 Steelmaking slag

In order to efficiently remove phosphorus in the BOF, the slag formation process is crucial. As iron and silicon are oxidised, a fayalite slag is formed, which, as quickly as possible, shall take up CaO from slag formers added to the BOF (i.e. mostly dolomite, lime and limestone). Only then can phosphorus be oxidised and bound into the slag matrix and, in turn, be stabilised. [19] The following equations **Equation (2-1)**, **Equation (2-2)** and **Equation (2-3)** describe the binding of phosphorus into the slag using molecular theory. [12]





According to the ion theory of slags, slag is composed of ions that interact with each other. Depending on the binding energy of oxides, they can be categorised by their tendency to donate or accept oxygen ions according to **Equation (2-4)** and **Equation (2-5)** (adapted from [20]).



Metal oxides donating oxygen ions are called basic and those accepting oxygen ions are referred to as acidic. An important parameter to quickly describe the behaviour of slags regarding their stability in contact with other oxides as well as slag flowability is the so-called basicity. The basicity is a ratio of certain oxides in m.-%. Depending on the considered species, the basicity can be expressed as seen in **Equation (2-6)**, **Equation (2-7)** and **Equation (2-8)**: [20]

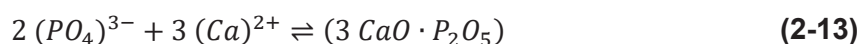
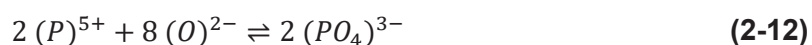
$$B_2 = \frac{\text{CaO}}{\text{SiO}_2} \quad (2-6)$$

$$B_3 = \frac{\text{CaO} + \text{MgO}}{\text{SiO}_2} \quad (2-7)$$

$$B_4 = \frac{\text{CaO} + \text{MgO}}{\text{SiO}_2 + \text{Al}_2\text{O}_3} \quad (2-8)$$

If not indicated otherwise, the term basicity will be used in this thesis only to refer to the value B_2 .

Applying this theory to the formation of $3 \text{CaO} \cdot \text{P}_2\text{O}_5$ (also referred to as tricalcium phosphate, C_3P or $\text{Ca}_3(\text{PO}_4)_2$), the following reactions can be used to describe the mechanism (**Equation (2-9)**, **Equation (2-10)**, **Equation (2-11)**, **Equation (2-12)**, **Equation (2-13)** and **Equation (2-14)**): (adapted and combined from [8], [12] and [21])



It has been shown that phosphorus accumulates preferably in dicalcium silicate phases and, if the SiO_2 content is low, in a calcium phosphate phase. [21] In any case, according to the ionic theory of slags, PO_4^{3-} ions exist and it is further assumed for theoretical considerations that C_3P is the predominant P-containing species in BOFS.

In terms of oxide content, average BOFS shows the composition shown in **Table 1**. [5]

Table 1: Average basic oxygen furnace slag composition at voestalpine Stahl Linz GmbH in 2014 [5]

species	element content [m.-%]
MnO	6.25
MnS	0.11
FeO	27.23
SiO ₂	12.77
CaO	40.21
MgO	6.66
Al ₂ O ₃	2.17
P ₂ O ₅	1.22
TiO ₂	0.38
Cr ₂ O ₃	0.39
total	97.40
B ₂	3.15

B₂ is roughly 3.2. FeO, Al₂O₃ and SiO₂ are also referred to as network-forming oxides and typically increase the viscosity of the slag. The basic oxides, which are also called network-modifying oxides, lead to lower viscosity. [22] If a reduction process is proposed to treat BOFS – as it is in this thesis – FeO and parts of the SiO₂ are removed from the slag and the viscosity changes drastically. Iron is amphoteric and can act as both network-forming and -modifying, depending on the slag composition.

Therefore, additives must be used to ensure the flowability required by the respective processes. The determination of the viscosity as used in this thesis occurred empirically regarding only the desired, highly specific application. In general, the positive effect of FeO on the flowability and the thickening of BOFS during reduction is a well-known effect which limits the slag handling without SiO₂ addition. [10] In addition, a simplified deduction can be made using **Figure 3**. [17]

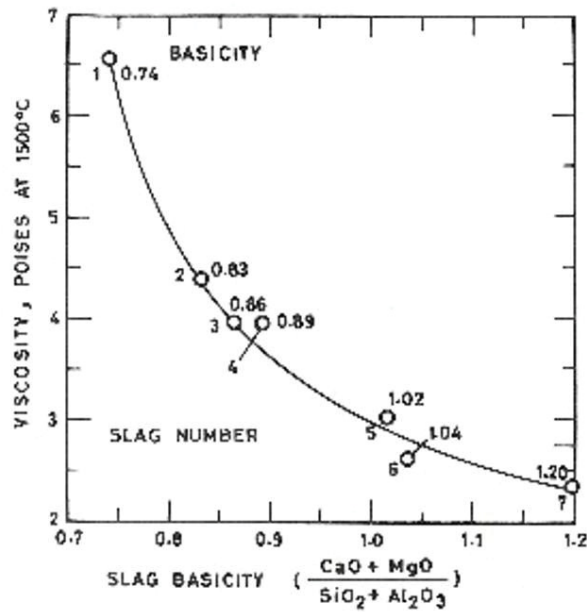


Figure 3: Relation between basicity and viscosity of slags [17]

This general assumption is true only for simplified slag systems. Real systems are highly complex and a high number of compounds are involved. Therefore, the slag viscosity in this thesis is evaluated empirically.

Using a CaO-FeO_n-SiO₂ phase diagram, BOFS, its composition as well as its liquidus temperature as a function of the SiO₂ content can be depicted. Such a phase diagram with the approximate location of BOFS (using the diagram as CaO-FeO_n+MnO+MgO-SiO₂+P₂O₅ diagram and neglecting Al₂O₃ and traces of other components) is shown in **Figure 4**. [23]

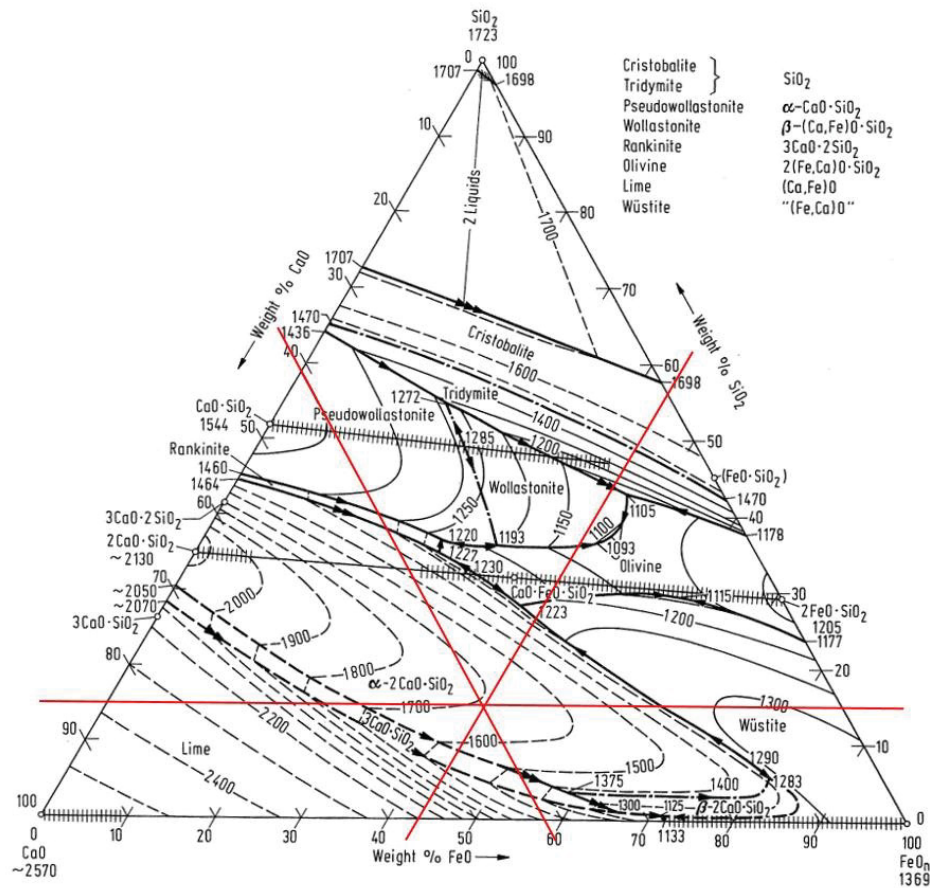


Figure 4: CaO-FeO_n-SiO₂ phase diagram [23]

Mineralogically, the slag consists of the following phases (with the letters indicating the respective oxide, e.g. F is short for FeO, CS is short for CaO·SiO₂):

- C₂S (β-modification, larnite)
- CS
- C₂F (including brownmillerite containing Al)
- FeO
- CaO (free lime)
- metallic iron [24]

2.1.2 State of the art in BOFS treatment and utilisation

Due to the high potential of BOFS recycling, a vast number of treatment processes have been proposed and extensive research has been conducted. The state of the art is reviewed in this chapter. In order to provide a clear overview, the presented treatment methods are categorised as follows:

- mechanical processing of BOFS
- pyrometallurgical processing of BOFS
 - partial reduction
 - full reduction
 - other pyrometallurgical approaches
- hydrometallurgical processing of BOFS
- other treatment processes/applications of BOFS

Hydrometallurgical processes are mostly applied to chromium- and vanadium-rich slags and are therefore shortly presented in chapter 2.1.6.

2.1.2.1 Mechanical processing of BOFS

Mechanical treatment of BOFS was reported to be the main processing route in Japan in 2013. Typically, the slag is cooled in ambient air and metallic iron is recovered as completely as possible by crushing and sieving. In order to stabilise free lime, hydration and carbonation are not suppressed, but observed, controlled and even supported. The slag is then used as a construction material (soil improvement or road construction). Other fields of application are the cement industry (clinker material delivering FeO) or fertiliser production (as a source of, amongst other elements, P). [25, 26]

Stabilising cooled BOFS in order to produce a construction material is not the only objective in the area of mechanical processing. Since the iron oxide containing parts of the slag could be reused within integrated steelworks if it were not for the phosphorus content, the mechanical separation of iron- and phosphorus-rich phases has been investigated. Milling and magnetic separation enable an iron enrichment in the concentrate of up to 40%. However, the structures are finely intergrown and so far the separation results have not been sufficiently promising, especially regarding the lacking possibility of reusing chromium and manganese. [10]

Efforts made to produce clinker materials are described in chapter 2.1.2.2, because they are often based on the quick cooling of modified BOFS. Ludwig et.al. report, however, that by special, very fine milling, existing cement phases (mostly belite) can be activated to participate in hydration reactions. [27]

Lastly, slag utilisation is practised in Europe also by using it in landfill construction (as a drainage, a base sealing or as a cap layer material). Research on the leaching behaviour of slags, especially regarding chromium, is intensified. [28]

2.1.2.2 Pyrometallurgical processing of BOFS

Literature research results show that there are two main objectives of pyrometallurgical BOFS treatment – the production of a construction material and the recovery of valuable metals by reduction.

In the field of the production of construction materials, (latently) hydraulic activity shall be developed in BOFS. The objective is mostly simplified by evaluating the formation of amorphous structures in the slag after modification and quick cooling. Ferreira Neto et.al. report that in slags with a high SiO_2 and Al_2O_3 content (network formers, s. 2.1.1.2) – in this case $B_2=1.1$ – cooling at roughly 4 Ks^{-1} can result in an amorphous slag content of over 90%. The slag phases that occur are merwinite ($3 \text{ CaO} \cdot \text{MgO} \cdot 2 \text{ SiO}_2$), monticellite ($\text{CaO} \cdot \text{MgO} \cdot \text{SiO}_2$), akermanite ($2 \text{ CaO} \cdot \text{MgO} \cdot 2 \text{ SiO}_2$) or melilite and, if the aluminium oxide amount is increased, gehlenite. [29] These phases have also been detected in the reduced slags produced in the experiments conducted in the course of this thesis (s. 3.2.4). The positive effect of the Al_2O_3 amount on the formation of amorphous phases in slags has been repeatedly reported. If the benefit of the addition of Al_2O_3 is expressed by its effect on the critical cooling rate, above which no crystal can be formed anymore, it can be seen that this cooling rate is immensely decreased by Al_2O_3 addition. [30] Modification and quick cooling has also been investigated using dry slag granulation. [31] The use of BOFS after stabilisation is applied in several countries. In China, a special stabilisation process is used before recovering magnetic components of the steelmaking slags. [32] In 2005, a report on a research project in Germany presented similar results. In order not to just cool BOFS, dry granulation was tested and it was concluded that the granulation is potentially feasible. [33]

Partial reduction is a treatment path standing between full reduction efforts and mere construction material production, trying to combine both aspects. Its objective is to reduce iron oxide, producing a hydraulically active alite phase independent from cooling rates. It has been shown that this objective can be achieved, indicating that other elements (foreign ions) stabilise the alite phases – which make up more than 60% in the reduced slags – in BOFS. Even at a reduction temperature of 2073.15 K, however, the phosphorus content is hardly reduced and neither are the contents of chromium and manganese. If the slags are diluted with synthetic slags that show the same mineral composition except for foreign ions like Na or Cr, the alite phases cannot be stabilised. [34] C_2S is formed, which transforms from its β -modification to its γ -modification, leading to its decay due to a volume increase of roughly 10%. This has been reported in respective literature and must be considered during the full reduction of BOFS. [35] It is reported that P stabilises C_2S phases as well. [36] In spite of being highly promising with regard to clinker formation, partial reduction does not solve the phosphorus accumulation

problem with BOFS but transfers it to cement production. Residual iron, chromium, manganese and phosphorus of partially reduced slags limit the utilisation of the reduction product in the rotary kiln. Phosphates (more than 2 m.-%) reduce the ability for hardening of the cement products. They stabilise C_2S , inhibit the formation of C_3S and raise the amount of free lime, reducing the strength. [37]

Full BOFS reduction is investigated in order to achieve all the objectives mentioned so far simultaneously:

- recovery of a manganese- and chromium-rich iron alloy
- removal of phosphorus during reduction via the gas phase
- production of a metal oxide-free slag suitable as a construction material

In addition to phosphorus posing a major challenge, the charging of molten slag into a reduction unit is also highly critical due to slag foaming. In Japan, reduction processes have been intensively investigated. Since the Japanese steelmaking route involves desiliconisation and dephosphorisation technologies, the slag from the BOF contains low amounts of phosphorus. However, molten slag charging has been improved, which is relevant to European BOFS treatment just the same. If carbon and molten slag get in contact, an immediate high CO production rate can cause slag foaming, destabilising the reduction process. If the feeding rate is too slow, on the other hand, the slag might solidify. It is highly demanding to optimise this process so that both problems can be tackled. Harada et.al. report that the positioning of a refractory block in the dropping area prevents foaming and that off-gas combustion can supply enough energy to avoid slag solidification. [38]

If dephosphorisation is not applied, the metal product obtained by full reduction is not reusable within integrated steelworks, because phosphorus fully accumulates in the metal phase as it does in the BF. Resistance furnaces, standard induction furnaces and EAF have been investigated as reduction units by Schmid et.al. High phosphorus amounts were analysed in the metal product after nearly complete iron oxide reduction. In BOFS without additives, the P content could be as high as 2 m.-%. This thesis focuses on the phosphorus gasification in order to significantly reduce this amount. The experiments regarding this task are described in chapter 3.2. If the metal product were refined, however, low iron losses could be expected since its composition is similar to the historic Thomas phosphate, but the chromium that was reduced would also be re-oxidised. The product slag containing high amounts of Cr and P does not yet have a designated utilisation. [10] Its treatment is investigated in the course of this thesis. The state of the art as well as the conducted experiments are described in chapters 2.1.6 and 3.4.

Efforts to remove P via the gas phase are already patented. One approach aims at the reduction of iron and phosphorus compounds in individual steps but in the same aggregate, removing iron before phosphorus is removed. In a rotary kiln P is accumulated in Fe and the patent suggests the prior reduction of the iron content with the help of mechanical processing. If conducted in two steps (reduction, separation of Fe, second reduction), the P-content in the iron from the second step is stated to be roughly 0.4-1.0 m.-%. [39] In a prior patent application, an equation for the ideal reduction temperature as a function of the basicity is stated. It suggests higher temperatures with increasing basicity and can be seen in **Equation (2-15)**. [40]

$$T[{}^{\circ}C] \geq 200 \cdot B1 + 1050 \quad (2-15)$$

Temperatures chosen for reduction experiments in this thesis are much higher than the ones suggested by this equation. The desired application of the gaseous phosphorus in the patent is the production of phosphoric acid. [40]

Finally, other pyrometallurgical research efforts investigate the separate recovery of individual elements. As an example, the selective reduction of Mn and P is mentioned and has been investigated by Shin et.al. If the composition of BOFS is modified by Al₂O₃ addition, the relative time at which P- and Mn-compound reduction occurs can be altered. However, phosphorus is almost completely accumulated in the metal phase. [41] Another approach aims at the enrichment of P-rich C₂S phases by density separation in the liquid slag state as a pre-treatment for mechanical processing. [42]

2.1.2.3 Other treatment processes and applications of BOFS

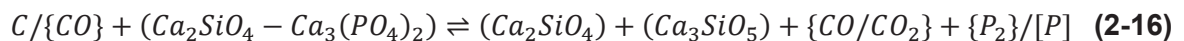
In Japan, BOFS has also been used to restore marine environments. It is supposed to improve plankton growth and in some applications prevent eutrophication. [25] Seaweed production, which is highly demanded in the country, is also supposed to benefit from this method of BOFS utilisation. [26]

The enormous number of proposed slag utilisation and processing methods show that the industry is in need of a recycling process that is able to tackle the challenges posed by this highly valuable secondary resource.

2.1.3 State of knowledge in BOFS reduction with simultaneous phosphorus gasification

Since the research topic of this thesis is the full reduction of BOFS with simultaneous phosphorus gasification, the state of knowledge in this specific research area is presented separately.

Recent experimental groundwork on BOFS reduction under consideration of phosphorus reduction has been done by Liu et.al. Slag mixtures representing BOFS were prepared and the influence of carbon addition on the phosphorus uptake of the produced metal were investigated. Naturally, higher carbon rates lead to higher P-compound reduction rates and, in turn, to P-accumulation in the iron phase. Combining possible indirect and direct reduction of C_2S – C_3P phases under production of C_2S and C_3S , CO_2 and phosphorus – dissolved in the molten metal bath or in its gaseous form – leads to the fundamental reaction equation relevant to the reduction process of BOFS (**Equation (2-16)**). [43] It includes all the potential reagents and products but neglects stoichiometric balancing due to the combination of reaction mechanisms it depicts.



The suggestion, however, is that P is present in its gaseous state only in minute amounts and that therefore the carbon content should be controlled in a way that P-reduction is limited. [43]

The effect of Al_2O_3 and SiO_2 addition to BOFS before reduction has been investigated by Liu et.al. It has been shown that the addition of Al_2O_3 increases the influence of liquid mass transport and in turn the size of iron particles separated after reduction. The SiO_2 , naturally, binds free lime and supports C_2S phase formation. [36]

Morita et.al. investigated the reduction of iron- and phosphorus-containing slag at 1823 K by microwave irradiation and the influence of SiO_2 addition in 2002. SiO_2 improves the slag flowability and therefore the reduction kinetics. It also increases the activity coefficient of P_2O_5 . The basicity was set at roughly 1.6 and the P_2O_5 content of the slags was 4 m.-%. Significant amounts of P accumulate in the metal phase. Phosphorus being distributed between a slag and metal phase accounts for 80% of the input phosphorus (lowest value). A gasification of a maximum of 20% is therefore achieved, assuming that the “unknown” phase mentioned is the gaseous phase. [44]

In 2008, Matinde et.al. described the separation of phosphorus from sewage sludge during reduction via the gas phase. Solid state reactions below 1273 K show that PO and PO₂ can be formed, whereas at temperatures between 1373 K and 1700 K, mostly P₂ (and not P₄) are formed out of liquid P₂O₅ compounds. If iron oxide contents are high, an Fe-P alloy is formed and the distribution rate of P to the gas phase decreases. [45]

By adding carbon to slag and stirring, slags containing different iron oxide fractions and showing different basicity values were reduced by Nakase et.al. If a slag with a basicity B₂ of 4.0, a mass fraction of iron oxides (FeO) of 10.4% and a P₂O₅ content of 2.8% is reduced at 1773 K (and 1873 K), up to 30% of P can be gasified. [46] This procedure of carbo-thermal reduction is referred to as “standard” carbo-thermal reduction in this thesis (though stirring is not required for a process to be included in the definition).

In 2017, Nakase et.al. investigated the influence of the FeO content on the P gasification possibilities. Its huge influence suggests the absorption of P in liquid Fe occurs as assumed. By reducing slags with an FeO content of 2.0-2.4 m.-% and a basicity B₂ of 1.0 at a temperature of 1673 K, 55% of the P could be gasified. [47] In the paper’s reference list, Nagata K. 1997 is mentioned to have achieved a 70% phosphorus gasification rate from pre-treatment slags (high P/Fe ratio) at temperatures above 1896 K. [48] However, for BOFS, 55% is the highest value reported in respective literature to date.

2.1.4 InduRed reactor and process

The InduRed process has been advanced in the course of this thesis. It is a reduction process that aims at the full reduction of BOFS. A pilot-scale plant to execute the InduRed process was constructed at the Chair of Thermal Processing Technology of the Montanuniversitaet Leoben, Austria. Its main component, the InduRed reactor, is supposed to tackle the problems related to BOFS reduction as explained in the previous chapters. The reactor consists of a cylindrical arrangement of refractory materials, containing pieces of electrode graphite. Its novelty is founded in the inductive heating of this bed of graphite pieces and by achieving a homogeneous temperature distribution, horizontally as well as radially. It is depicted in **Figure 5**.

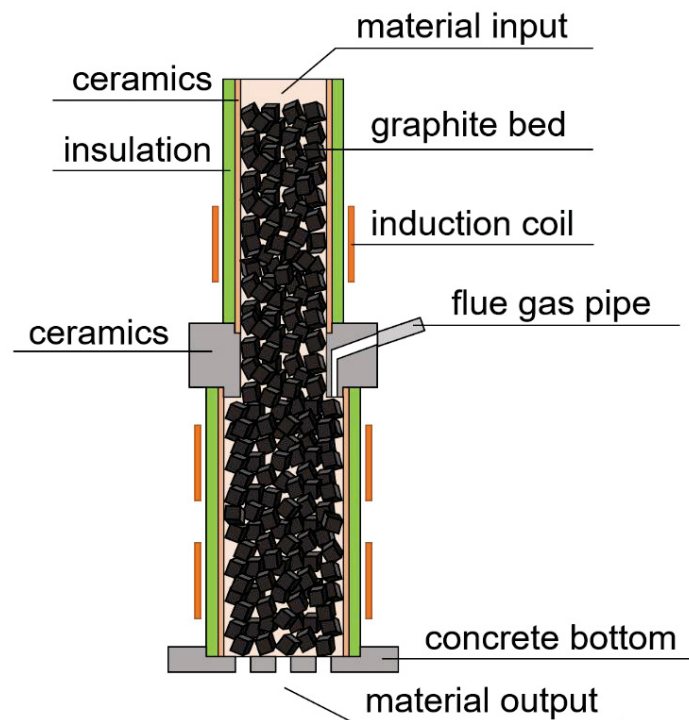


Figure 5: InduRed reactor [49]

Material that is fed to the reactor from the top melts almost immediately as it gets in contact with the first layer of graphite pieces. A thin, molten film moves towards the bottom of the reactor. A large surface area for reactions as well as short mass transport distances for reagents and products are provided. Argon is led into the reactor from the top and the bottom. Its purpose is not mainly to provide an inert atmosphere but to transport fine particles directly to the graphite surface as well as to prevent the suction of false air.

The refractory materials used all have Al_2O_3 as their main component. The reactor wall is constructed using high purity aluminium oxide and the middle part for gas suction as well as the bottom for liquid material output are cast, high-alumina concrete parts. The suction of exhaust gas is enabled by an induced draft fan, securing a minute under-pressure of roughly 0.3 mbar. The reactor in the pilot plant is close to 1 m in height and has an inner diameter of roughly 20 cm.

Liquid products of BOFS reduction are metal and slag. Both leave the reactor at its bottom and are not separated at this point. The feed is cold and needs to be heated and molten in the reactor.

The graphite is not supposed to participate in the reduction reactions. It shall provide the bed structure and a possibility for heat input directly at the graphite pieces' surface. Carbon powder is added as a carbon source for direct reduction reactions. Graphite has an estimated

sublimation point of 4000 K. Its thermal conductivity at 298.15 K is $398 \text{ Wm}^{-1}\text{K}^{-1}$ in directions within layers and close to zero between layers. For highly crystalline graphite, much higher values in the range of 10^3 have been reported. Its electrical resistivity is also high within layers, close to zero between layers and increases with temperature. It possesses a high strength of 1060 GPa in a direction within a layer. It is highly chemically resistant (except in reaction with oxygen, sulphur, selenium and tellurium). Synthetic graphite can be highly anisotropic and close to the ideal crystal and the change of its properties depending on direction can be reduced. [50] In conclusion, graphite is a highly suitable material for the reactor bed construction.

The pilot-scale plant also includes a feed vessel, a slag and metal collector bin, a post-combustion chamber for product gases and a gas scrubber. It is shown in **Figure 6**.



Figure 6: InduRed pilot-scale plant and its main components (1: reactor, 2: combustion chamber, 3: gas scrubber)

The whole process aims at the post-combustion of the product gas, mainly consisting of P_2 and CO , and treating it in a gas scrubber so that phosphoric acid can be produced. A simplified flow-chart is shown in **Figure 7**.

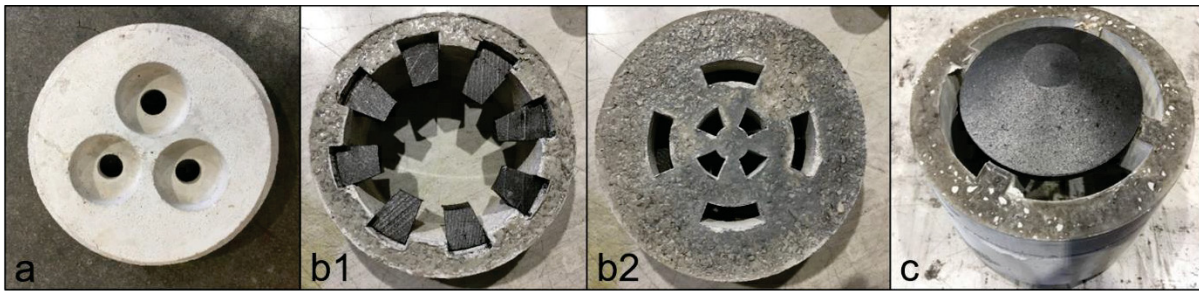


Figure 8: Development of the reactor bottom design in the InduRed pilot-scale plant (a: tapping holes, b1: internal inductive heating by graphite pieces, b2: slits for larger tapping area, c: graphite frustum)

The initial design that was likely to clog can be seen in picture a. The pictures b1 and b2 belong together. The slits in b2 provide a bigger outlet surface while the graphite pieces in b1 are meant to serve as an internal heating of the output area. Design concept b still led to clogging over time. The most successful solution that has served well in its desired application is design c. The last material slag is in contact with before leaving the reactor is graphite that is inductively heated. The power input per volume was calculated for the frustum as well as the graphite pieces it replaces. The two values were balanced so that the power input in the area was not influenced as a result of the replacement.

The desired application of the InduRed reactor is for it to serve as a BOFS treatment unit that produces an iron alloy that can be reused internally in integrated steelworks. The process and the projected goods balance are shown in **Figure 9**. The stated figures are based on actual production data from voestalpine Stahl Linz GmbH and are normalised.

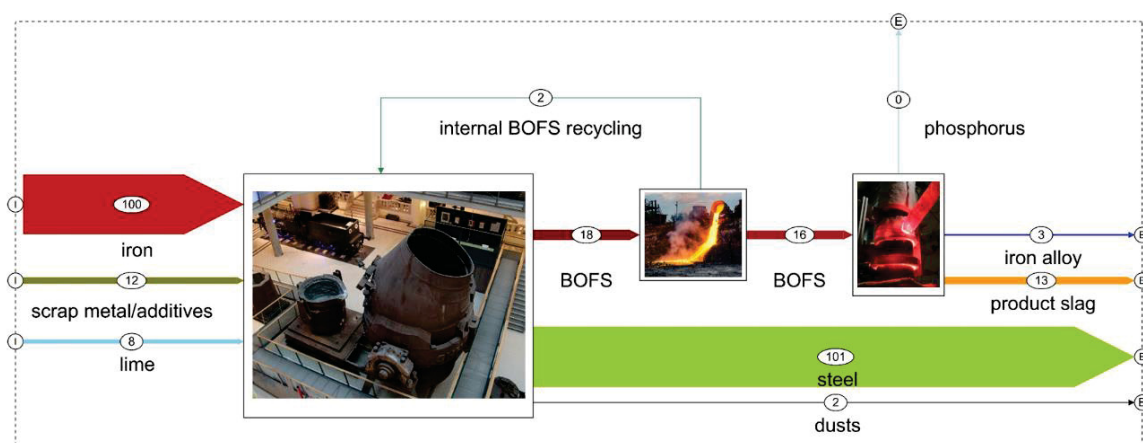


Figure 9: Goods balance of the steelmaking process including the proposed InduRed process

The main objective of the application of the InduRed reactor and process is to remove phosphorus from the BOFS during reduction via the gas phase. Respective literature does not

yet state results regarding this challenge that would enable the metal product to be reused directly in the BOF. The main advantages of the reactor are:

- The graphite bed possesses a large surface area that supports reaction kinetics.
- The induction units are designed to enable the heat input just beneath the surface of the individual graphite pieces. Slag solidification is therefore eliminated as a problem during treatment.
- The negative impact of slag foaming on the treatment should be less crucial due to the formation of a slag film (to be investigated).
- Direct reduction accounts for most of the reduction processes occurring in the reactor. This limits the carbon consumption (while, on the other hand, it increases the energy demand).
- A thin slag layer facilitates mass transport by shortening transport distances. This is especially crucial for the diffusion of P and its removal as gaseous, elementary P_2 .
- No molten bath of metal is formed. Therefore, the P_2 (g) – Fe (l) contact probability and therefore the kinetics of P-dissolution (and iron phosphide formation) can be decreased immensely.
- Dry slag granulation (or other quick cooling of product slag) provides a possibility to stabilise the slag even after full reduction.

The sources used in this chapter are partly unpublished. Results from previous research projects at the Chair of Thermal Processing Technology (Montanuniversitaet Leoben) under the leadership and management of Univ.-Prof. DI Dr.techn. Harald Raupenstrauch are presented. The pilot-scale plant and the reactor (including the oscillating circuit) were constructed in the course of the project RecoPhos. Basic information on the project is published in Schönberg et.al. [51] and documented (yet unpublished) by Kasra Samiei and Andreas Schönberg in 2014. [52] The author does not claim any contribution to the development of the InduRed reactor concept. The basic reactor concept as well as the idea of its application to treat slags are patented. [53, 54] The presented adaptations (e.g. bottom design), the work done on the InduRed process (e.g. balancing, heat input tests) and the operation with BOFS were part of the work conducted in the course of this thesis. The major contribution of this thesis to the research project is described in chapter 3.

2.1.5 Thermodynamics and kinetics of BOFS reduction

In order to properly describe the expected and observed phenomena occurring during BOFS reduction, fundamental thermodynamic and kinetic considerations are taken into account. The

bases for the theoretical scientific work conducted in the course of this thesis are explained in this chapter.

Reduction reactions of metal and phosphorus compounds in BOFS are described and, specifically, the FeO and C_3P reduction reactions are investigated. With the help of the reduction of FeO, the difference between the applied reactor concept and well-known aggregates, especially a BF, is highlighted. The C_3P reduction combined with the formation of iron phosphides is described so that the gasification of phosphorus can be explained.

2.1.5.1 Reduction reactions and iron phosphide formation

In a BF, the reduction of iron oxides progresses in several steps depending on the temperature conditions in the respective zones. A model of a BF is shown in **Figure 10**. [55]

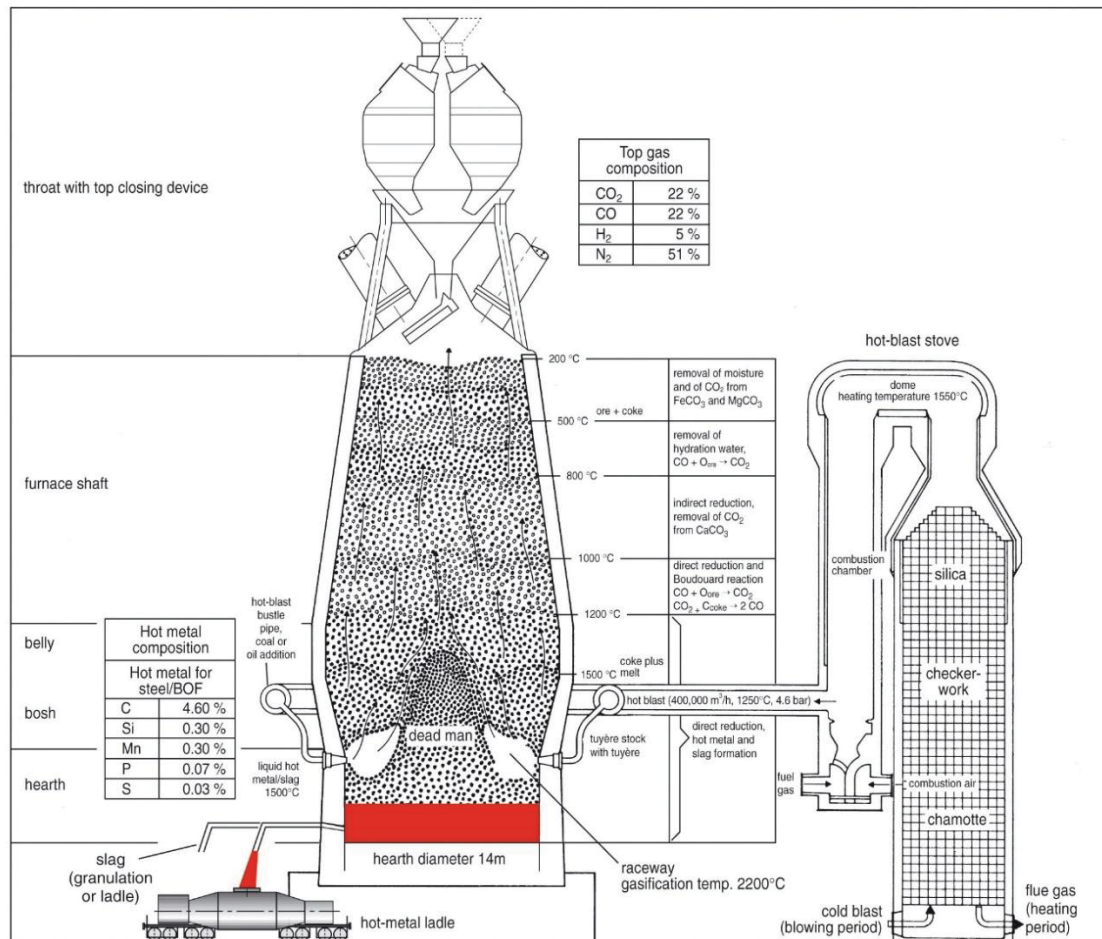


Figure 10: Blast furnace model [55]

In the belly, oxides start melting and the direct reduction of FeO occurs. The indirect reduction with CO and the formation of new CO via the Boudouard reaction (**Equation (2-17)**, **Equation (2-18)** and **Equation (2-19)**) decreases in relevance. [55, 56]



In the proposed reactor concept used for the reduction of BOFS in the course of this thesis, only the direct reduction (**Equation (2-19)**) plays a significant role. CO is produced and removed constantly from the reactor. The lack of a Boudouard zone and the gas removal in the zone with the highest P production rate are significant differences between the reduction of iron oxides in a BF and the InduCarb reactor.

Iron forms spheres (found as such after experiments) and moves through the reactor without forming a molten bath. Therefore, the contact between Fe (l) and P₂ (g) is reduced to a minimum. In a BF, C₃P is reduced in the bottom zone of the aggregate (high temperatures required). Iron moves through the slag layer and phosphorus originates in direct contact with the metal bath (derived from [55] and thermodynamic considerations described in chapter 2.1.5, [17]). Due to the thin slag layer in the InduRed reactor, however, the chances of the element getting in contact with Fe (l) is limited.

Carbon is used as a reducing agent in a BF as well as in the reduction experiments conducted in the course of this thesis. In order to estimate required reduction temperatures as well as CO/CO₂ ratios, a Richardson-Ellingham diagram can be used.

In a Richardson-Ellingham diagram, the oxygen potential of reactions of species with 1 mole of oxygen at a pressure of 1 atm is plotted against the temperature. The oxygen potential is derived and defined as follows (**Equation (2-21)**, **Equation (2-22)**, **Equation (2-24)** and **Equation (2-25)**) and explained using the oxidation of Fe and the equilibrium constant of this reaction (**Equation (2-20)** and **Equation (2-23)**) as an example. (derived from [17], [57] and [58])



$$\Delta G_{TD}^{\theta} = \Delta H^{\theta} - T \cdot \Delta S^{\theta} \quad (2-21)$$

$$\Delta G^{\theta}_{EQU} = -R \cdot T \cdot \ln K \quad (2-22)$$

The activity for FeO and Fe is one for pure substances at standard conditions [58], hence:

$$K = \frac{1}{p_{O_2}} \quad (2-23)$$

$$-R \cdot T \cdot \ln \frac{1}{p_{O_2}} = \Delta H^{\theta} - T \cdot \Delta S^{\theta} \quad (2-24)$$

$$R \cdot T \cdot \ln p_{O_2} = \Delta H^{\theta} - T \cdot \Delta S^{\theta} \quad (2-25)$$

The expression $R \cdot T \cdot \ln p_{O_2}$ is defined as the oxygen potential. [57] The activity of iron is not one if Mn, Cr, P, C, Si, Ti and other elements are dissolved in the liquid metal. At this point, the influence of a changing iron activity on the slope of the Richardson-Ellingham diagram plot of any reaction is explained by rearranging the equations above and depicted in **Equation (2-26)**.

$$R \cdot T \cdot \ln p_{O_2} = \Delta H^{\theta} - T \cdot \left[\Delta S^{\theta} + R \cdot \ln \left(\frac{a_{Fe}^2}{a_{FeO}^2} \right) \right] \quad (2-26)$$

Therefore, if the iron activity increases, the logarithmic expression moves towards higher values and, in turn, the term in brackets determining the slope of the curve in the Richardson-Ellingham diagram increases and the slope becomes flatter (since the change in entropy is below zero). Flatter slopes cause a shift towards higher reduction temperatures.

A Richardson-Ellingham diagram is shown in **Figure 11**. [17]

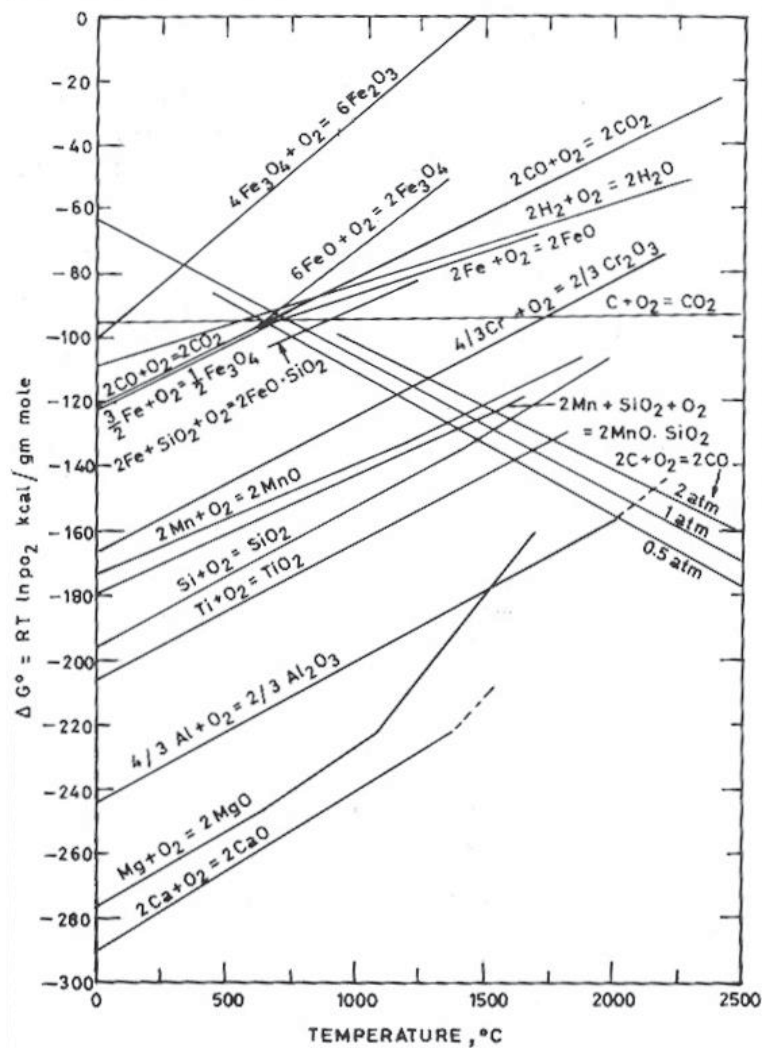


Figure 11: Richardson-Ellingham diagram [17]

Most current depictions include a CO/CO₂ scale on the side that indicates the required minimum ratio of CO and CO₂ partial pressures for a reduction. If this scale is translated into a scale indicating the CO₂ content in a CO – CO₂ gas mixture (i.e. a molar ratio of O/C, which is 1 for CO and 2 for CO₂), a so-called Baur-Glaessner diagram can be drawn. The other scale indicates the temperature and the resulting Baur-Glaessner diagram shows the stability of iron oxides in regions of certain temperatures and CO/CO₂ ratios. An example for the stability regions of iron oxides and metallic iron is shown in **Figure 12**. [59]

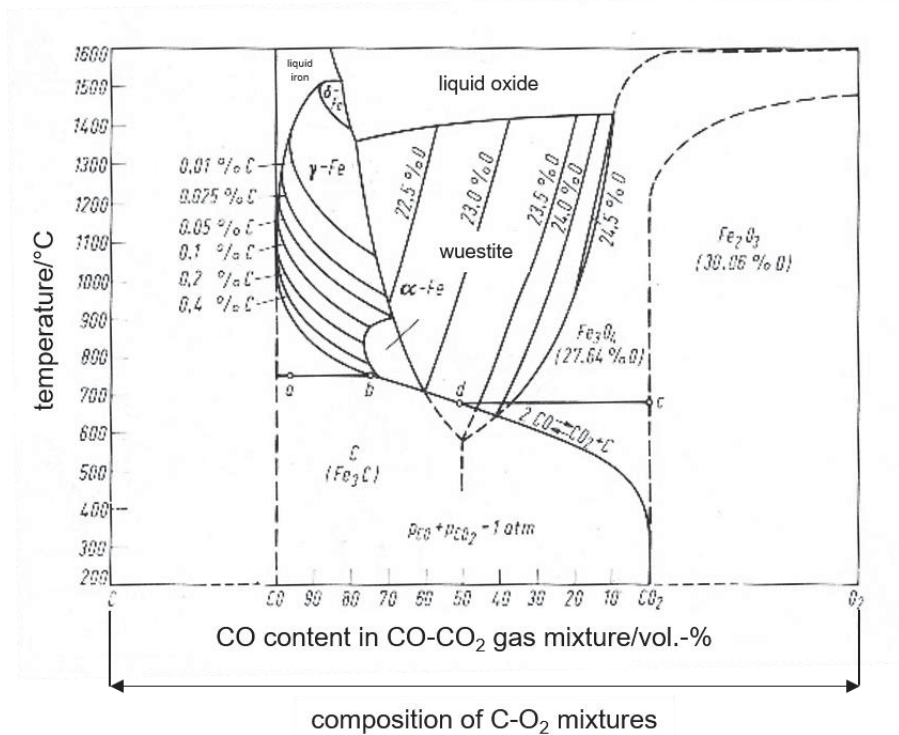
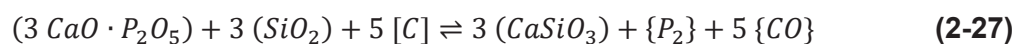


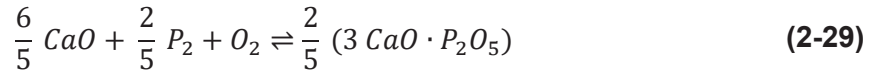
Figure 12: Baur-Glaessner diagram [59]

It is needed later to describe the ratio of indirect and direct FeO and C_3P reduction and the required carbon addition. It can be derived by plotting the O/C molar ratio against the O/Fe or, respectively, the O/P molar ratio at a certain temperature in a so-called Rist diagram (s. chapter 3.1). [60]

The calcium phosphate reduction is a reaction described in detail with regard to primary phosphorus production. Reaction pressure investigations have shown that SiO_2 participates in the reduction according to **Equation (2-27)**. The reduction with CO might play a role in the reduction process only if the phosphate is in its solid state. The dissociation of C_3P into CaO and P_4O_{10} has been refuted by these investigations. The accumulation of P in a metal phase is not relevant to the primary P production, because fluorine-apatite has low iron contents. [61] The direct reduction of P_4O_{10} – or P_2O_5 (**Equation (2-28)**) – is still important to BOFS reduction because of potential iron phosphate contents and their dissociation to P_2O_5 and FeO.



In order to describe the C₃P reduction using a Richardson-Ellingham diagram, the calcium phosphate line must be drawn. Since CaO is needed – according to the dephosphorisation mechanism described in 2.1.1.2 – to bind oxidised phosphorus, the reaction used to draw said line is the following **Equation (2-29)**. [36] The Richardson-Ellingham diagram drawn can be found in chapter 3.1.1.



The direct MnO reduction happens according to **Equation (2-30)**. [62]



High temperatures, high initial FeO contents as well as a low initial basicity support the MnO reduction. [62]

With increasing carbon, silicon or aluminium contents in the metal, the Cr activity is decreased drastically. It is increased, however, with rising temperatures. The activity of chromium oxide increases with increasing basicity. [63] The reduction of Cr₂O₃ in BOFS directly with carbon is shown in **Equation (2-31)**.



The reduction reactions for SiO₂ and TiO₂ are shown in **Equation (2-32)** and **Equation (2-34)**. SiO₂ can also be reduced to gaseous SiO (**Equation (2-33)**). [17]



As mentioned before, Matinde et.al. reported Fe-P alloy formation during the reduction of iron oxide containing sewage sludge. [45] In primary phosphorus production from fluorine-containing C_3P (apatite), the formation of Fe_2P is known. [64] In this thesis, the formation of iron phosphides is assumed to happen as soon as liquid iron and gaseous phosphorus get in contact. Whenever P is dissolved in iron – [P] – the following reaction or reaction sequence occurs (**Equation (2-35)**, **Equation (2-36)** and **Equation (2-37)**, s. also 3.1.2). [65]



Thermodynamic data on iron phosphide formation is provided by the work of Schlesinger 2002. [66] It is implemented in the databank of HSC Chemistry and used later to investigate the formation of relevant compounds.

2.1.5.2 Activity of Fe(O) and P_2O_5 in metal and slag phases and thoughts on kinetics

The equilibrium constant for the reduction of iron oxide directly with carbon is expressed as follows (**Equation (2-38)**).

$$K = \frac{p_{CO} \cdot a_{Fe}}{a_{FeO} \cdot a_C} \quad (2-38)$$

High C activity supports the reaction whereas a high iron activity moves the equilibrium to the side of the reagents. The activity coefficient is related to the activity as expressed in **Equation (2-39)** (adapted from [17, 58]).

$$a = \gamma \cdot x \quad (2-39)$$

The influence of other elements on the activity is expressed by influence parameters. The dependence of the activity coefficient on those parameters is expressed as shown in **Equation (2-40)** in metal baths that are considered to be iron with small amounts of other elements. (adapted from [17, 58])

$$\log \gamma_i = \log \gamma_i^{(H)} + \sum_j \varepsilon_i^j \cdot x_j \quad (2-40)$$

In **Equation (2-27)** the reduction of C_3P is shown. The equilibrium constant for this reaction can be seen in **Equation (2-41)**.

$$K = \frac{p_{CO}^5 \cdot p_{P_2} \cdot a_{CS}^3}{a_{SiO_2}^3 \cdot a_{C_3P} \cdot a_C^5} \quad (2-41)$$

The equilibrium composition is strongly influenced by the partial pressure of CO. Deviations from one in the activity of CS, C and SiO_2 also influence the equilibrium significantly. Sufficient carbon supply, SiO_2 addition to the slags and gas removal from the reactor positively influence the progress of the reduction reaction.

The equilibrium constant for the iron phosphide production can be found in **Equation (2-42)**.

$$K = \frac{a_{[Fe_xP_y]}}{a_{[Fe]} \cdot a_{[P]}} \quad (2-42)$$

High iron and phosphorus activities in the melt facilitate the phosphide formation. The influence of P and C on the P activity in liquid iron is expressed by their influence parameters in respective literature as $e_P^P=0.054$ and $e_P^C=0.126$. [47] Both elements increase the phosphorus activity.

The activity coefficient of P_2O_5 in the slag phase has been thoroughly investigated. Basu et.al. state the determination seen in **Equation (2-43)** based on mole fractions of other oxides. [67]

$$\log \gamma_{P_2O_5} = -6.775N_{CaO} - 4.995N_{FeO} + 2.816N_{MgO} - 1.377N_{SiO_2} + \frac{1007}{T} - 13.992 \quad (2-43)$$

The aluminium oxide influence is not considered. High temperatures and SiO₂ contents decrease log $\gamma_{P_2O_5}$ whereas a decreasing FeO content increases it.

In most research focusing on the reduction reactions between a metal and a slag phase, the transport mechanisms are defined as the rate-determining steps. The fast reaction kinetics in reduction metallurgy in the liquid state are well-reported. [62]

In the proposed reactor concept, the graphite is supposed to not participate in the reduction reactions. If it does, due to its density, a metal layer is formed on the graphite cubes instead of metal spheres as a product with carbon from the powder. The formation of such a layer during the reduction of iron ore is described in Biswas 1981. [17]

2.1.6 Chromium- and phosphorus-rich slags

Chromium recovery from slags is done mostly by applying hydrometallurgical techniques, which will not be discussed as a part of this thesis.

A process in which BOFS is reduced and the phosphorus-containing metal is refined a second time is already patented. The residual slag after the reduction step is supposed to serve as a lime donor in the sintering plant. [68] As described in a research approach by Nakase et.al., metal obtained by BOFS reduction is refined and oxidised and the P and Cr oxides are bound with CaO. The resulting slag is supposed to be P-rich and might serve as a secondary phosphorus ore. [46] After full reduction of BOFS, however, refining will ultimately lead to Cr (and Mn) enrichment in the newly produced slag in the form of their oxides.

The refining step necessary should aim at low Fe oxidation and almost complete Cr and P oxidation (and binding), which will also cause Mn to be oxidised. Examples for P-rich slags stem from the LD-AC process. In the course of the process, P-rich metal is refined. It is similar to the LD process, though the slag-forming additives are not added in the very beginning but over time together with oxygen via the blowing lance. The produced slag containing mostly CaO, FeO and P₂O₅, is not homogeneous. Removal of slag occurs at least once between the beginning of the refining process and the end. Slags with an FeO content of <10% and a P₂O₅ content of >20% can be produced. [69] The phosphorus-rich slag is suited as an existing

example for the slag composition proposed in chapter 3.3.2. The resulting slags can be described using a $\text{CaO-FeO}_x\text{-P}_2\text{O}_5$ phase diagram as depicted in **Figure 13**. [23]

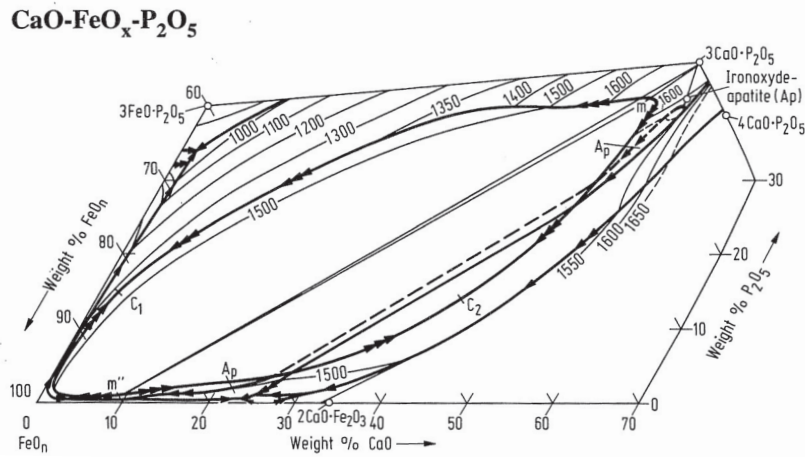


Figure 13: $\text{CaO-FeO}_x\text{-P}_2\text{O}_5$ phase diagram [23]

The reduction of high-Cr slags is also relevant to the field of stainless steel production. Preliminary experiments with slags from stainless steel production have been conducted but will not be further discussed in this thesis.

With regard to the objective of this thesis, the occurrence and formation of chromium phosphides is of importance. CrP , Cr_3P and Cr_{12}P_7 exist in commercially available databanks. [65] Broll et.al. in 1995 reported that they experimentally created $\text{Cr}_8\text{P}_6\text{C}$, a phosphide carbide. [70] However, thermodynamic data is not available for the temperature range of the desired treatment process. If the formation of the phosphides from $\text{Cr}(\text{l})$ and $\text{P}_2(\text{g})$ is calculated, only Cr_{12}P_7 seems to be built at temperatures above 1673.15 K. [65] Therefore, the stoichiometric ratio of $\text{Cr}:\text{P}_2$ would have to be 12 : 3.5, which is unlikely, considering the low amounts of chromium in BOFS and – even – in the Cr-rich slags produced for the experiments described in chapter 3.4.

In any case, the data basis for the prediction of chromium phosphide formation is not sufficient to judge the behaviour in a Cr- and Mn-rich alloy. Manganese phosphides are also reported to be formed, which is why it is difficult to make out the reasons for low gasification rates during reduction of slags containing Fe, Mn and Cr oxides without extensive experimental work. [66] Zaitsev et.al. (1998) provide the most extensive insight on Cr-P systems so far. While the formation of Cr_xP_y might occur spontaneously (free enthalpy <0), the driving force for the reaction decreases with increasing temperatures. [71] The free enthalpy for the formation of reported manganese phosphides is lower on average than that of the chromium phosphide formation reactions. [66]

2.2 Practical fundamentals – construction of a lab-scale plant

The InduRed process and the reactor concept it uses are highly promising regarding the tackling of problems related to BOFS reduction. However, the pilot-scale plant is cost- and personnel-intensive in its application. In order to determine a point of operation for the treatment of BOFS with an optimised B_2 and temperature, preliminary experiments at a smaller scale were required. Therefore, a lab-scale plant called InduMelt was planned and built.

The lab-scale plant is an induction furnace that consists of an oscillating circuit, a cooling circuit, a power supply unit, a royer converter and a microcontroller. It is schematically depicted in **Figure 14** and a realistic illustration can be seen in **Figure 15**.

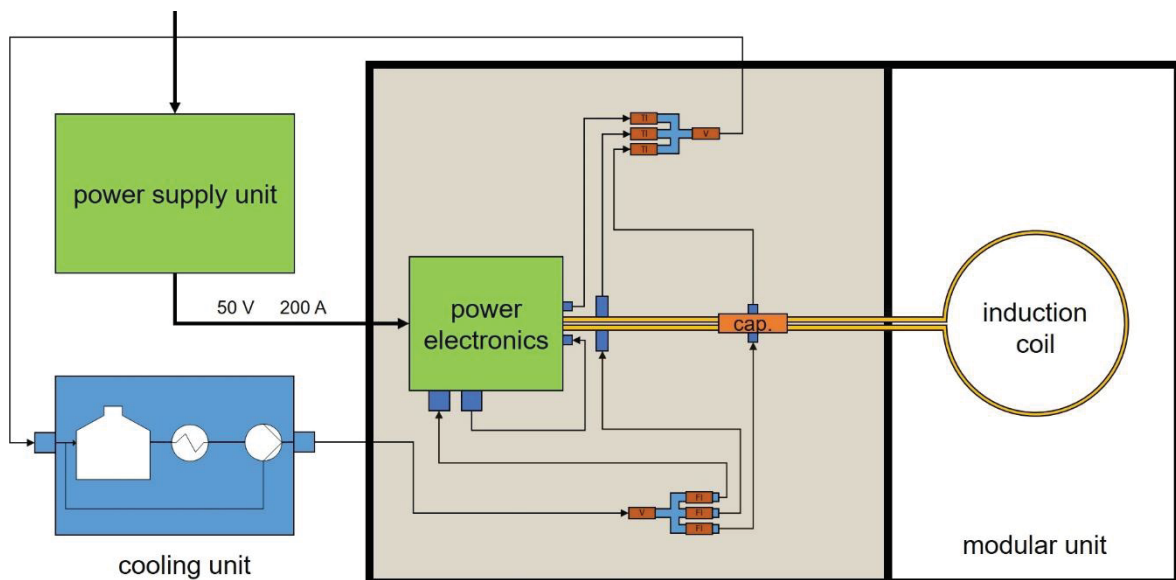


Figure 14: Schematic setup of the lab-scale plant InduMelt

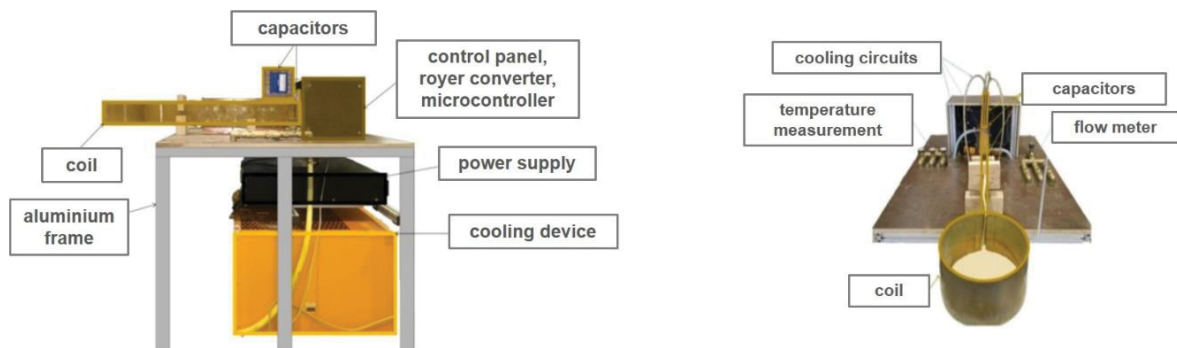


Figure 15: Realistic illustration of the InduMelt plant and its main components

Its operational frequency – roughly 50 kHz – and the associated oscillating circuit are designed to induce currents in individual particles instead of a homogeneous susceptor. The coil has a diameter of 20 cm and a height of 12 cm, and the circuit is supplied with a maximum power of 10 kW. At 50 kHz, the maximum power loss is in the range of 3.1 kW. For safety reasons, the capacitors, the power electronics as well as the induction coil each have their individual cooling circuit. Volume flow indicators are positioned on the intake side of the respective circuits and temperature measurement installations are integrated in the effluent side.

The construction of the lab-scale plant was completed in the course of this thesis. The plant design and construction was led by and completed in cooperation with Valentin Mally (Chair of Thermal Processing Technology). The design of the oscillating unit is based on the knowledge about the InduRed reactor mentioned in chapter 2.1.4. The royer converter and the micro-controller units were designed and constructed with the external help of Dipl.-Ing. Harald Noack. The setup of the reactor construction methods used were developed in the course of this thesis.

The plant is constructed to induce currents in graphite, and, by changing the position and form of the respective susceptor, can be used as a general smelting unit. Therefore, a graphite crucible is positioned below the induction coil. If contact between sample and graphite is not desired, a graphite ring can be positioned around a refractory material crucible with a small gap left between the two rings to allow for differences in thermal expansion during heating. For the reduction experiments using the inductively heated graphite bed, a crucible from refractory materials is filled with cubes of graphite. In the experiments conducted in the course of this thesis, Al_2O_3 rings, Al_2O_3 mortar and Al_2O_3 -rich concrete were used to construct a suitable crucible. In spite of possible reactions between basic slag and an argillaceous refractory material, Al_2O_3 provided higher heating rates, high maximum temperatures as well as good thermal shock resistance during tapping (when the insulation is removed in order to pull the slag stopper) and was therefore chosen. The setups for the smelting and reduction experiments are shown in **Figure 16**.

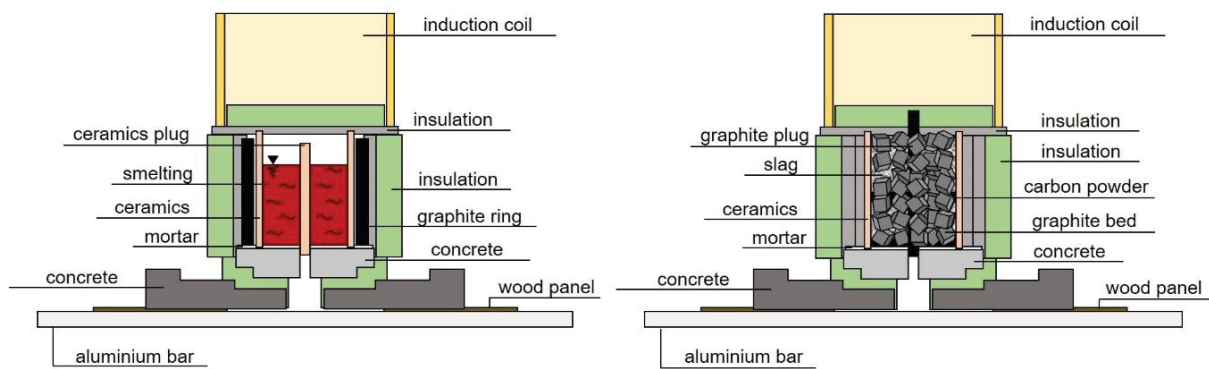


Figure 16: Experimental setups for smelting and reduction in the lab-scale InduMelt plant [49]

The electrodes used for the bed material have an average purity of 99% C. Their electrical resistance is 4-8 $\mu\Omega\text{m}$ and their density is 1.55-1.75 gcm^{-1} . [72] A number of amendments to the susceptor geometry and its influences on the power input have been investigated in the course of the work conducted in cooperation with Elias Obererlacher (Chair of Thermal Processing Technology). Remarkably, expected power input reduction by holes or cut-outs have not been observed as long as induced eddy-currents were provided a certain flow circumference. The reactor setup was developed by investigating the power input in cylindrical susceptor materials of different lengths as well as power input into graphite pieces. Exemplary results are shown in **Figure 17** and **Figure 18**.

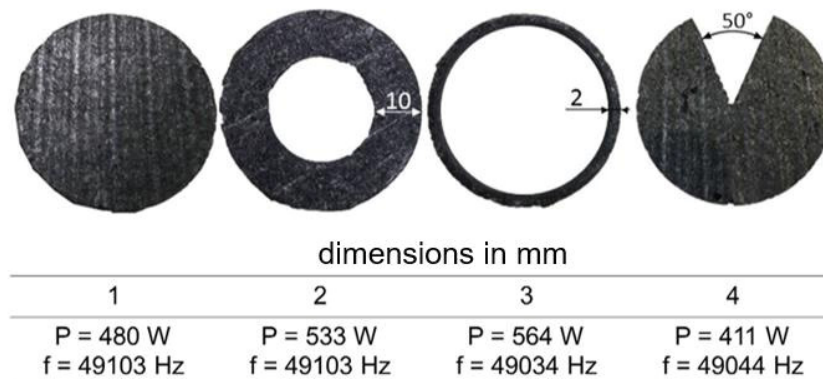


Figure 17: Power input in different susceptor geometries investigated in the InduMelt plant in cooperation with Elias Obererlacher (Chair of Thermal Processing Technology)

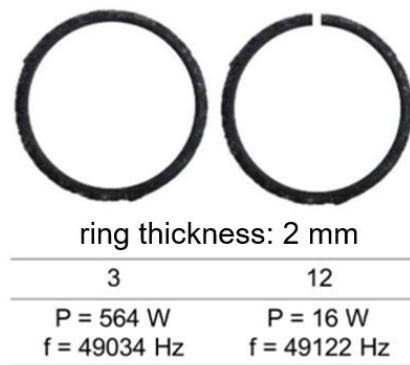


Figure 18: Power input in thin susceptor rings investigated in the InduMelt plant in cooperation with Elias Obererlacher (Chair of Thermal Processing Technology)

As long as the susceptor thickness is in the range of the penetration depth of the magnetic field, enlargement of the cut-out hole does not lead to a decrease in the power input but might even cause an increase due to field concentration.

These experiments as well as respective calculations have led to the positioning of the susceptors used for smelting and reduction in the course of this thesis.

3 Original scientific work

The results of extensive literature research and theoretical work on the reductive treatment of BOFS suggest that the applied reactor concept provides a number of advantages over standard units. In the course of the scientific work conducted for this thesis, the possibility of high percentage phosphorus gasification was demonstrated. Based on this newly gained insight, the process parameters were optimised in preliminary experiments and the behaviour of the slags during reduction was evaluated.

Subsequently, the focus shifted to the product quality of the liquid product streams of slag and metal. Work regarding the metal quality led to the investigation of an alternative process route that also applies the novel reactor concept to chromium- and phosphorus-rich slags.

3.1 Theoretical work

In order to understand the advantage of the proposed reactor concept for the treatment of BOFS and the possibilities coming from its application, two important aspects are investigated in greater detail: The required reduction temperature in order to fully reduce the BOFS as well as the carbon requirement of the iron oxide reduction. Reaction schematics are drawn to illustrate the thermodynamic processes in combination with simplified kinetic deliberations.

3.1.1 Temperature requirements and carbon consumption

The free enthalpy of the reactions of one mole of oxygen with metal to their oxides is illustrated in the Richardson-Ellingham diagram (s. chapter 2.1.5.1). Phosphorus is also

included in most versions of the diagram. However, phosphorus does not exist in the form of P_2O_5 in BOFS. Mostly it consists of calcium phosphate as $3 CaO \cdot P_2O_5$, which cannot be found in a standard Richardson-Ellingham diagram. The formation of C_3P out of CaO , P_2 and one mole of O_2 is described in chapter 2.1.5.2.

It is assumed that the partial pressure of P_2 (g) as well as the activities of C_3P (l) and CaO (l) are one or close to one and that the slag components are liquid (since they are in the relevant temperature interval).

Using thermodynamic data from HSC Chemistry 7 [65], the Richardson-Ellingham diagram curve for C_3P can be drawn. The same is done for the oxidation of iron, carbon (C (s)) and CO (g), assuming that the activities of iron, iron oxide and carbon as well as the CO partial pressure (product of C oxidation) and the ratio of the CO and CO_2 partial pressures (reagent and product of CO oxidation) are one or close to one.

The Richardson-Ellingham diagram drawn is depicted in **Figure 19**. [65]

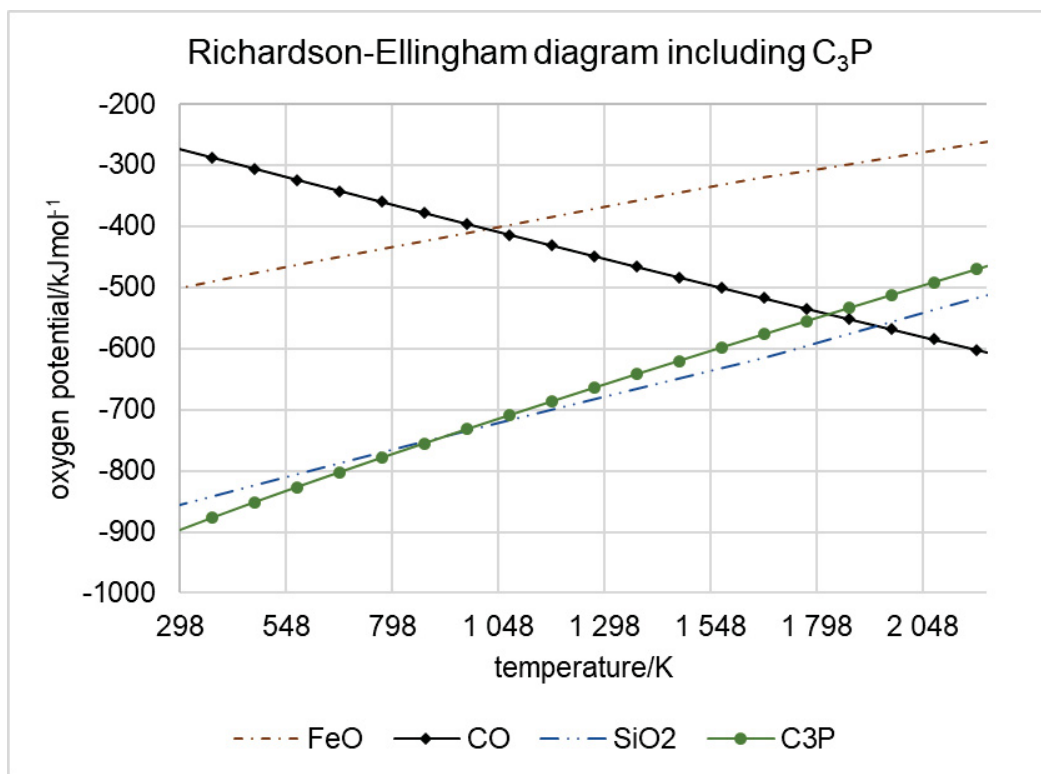


Figure 19: Richardson-Ellingham diagram drawn with data retrieved from HSC [65]

It can be seen that high temperatures are needed to reduce C_3P with carbon. The reaction is thermodynamically possible under standard pressure, with pure substances at a temperature of roughly $1550^\circ C$ or higher. The partial pressure of CO, however, is much higher in the proposed reactor concept.

In reality, the activities of Fe (l), CaO (l) and the partial pressure of P_2 (g) will be lower than one. If a_{Fe} decreases, the slope of the curve for the iron oxidation in the Richardson-Ellingham diagram becomes steeper (s. 2.1.5). It cuts the C oxidation slope at lower temperatures. The same effect is assumed for C_3P .

In conclusion, even if lots of simplifications are assumed, temperatures over 1500°C are necessary to reduce C_3P at considerable rates. Equidistant temperatures 150 K below and above this temperature were chosen for the reduction experiments in order to empirically investigate the reduction behaviour of modified BOFS as well as the slag flowability.

The stability of the phases P_2 and C_3P as well as Fe and FeO can be illustrated in a Baur-Glaessner diagram (s. 2.1.5.1). It is depicted in **Figure 12** for temperatures up to 1600°C .

In order to estimate the minimum amount of carbon required to reduce iron oxide, a Rist diagram is used. For a temperature of 1650°C (chosen experimental temperature for reduction as described in 3.2.3), it is depicted in **Figure 20** based on the Baur-Glaessner diagram shown before (adapted from [17, 60]).

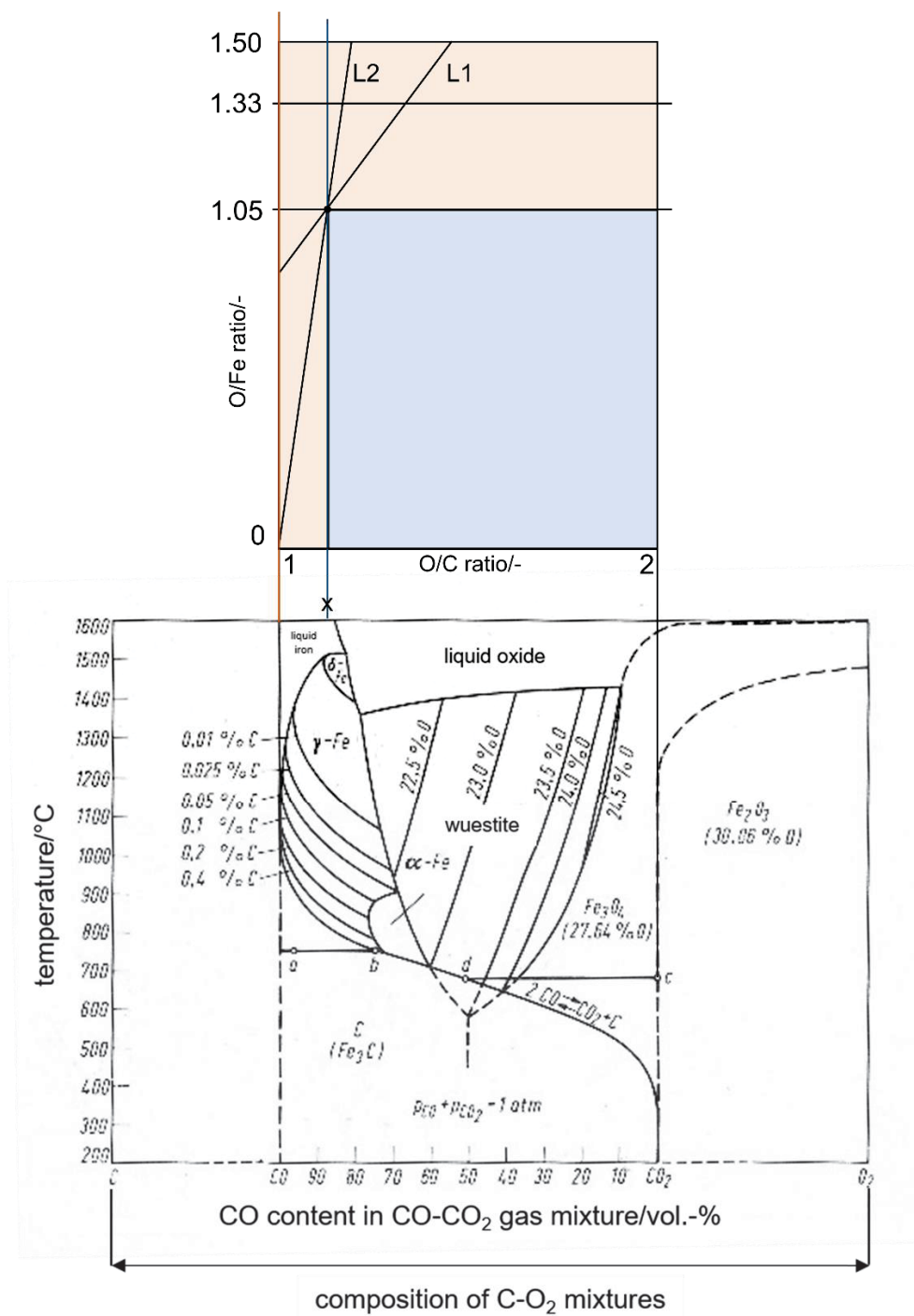


Figure 20: Rist diagram for C₃P and FeO reduction and its relation to the Baur-Glaessner diagram (adapted from [17, 60])

The line for the P₂/C₃P equilibrium can be seen on the very left and is almost perfectly vertical (red line aligning with the vertical line for x_{CO}=100%). Indirect reduction plays hardly any role in the reduction of C₃P at 1650°C (and even much lower temperatures) [65] and the carbon consumption can be estimated stoichiometrically. Therefore, the stability areas of C₃P and P₂ are not shown in the Baur-Glaessner diagram.

The axes of the Rist diagram are the molar ratios O/C and O/Fe (or O/P respectively, which is not considered because of the almost perfectly vertical slope). For iron, 1.05, 1.33 and 1.50 represent the species FeO_n , Fe_3O_4 and Fe_2O_3 . The incline of the black lines in the diagram represent the carbon demand (C/Fe). The lowest carbon demand can be achieved if the C/Fe curve is the diagram's diagonal. However, a curve reaching into or through the blue area is not possible since gas compositions that are thermodynamically impossible would be required. If the diagonal is moved as a parallel through the upper left corner of the blue area (called the wuestite point), the minimum carbon amount is used ($C/Fe=1.5$, L1), but only roughly 15-20% of the FeO could be reduced indirectly. [17, 60]

If complete indirect reduction with CO is desired, the curve must start in the lower left corner of the diagram ($0/0$) and reach through the wuestite point (L2). The carbon demand would be immense (approximately $C/Fe=8.3$).

Assuming a minimum amount of carbon, direct reduction accounts for roughly 80-85% of the FeO reduction and makes the process more energy intensive (the higher the percentage of indirect reduction, the more CO is produced according to the highly endothermic Boudouard reaction [17]). **Figure 21** shows an extended Rist diagram for the proposed application based on assumptions for false air compensation and the reduction of other oxides and phosphates schematically (adapted from [17, 60]).

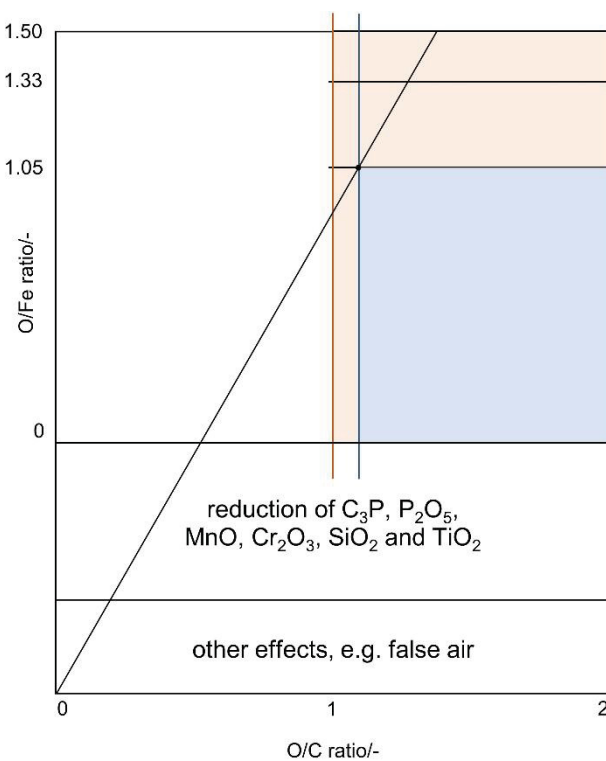


Figure 21: Extended Rist diagram for the reduction of basic oxygen furnace slags
(adapted from [17, 60])

The carbon addition has to compensate the amount of indirect reduction according to the Rist diagram. Direct reduction accounts for the remaining iron oxide, manganese oxide, chromium oxide, phosphorus oxide, calcium phosphate, titanium oxide and silicon oxide reductions. The respective reaction equations can be found in chapter 2.1.5. Based on the mixture composition (calculated) used for the preliminary reduction experiments (presented in chapter 3.2), the required carbon addition can be calculated stoichiometrically assuming direct reduction. Thermodynamic data suggests that the direct reduction reactions play a major role and high amounts of excess carbon are added in order to compensate false air influences, CO production and to protect the graphite bed.

3.1.2 Reaction schematics

Thermodynamically, the reactions for indirect and direct reduction are powered by high driving forces (high negative free enthalpy values). The reduction feasibility has been demonstrated in reduction experiments in other units as well as in the blast furnace in the ironmaking process.

Kinetically, the availability of carbon is crucial. Carbon powder is evenly spread within the slag feed by mixing of the input material and additional carbon is provided by the graphite from the reactor bed. The graphite is not supposed to participate in the reactions since it is used to provide the reaction surface as well as the possibility of direct heat input. The experiments conducted and presented in the following chapters showed that the carbon cubes are hardly participating in the reduction reactions. The cut surface of the cubes is a good indicator for this assumption.

If carbon is not available and the cubes interact with the slag, a layer of metal is formed on the graphite cubes in some places. This phenomenon was sometimes observed and can be seen in **Figure 22**.



Figure 22: Metal layer formed on graphite cubes during the reduction of basic oxygen furnace slags in the InduMelt plant

The transport limitation of both carbon as a reagent as well as phosphorus as a product is reduced to a minimum by applying the reactor concept as presented in this thesis. A thin molten slag film provides short mass transport distances for gaseous reaction products. This time is critical due to the reaction between liquid iron and gaseous phosphorus. The immediate melting of the input materials favours direct reduction as the predominant reduction mechanism (s. also Rist diagram). The gas suction as well as the missing, long-lasting metal-slag interface are the main differences to a blast furnace and enable the removal of gaseous phosphorus. The reactions and kinetic conditions are depicted in **Figure 23**.

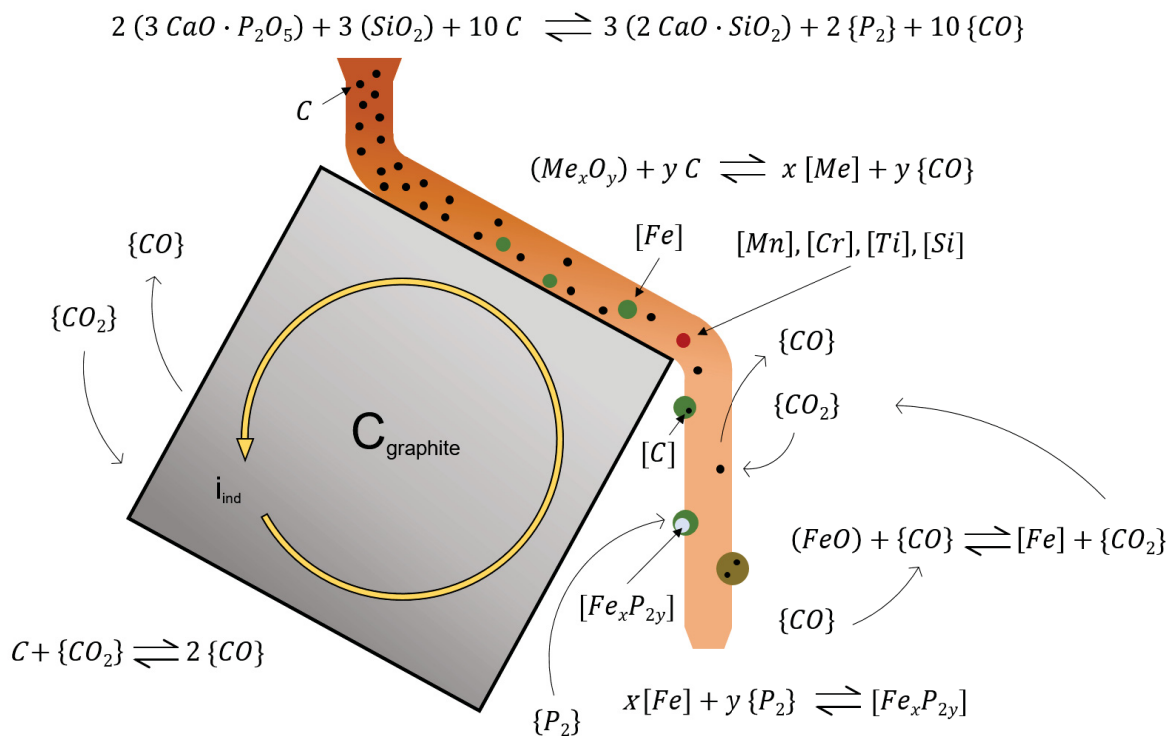


Figure 23: Schematics of reduction reactions and phosphide formation during the treatment of basic oxygen furnace slags in the InduRed reactor

Iron oxide is immediately reduced, the slag is instantly molten and the carbon uptake of the metal phase lowers its melting point to 1320°C upon saturation. [7] If collected as a molten bath after complete reduction, the metal phase forms a layer beneath molten slag and the two phases can be separated due to the difference in density.

In order to support the schematics drawn above, thermodynamic data is used to calculate theoretical equilibrium compositions. The most important reduction reactions are shortly described in the following paragraphs. The following points are derived from data and application of HSC Chemistry 7. [65]

- FeO reduction: The free enthalpy of the direct reduction at 1923.15 K is roughly $-133.4 \text{ kJmol}^{-1}$, for the indirect reduction it is $+30.3 \text{ kJmol}^{-1}$. The amount of indirect reduction can be derived from the Rist diagram shown before.
- SiO_2 and TiO_2 reduction: Thermodynamically, the reduction of SiO_2 to Si (l) or SiO (g) does not occur spontaneously at 1923.15 K. However, Si can be found in the metal phase and the basicity is slightly altered due to Si loss during the process because of the reduced iron activity and the amount of carbon present in the reactor. Also, temperature peaks might occur within the reactor. The same is true for TiO_2 .
- MnO, Cr_2O_3 and P_2O_5 reduction: These elements are spontaneously reduced directly with carbon. Elementary Mn and Cr can be dissolved in Fe. P in its elementary form at 1923.15 K exists as $\text{P}_2 \text{ (g)}$ and can be dissolved in iron and react to Fe_xP_y or is removed as a gas as desired.
- iron phosphate reduction: Iron phosphates might occur in the BOFS as $\text{Fe}_3(\text{PO}_4)_2$ or $3 \text{ FeO} \cdot \text{P}_2\text{O}_5$, short F_3P . At very low temperatures of roughly 673 K it dissociates into FeO and P_2O_5 . Both species are directly reduced with carbon.

The most important reduction reaction is the calcium phosphate reduction. As reported in respective literature, C_3P is reduced in the presence of SiO_2 , forming a silicate (C_xS) rather than it being directly reduced with carbon. The equilibrium compositions of the slag and gas phases during the reduction of C_3P with carbon as a function of the temperature are shown in **Figure 24** and **Figure 25**. [65]

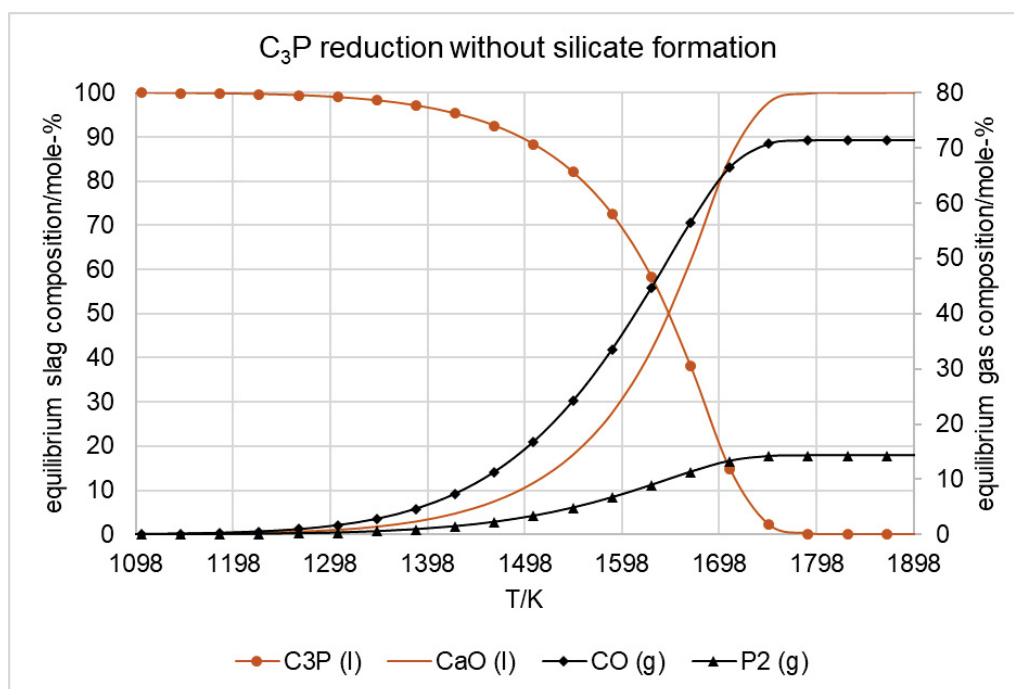


Figure 24: Equilibrium composition during the direct reduction of C_3P [65]

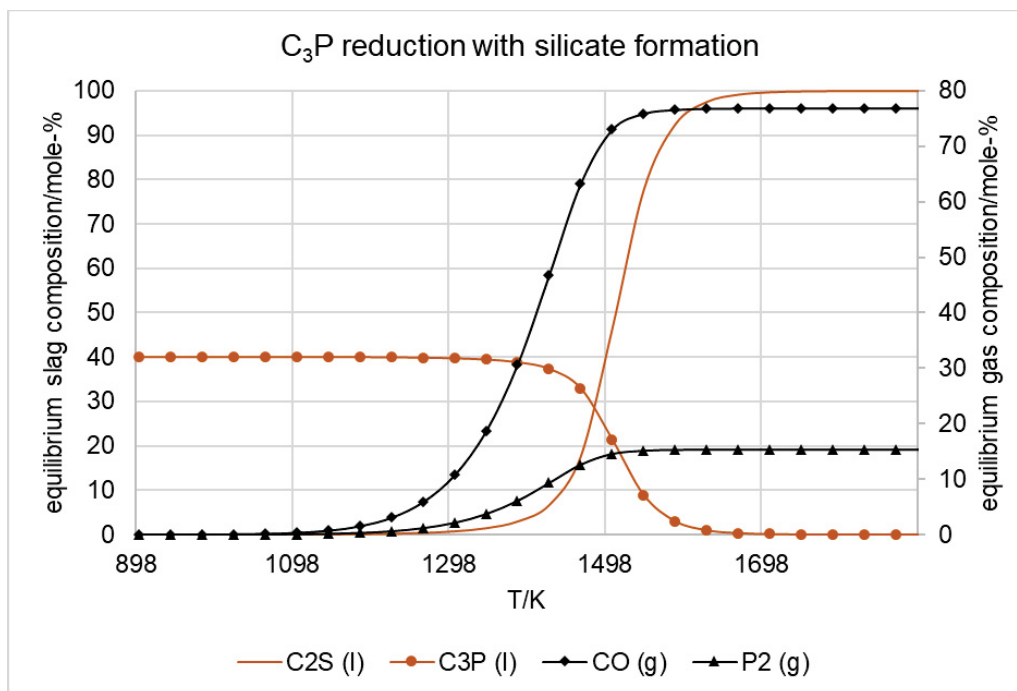


Figure 25: Equilibrium composition during the direct reduction of C_3P with simultaneous silicate formation [65]

At 1760 K (without silicate formation) and 1698 K (with silicate formation), respectively, the equilibrium amount of C_3P in the slag phase is 0. However, the second reaction process is dominant. The free enthalpy of the reduction of C_3P with silicate formation at 1923.15 K is $-414.8 \text{ kJmol}^{-1}$, whereas the value for the direct reduction without silicate formation is $-180.5 \text{ kJmol}^{-1}$. [65] Carbon (s), SiO_2 (l) and Ar (g) are not shown in the diagram for reasons of clarity and account for the missing amounts. Ar (g) is not used in the preliminary batch experiments described in this thesis (only small amounts to ensure the gas flow direction towards the reactor core in the continuous experiments), but is required for the calculation of the equilibrium compositions in HSC.

Higher temperatures are still desired because of slag flowability and the formation of iron phosphides. Depending on the local stoichiometric availability of liquid iron and gaseous phosphorus, the reactions described in chapter 2.1.5.1 occur. The driving force for the formation of Fe_3P is the highest, closely followed by Fe_2P . FeP and FeP_2 are hardly produced. [65] The production rate of all phosphides is reduced when the temperature is increased. The equilibrium compositions of the metal phase and gas phase for the respective reactions are shown in **Figure 26**.

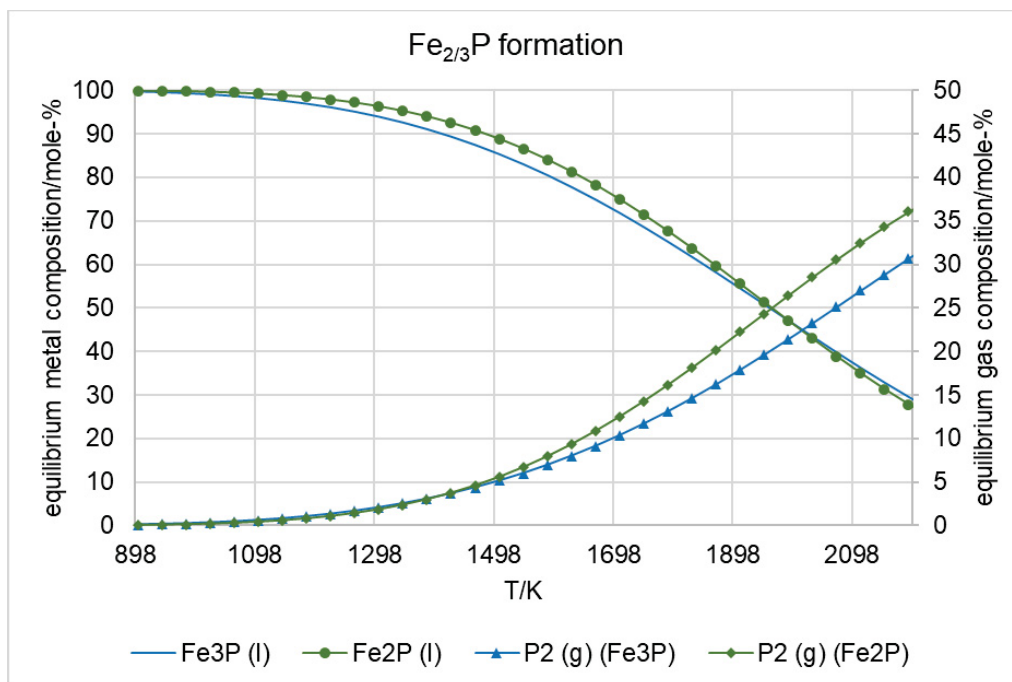


Figure 26: Fe_{2/3}P formation as a function of the temperature [65]

Fe (l) in the metal phase as well as Ar (g) (used for the calculation in HSC) account for the missing amounts in the diagram.

If only Fe₃P was formed during the reduction of one of the mixtures for the preliminary experiments (s. chapter 3.2.3, mixture 3), containing 21.7 m.-% Fe and 0.95 m.-% P, and the whole phosphorus was found within the metal phase, its maximum mass fraction could be as high as 2.4%.

3.2 Preliminary experiments

The phosphorus gasification – as the state of knowledge suggests – requires a certain amount of SiO₂ in the slag in order to increase the phosphorus activity. Silica dioxide also improves the flowability of the slag, which is necessary to reduce the hold-up and retention time of slag in the reactor. A certain amount of silica dioxide is expectedly reduced during the treatment. Combined with the effect of an increasing viscosity due to the reduction of iron oxides, the SiO₂ addition must be substantial. Some potential building material applications for the product slag, however, might require a higher basicity and therefore less silica addition. Furthermore, silica does not have to stem from quartz sand (QS) but might also be provided by siliceous slags like BFS.

The pressure in the reactor is set slightly below the atmospheric pressure in order to remove CO and P₂ gases from the reactor constantly. The reaction pressure, hence, has not been one of the parameters varied in the course of the conducted experiments.

In contrast, the reaction temperature, naturally, is the most influential parameter to be varied. High temperatures support endothermic reduction reactions, improve flowability and inhibit the iron phosphide formation. However, high temperatures in the upper part of the reactor might cause slag foaming. In general, high temperatures increase the reduction of silica dioxide, heat loss and the stress put on refractory materials.

Figure 27 visualises the fields of conflict between the main parameters of basicity alteration and reaction temperature by stating the advantages of each factor of influence.

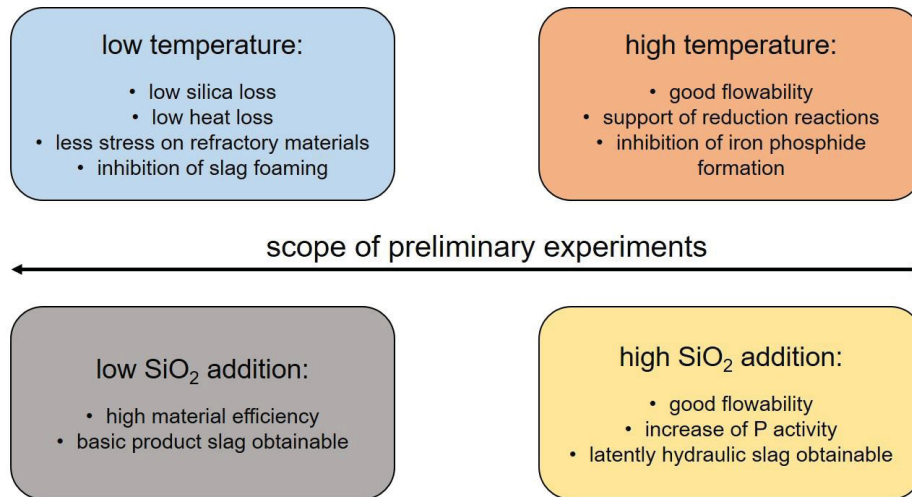


Figure 27: Fields of conflict between basic oxygen furnace slag processing parameters

3.2.1 Objectives

The main objective of the preliminary experiments is to alter the parameters explained above and to evaluate the reduction degrees of key elements as well as the distribution of phosphorus between the metal, slag and gas phases. Additionally, the processability of the BOFS after each alteration, especially regarding the flowability, shall be assessed.

3.2.2 Methodology

The smelting and reduction temperatures were chosen by evaluating theoretical melting points and by determining minimum temperatures required for the reduction of individual oxides (iron, chromium and phosphorus oxides) according to phase diagrams and the Richardson-Ellingham diagram. Temperature measurement was a highly demanding task due

to high process temperatures, current induction in metallic conductors and the high temperature difference between the sample and the graphite bed in the beginning of each heating phase. In order to measure as precisely as possible, three thermocouples (TC) of type K were positioned in different heights of the graphite bed and bent to make sure they touched at least one cube each. On the outside of the ceramics ring, a TC of type S was positioned at medium height. With the help of the TC, a temperature difference between the inside and the outside of the reactor could be measured up to 1473 K (melting point of type K TC). A good correlation was seen and used to describe the inner temperature up to the reduction temperature based on the outer temperature. Additionally, a thermal imaging camera was pointed at the graphite slag stopper. By shortly lifting the upper insulation layer, the slag stopper temperature was determined without contact.

The setup during operation, including temperature measurement equipment, can be seen in **Figure 28**.



Figure 28: InduMelt plant and temperature measurement equipment in operation (1: optical temperature measurement, 2: induction coil with reactor, 3: thermocouples, 4: cooling water distribution, 5: laptop)

Two basicity values, 2.5 and 1.5, were chosen as possible points of operation, aiming for either minimal SiO_2 addition (2.5) or high P activity and good flowability (1.5).

The carbon demand for the reduction was calculated according to the stoichiometric coefficients of the direct reduction reactions, adding excess carbon powder (+20%) to limit the influence of potential false air and CO production (Boudouard reaction). The carbon powder stems from pellets that were ground in a hammer mill. Added carbon powder with a high specific surface area serves as a reducing agent, as a producer of reduction gas (CO) as well

as a preventive measure to avoid the participation of the graphite bed in the reduction reactions. The graphite bed shall provide a long-lasting structure for a liquid film to form as well as a means of heat input.

The reaction atmosphere was not altered due to the internal production of CO and the batch operation applied in the lab-scale plant (no counter-flow of any iron source). Therefore, gas suction above the reactor setup is only needed for health and environmental reasons and not for operational reasons.

Al₂O₃ refractory materials allow for a certain heating rate that shall not be exceeded. A rate between 200 Kh⁻¹ and 250 Kh⁻¹ was chosen. The reaction temperature was held constant for an hour in each experiment before tapping. This is true for both smelting and reduction experiments.

Lastly, sampling is an important step in the experiment evaluation process. Due to the high surface tension of liquid iron and the relatively small sample amount, iron spheres are found within the tapped slag. Only some larger agglomerations of metal can be detected. Therefore, the slag is crushed manually and the metal phase is mechanically separated from the slag phase. Some slag particles show a metal coating, which is also separated from the slag. All attained metal and slag particles are mixed and a representative sample is gathered. The selected particles for analysis are then sorted by size and weighed to make sure the slag particles with coating are not mistaken for metal particles or significant amounts of metal occur inside a slag particle. In addition, Ca is analysed in the metal phase, which, if found, can – for the most part – only stem from slag within the metal particle and therefore can be considered during the evaluation process. The analysis methods used were mass spectroscopy for the individual element contents in both phases (ICP-MS) as well as X-ray diffractometry (XRD) and scanning electron microscopy (SEM) for the mineral phase analyses.

3.2.3 Experiment execution

The following **Figure 29** illustrates the experiments conducted. It shows the additives used for basicity alteration, the set basicity as well as the reduction temperatures of the initial experimental campaign. The experiments described in this chapter were conducted in cooperation with Stefan Windisch (Chair of Thermal Processing Technology). Preliminary results and parts of the research presented in this chapter have been previously published. [49]

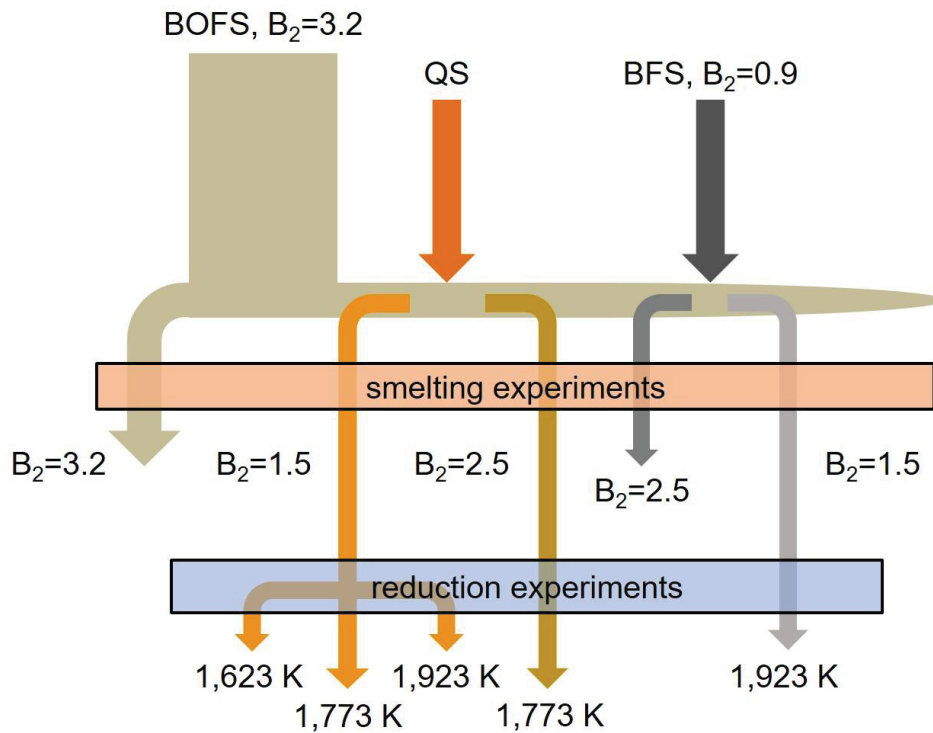


Figure 29: Overview of conducted experiments during the first experimental campaign [49]

3.2.3.1 Smelting experiments

The setup and the respective temperature measurement equipment used are described in 3.2.2. In order to alter the basicity, QS, BFS and BOFS are mixed according to their composition. The BFS and BOFS both stem from the production of steel at voestalpine Stahl Linz GmbH. The sand is commercially available quartz sand. **Table 2** shows the input material compositions. In **Table 3** the mixtures that were produced (a total of 2.5 kg each) are presented. [5]

Table 2: Compositions of blast furnace slag, basic oxygen furnace slag and quartz sand used for preliminary experiments in the InduMelt plant [5]

sample	Fe [m.-%]	SiO ₂ [m.-%]	Cr ₂ O ₃ [m.-%]	MnO [m.-%]
BFS	0.50	37.88	-	1.47
BOFS	19.44	12.40	0.40	4.40
QS	0.18	93.21	-	-
sample	CaO [m.-%]	MgO [m.-%]	Al ₂ O ₃ [m.-%]	P ₂ O ₅ [m.-%]
BFS	34.76	10.51	10.78	0.01
BOFS	40.00	7.10	1.50	1.10
QS	0.10	-	3.61	-

Table 3: Compositions of mixtures produced for preliminary experiments in the InduMelt plant

mixture no.	B ₂ [-]	BOFS [g]	BFS [g]	QS [g]
1	1.5	1,269	1,231	-
2	2.5	2,174	326	-
3	1.5	2,167	-	333
4	2.5	2,407	-	93

All of the input materials were pre-processed and had a grain size between 0.25 mm and 1.50 mm. The heating phase with a heating rate between 200 Kh⁻¹ and 250 Kh⁻¹ lasted roughly 8.5 h. The molten bath was held at 1823 K for approximately 0.5 h. The slag stopper – made from zirconia materials – was pulled and the homogeneous melt was cooled in air. The atmosphere was not altered. Ambient air could get in contact with the surface of the molten mass.

For pure BOFS as well as for mixture 2, tapping was impossible. The tapping hole was 8 mm in diameter for all of the experiments and led through the mortar as well as the concrete bottom. Only the mixtures tapped were used in the reduction experiments.

3.2.3.2 Reduction experiments

The tapped slags from the smelting experiments were crushed in a jaw crusher to an average grain size of roughly 3 mm after cooling. 500 g of each mixture were reduced together with carbon powder. The stoichiometric demand and the 20% excess carbon to counter false air influences were rounded up to 10% based on the mixture mass (50 g). The reactor was filled in layers, with carbon powder on the bottom, in the middle and on the top. The sample was filled between the middle and top third of the ceramics ring, so that a bit of movement is possible after melting even during batch operation.

For the reduction experiments the atmosphere was not altered either. Direct reduction as well as combustion of carbon powder produce CO and CO₂. CO₂, in turn, is converted into CO as long as solid carbon is present. Therefore, a CO atmosphere is maintained internally at all times.

The heating rate was between 200 Kh⁻¹ to 250 Kh⁻¹ up to the desired reduction temperature. At reduction temperature, it was held for approximately an hour before the graphite slag stopper was pulled. The tapped slag was cooled in ambient air. Tapping through a hole of 8 mm in diameter was possible for mixture number 3 at medium and high reduction

temperatures as well as for mixture number 1 at high reduction temperature. For these three experiments – abbreviated as 1h, 3m and 3h – the reduction degrees (s. chapter 3.2.4 for the definition used) as well as the phosphorus balances were evaluated. The InduMelt plant during operation as well as graphite cubes in the reactor shortly after tapping can be seen in **Figure 30**.



Figure 30: InduMelt plant during operation and heated graphite cubes shortly after tapping

Figure 31 illustrates the sequence of smelting and reduction experiments and shows intermediate as well as final products (from experiment 3h).

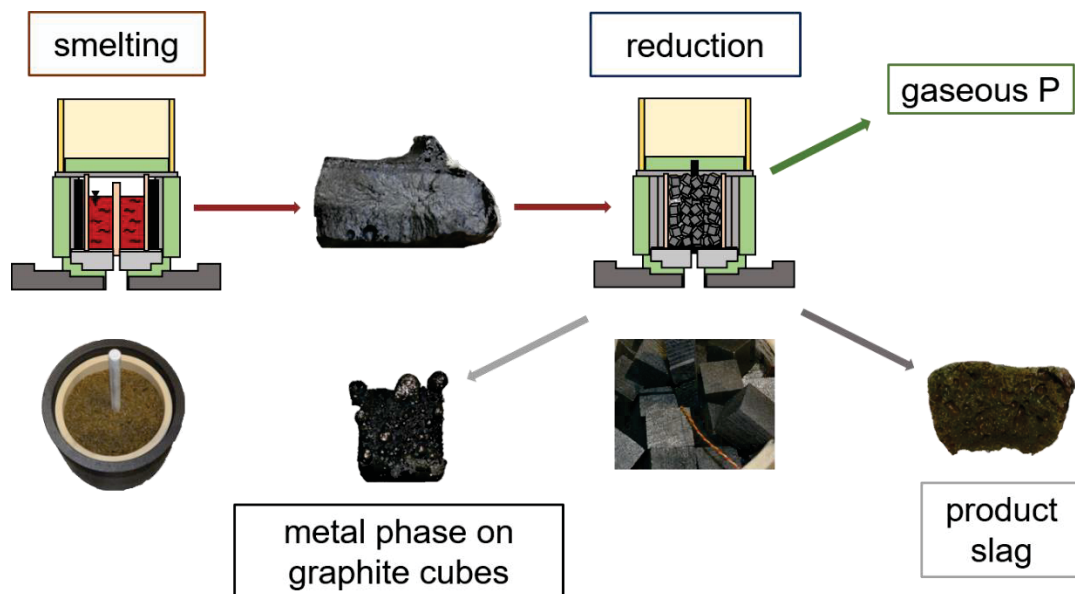


Figure 31: Experimental sequence for smelting and reduction in the InduMelt plant and images from preliminary experiments

3.2.4 Results

The smelting experiments were successful in providing the possibility to produce homogeneous slag mixtures for the reduction experiments. The four mixtures were produced

and analysed by ICP-MS as well as SEM and XRD, which showed a good correlation and supported the statement regarding homogeneity. If residual slag remained in the crucible, remaining slag was analysed as well. No significant deviation was found.

The calculated mixture composition and the analysed composition show a good correlation as well. The calculated compositions of mixtures 1-4 are shown in **Table 4**.

Table 4: Calculated mixture compositions for smelting experiments in the InduMelt plant

species/basicity	content in mixture 1 [m.-%]	content in mixture 2 [m.-%]	content in mixture 3 [m.-%]	content in mixture 4 [m.-%]
Fe as FeO	13.00	21.82	21.70	24.08
SiO ₂	24.94	15.72	23.16	15.41
Cr ₂ O ₃	0.20	0.35	0.35	0.39
MnO	2.96	4.02	3.81	4.24
CaO	37.42	39.32	34.69	38.52
MgO	8.78	7.54	6.15	6.84
Al ₂ O ₃	6.07	2.71	1.78	1.58
P ₂ O ₅	0.56	0.96	0.95	1.06
rest	6.07	7.56	7.41	7.88
total	100.00	100.00	100.00	100.00
B ₂	1.50	2.50	1.50	2.50

For the reduction experiments, the expected amounts of Fe, P, Cr and Mn in the obtained metal phase were calculated and metal and slag phase were analysed as described in chapter 3.2.2. ICP-MS analysis results and calculated values show a good correlation. For one experiment – 3h – the product phases were also weighed and the results match well with the analytical investigations. The correlation regarding the metal phase is shown in **Table 5**.

Table 5: Comparison of calculated, analysed and weighed amount of metal phase obtained in experiment 3h conducted in the InduMelt plant

phase/species	mass determined by ICP-MS [g]	mass determined by weighing [g]	calculated mass [g]
metal without P	89.88	-	92.97
P in metal	0.34	-	-
total	90.22	92.50	-

Weighing in general is hardly possible due to the distribution of small metal spheres. Metal layers on slag particles, small particles < 0.1 mm as well as bigger agglomerations > 2.0 mm

were found. Therefore, a gravimetric analysis was only made once to support analysis results and the evaluation method used. **Figure 32** illustrates the mentioned complexity.



Figure 32: Complexity of metal and slag samples after reduction of basic oxygen furnace slags in the InduRed reactor (left: metal spheres on graphite cubes, right: metal on cubes and green, partially reduced product slag)

The calculated value is based on the ICP-MS elementary analysis. Since a gravimetric analysis of product slag and metal is hardly possible, the analysed input P and Fe amounts as well as the Fe, P, Mn and Cr amounts in the product phases are used to iteratively determine the phase masses. A slag mass is assumed and the Fe amount in this slag is calculated. The remaining iron must then exist in elementary form and the iron content of the metal phase is known. Adding the amount of oxygen that is eliminated as well as a small, assumptive amount of Si (as SiO, included in volatiles/rest) and the eliminated P, the total mass must equal the input mass. The initial slag amount is then altered until this condition is fulfilled. The resulting product stream amounts are shown in **Table 6**.

Table 6: Product stream masses out of experiments 1h, 3h and 3m conducted in the InduMelt plant

product stream	stream out of 1h [g]	stream out of 3h [g]	stream out of 3m [g]
slag	400.19	359.70	365.63
metal	65.41	90.22	84.29
O	18.02	29.49	29.49
P	1.23	2.08	2.08
volatiles/rest	15.15	18.51	18.51
total	500.00	500.00	500.00

The reduction degree (RD) is defined as the ratio of the amount of the elementary form of each element to the sum of the elementary and oxidic forms. The elementary and oxidic amounts are calculated using the ICP-MS analysis results and the calculated slag and metal

product phases. Minute amounts of Cr stemming from type K TC and insulation materials are not mathematically evaluated because of the full reduction indicated by the low Cr amounts in the product slag.

The ICP-MS analysis results for the metal and slag phases are shown in **Table 7** and **Table 8**.

Table 7: ICP-MS analysis results for the metal phases from the basic oxygen furnace slag reduction experiments conducted in the InduMelt plant

species in metal	content after experiment 1h [m.-%]	content after experiment 3h [m.-%]	content after experiment 3m [m.-%]
Fe	75.40	93.10	92.40
P	0.61	0.38	0.37
Cr	1.02	0.77	0.63
Mn	1.23	4.49	1.32
Ca	0.12	0.15	0.33
S	-	0.03	-

Table 8: ICP-MS analysis results for the slag phases from the basic oxygen furnace slag reduction experiments conducted in the InduMelt plant

species in slag	content after experiment 1h [m.-%]	content after experiment 3h [m.-%]	content after experiment 3m [m.-%]
Fe	0.31	0.11	1.78
P	0.01	0.00	0.04
Cr	0.05	0.01	0.08
Mn	1.97	2.02	3.25
Ca	23.50	24.70	23.10
S	-	0.71	-

The sulphur amount was analysed because of the results of the XRD. Mn was found as MnS (as well as in some oxidic phases). Residual sulphur caused a falsification of the RD for manganese. MnO was reduced, but Mn is still found in the slag matrix during analysis. This has to be considered when reading the RD for Mn in **Figure 33** since the evaluation method does not consider the phenomenon observed with Mn. The values are also shown in **Table 9**.

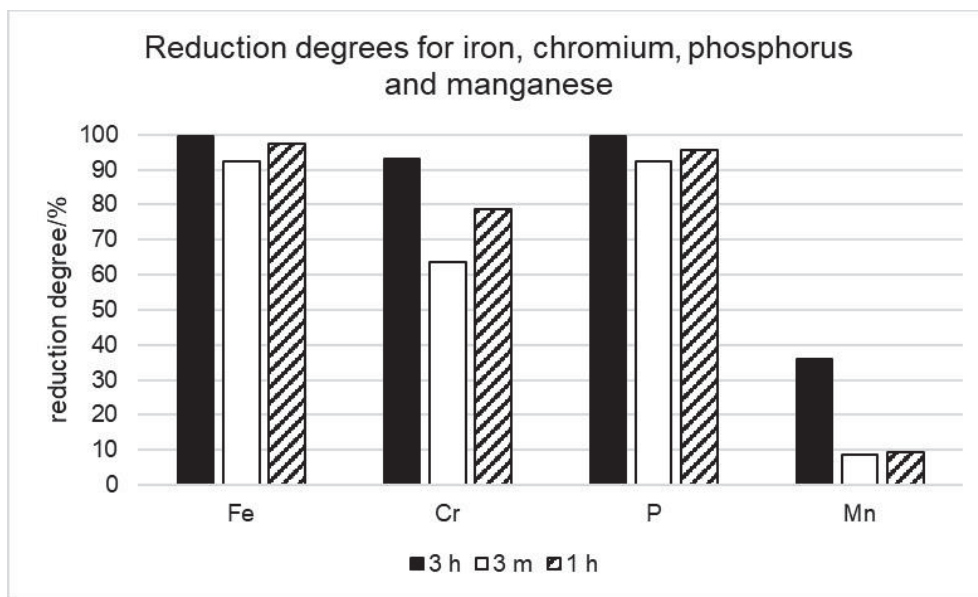


Figure 33: Reduction degrees for Fe, Cr, P and Mn based on ICP-MS analysis results for experiments 1h, 3m and 3h with basic oxygen furnace slags

Table 9: Reduction degrees achieved in the course of preliminary experiments with basic oxygen furnace slags

experiment	RD Fe [%]	RD Cr [%]	RD P [%]	RD Mn [%]
3 h	99.53	93.21	99.38	35.80
3 m	92.29	63.63	92.27	8.56
1 h	97.53	78.75	95.75	9.26

Mineralogical analyses (XRD) were not the main focus of the evaluation. However, they were conducted for a number of reasons:

- support of the ICP-MS analyses
- investigating the reason for low Mn reduction degrees
- supporting the assumption of homogeneity in the slag mixtures produced for reduction
- underlining the suitability of BFS as a potential silica source for basicity alteration due to the complete reduction of Fe, Cr, P and – mostly – Mn (similarity of product slag after reduction)
- phase analysis with regard to latently hydraulic slag properties
- Al_2O_3 enrichment from refractory materials

It has to be considered in future experiments that a certain amount of SiO_2 is reduced as well. Therefore, a shift towards higher basicity (and less flowability) occurs. However, while the number of phases occurring in the slag mixtures after smelting is high (especially the number of void phases and the extent of spinel formation), the product slags of the experiments 3h and 1h ($B_2=1.5$, mixtures with SiO_2 and BFS) are almost mineralogically identical after reduction. Melilite accounts for a big part of the slag mass and is co-existing with Merwinite and Monticellite. Minute amounts of residual P, Cr and Mn in the slag form void phases (Mn also exists as MnS). Cr from the insulation material and the TC might influence the metal mass. Due to the minute amounts of Cr in the slags, however, the RD calculation is not affected. The SEM images for selected slag samples are depicted in **Figure 34**.

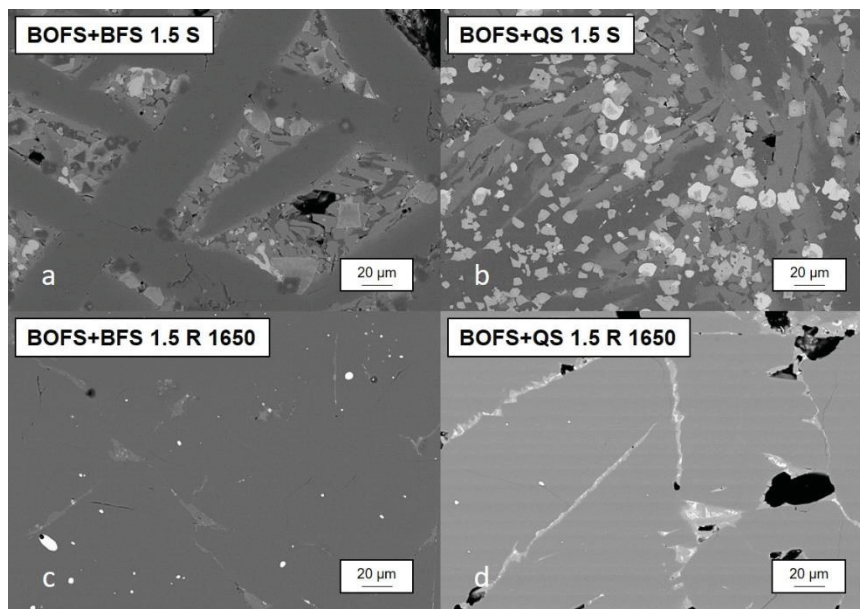


Figure 34: SEM images of produced slag samples: (a) BOFS+BFS, $B_2=1.5$, smelting step (b) BOFS+QS, $B_2=1.5$, smelting step (c) slag from experiment 1h (1650°C) (d) slag from experiment 3h (1650°C)

The phosphorus balance was calculated based on the ICP-MS analysis results and the calculated slag and metal masses. It is shown for the three experiments mentioned above in **Figure 35** and **Table 10**.

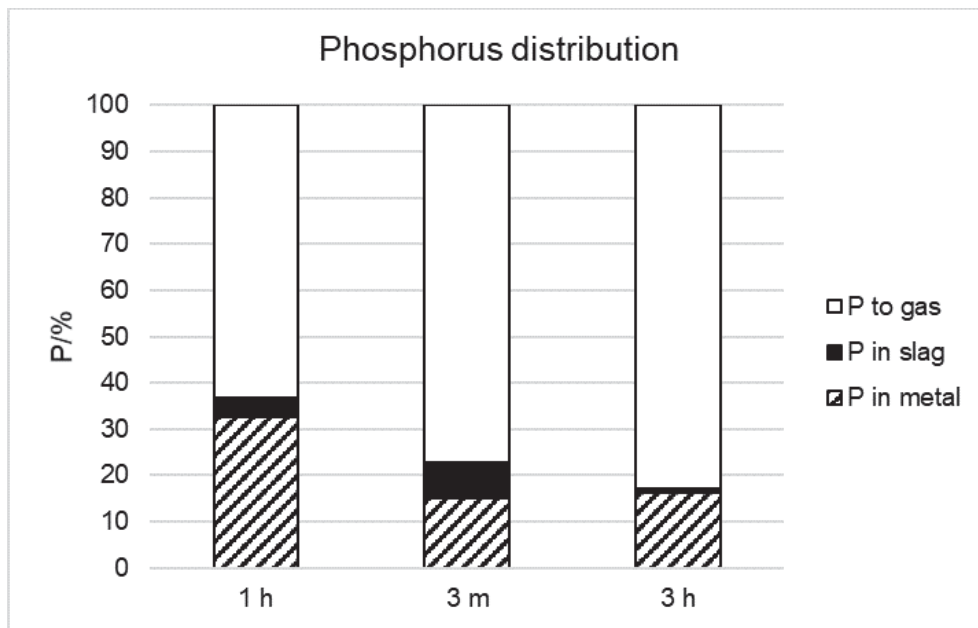


Figure 35: Input phosphorus distribution for experiments 1h, 3m and 3h conducted in the InduMelt plant with basic oxygen furnace slags

Table 10: Phosphorus distribution achieved in the course of preliminary experiments conducted in the InduMelt plant with basic oxygen furnace slags

experiment	P after 1h [m.-%]	P after 3h [m.-%]	P after 3m [m.-%]
total P	100.00	100.00	100.00
P in metal	32.50	16.43	14.98
P in slag	4.25	0.62	7.73
P to gas	63.25	82.95	77.29

The highest phosphorus gasification rate of 82.95% was achieved by reducing a BOFS-QS mixture at 1650°C and will be verified in future experiments. Remarkably, even by reducing slag mixture one with a very low initial P_2O_5 content (< 1 m.-%), high reduction degrees as well as phosphorus gasification rates were achieved.

The path the slag composition makes during the treatment is depicted using a $CaO-FeO_n-SiO_2$ phase diagram shown in **Figure 36**.

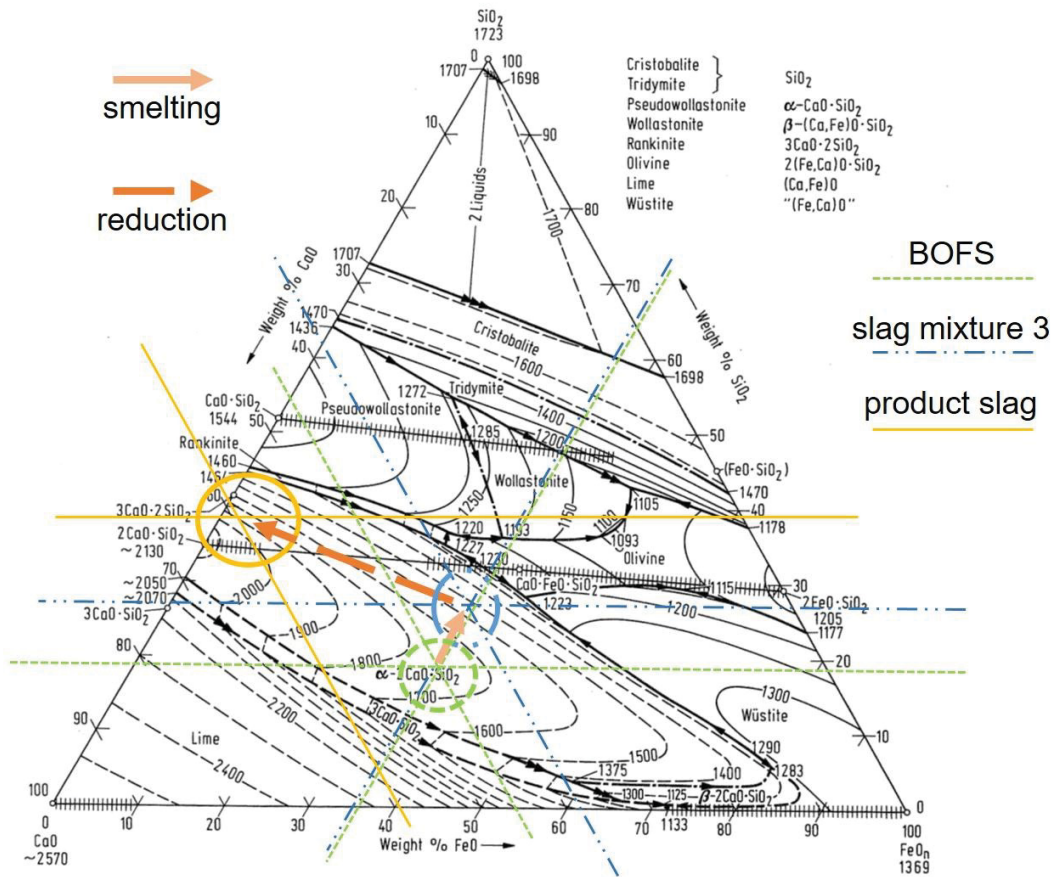


Figure 36: Path of the slag composition during the proposed treatment steps in a $\text{CaO-FeO}_n\text{-SiO}_2$ phase diagram [23]

The slag, starting from the BOFS composition (green circle), moves towards SiO_2 during the smelting step (blue circle). During the reduction step, the composition moves away from FeO towards C_2S (orange circle). P_2O_5 is added to SiO_2 and MgO as well as MnO are added to FeO . The amount of other components is equally distributed between the three species depicted in the phase diagram.

3.2.5 Research prospects

If balanced based on several assumptions, the influence of the internal reuse of the produced metal alloy can be estimated. The most important assumptions made are:

- Carbon, silicon, manganese, chromium and titanium amounts are not taken into account, especially when it comes to heat production/consumption in the BOF.
- Neither iron from the BF nor scrap metal are substituted. The iron alloy is simply fed to the BOF in addition to iron from the BF and scrap metal.

- The phosphorus input via the scrap metal stream is high and merely estimated. All estimations, however, are based on known material loads from an industrial scale steelmaking process.
- No phosphorus is transferred to the dust stream.
- Oxygen and carbon balances are neglected. Oxygen is used in the BOFS to remove carbon from the iron as CO. Carbon is added to the InduRed plant for the BOFS reduction. CO is produced. Furthermore, oxygen is removed via the gas phase (in the form of CO and minute amounts of CO₂) from the InduRed reactor.
- The additives used in the InduRed process are not considered, because they do not affect the phosphorus balance (which is also the case for O and C, s. above).

The phosphorus balances shown in **Figure 37** and **Figure 38** depict two different scenarios: The first one is the implementation of the InduRed process into the integrated iron and steel works. The second one assumes that no internal recycling of BOFS occurs, but the whole slag stream is processed and the whole iron alloy stream is reused.

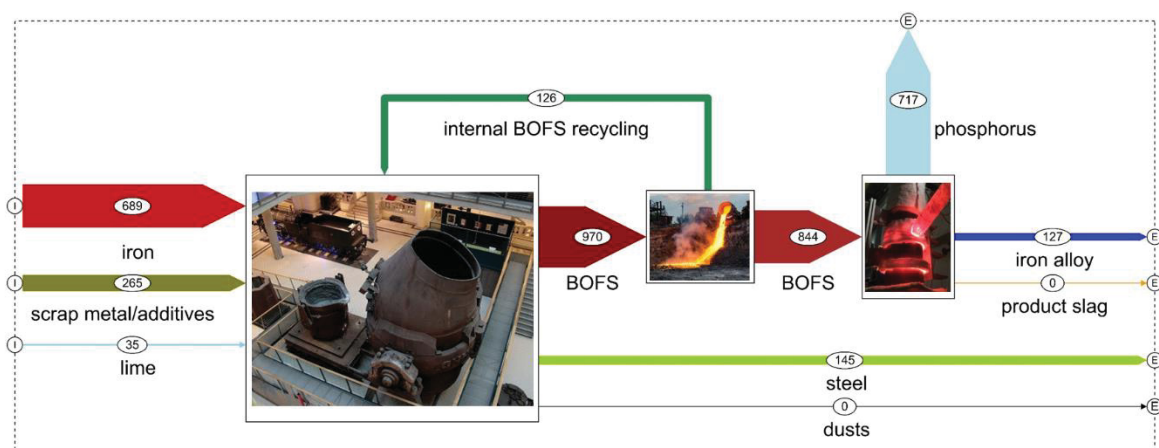


Figure 37: Phosphorus balance after implementation of the InduRed process

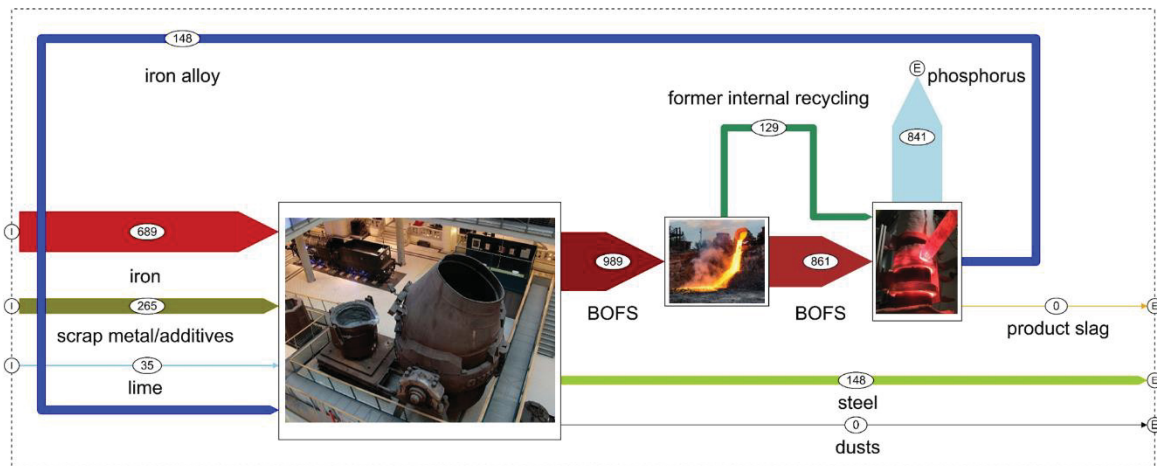


Figure 38: Phosphorus balance with internal recycling of the produced iron alloy

In order to protect sensitive data, the P-amount of the input streams is normalised. This is also true for the goods balance shown in **Figure 39** for better illustration of the amount of recycled metal.

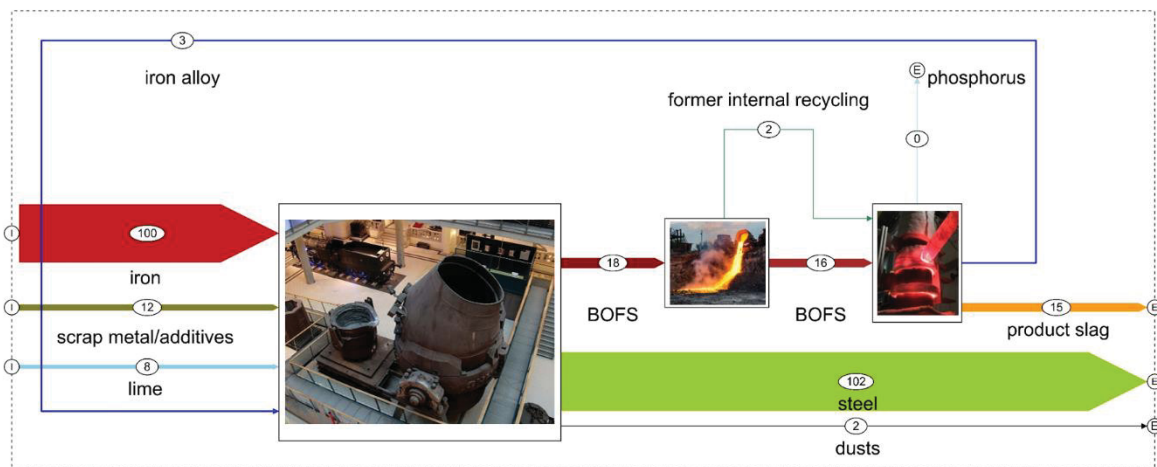


Figure 39: Goods balance with internal recycling of the produced iron alloy

However, the P-value in the steel stream is of interest for further consideration of the suggested process implementation. It is barely influenced by internally reusing the iron alloy product. The little influence that occurs is caused by a higher amount of recycled metal, because no BOFS is reused in the BOF in this scenario.

The results presented above are highly promising in that they exceed the state of knowledge reported in respective literature in terms of phosphorus gasification during the full reduction of BOFS. Future research will focus on the verification of the results. As a holistic approach, the

following areas were either covered and are not discussed in this thesis or will have to be worked on as a part of future research activities:

- continuous operation in the InduRed plant: Two continuous experimental campaigns have already been conducted. Due to sensitive pressure control within the plant and potential slag foaming, process stability could hardly be achieved. Therefore, small amounts of slag were processed and operational interruptions caused varying temperatures. The unequal distribution of small amounts of metal in the form of little spheres makes it hard to reliably evaluate research results at this point. Phosphorus gasification rates of roughly 40-65% have been achieved, depending on the underlying metal and slag analyses used (not constant). In order to tackle this problem, the pressure control (which at this point shuts down the induction units if unstable because of safety concerns caused by CO and the potential consequences of its release) has to be adapted so that longer trials with larger slag amounts are possible. The InduRed reactor in operation as well as slag and metal products from the first experimental campaign with continuous feed are shown in **Figure 40**.

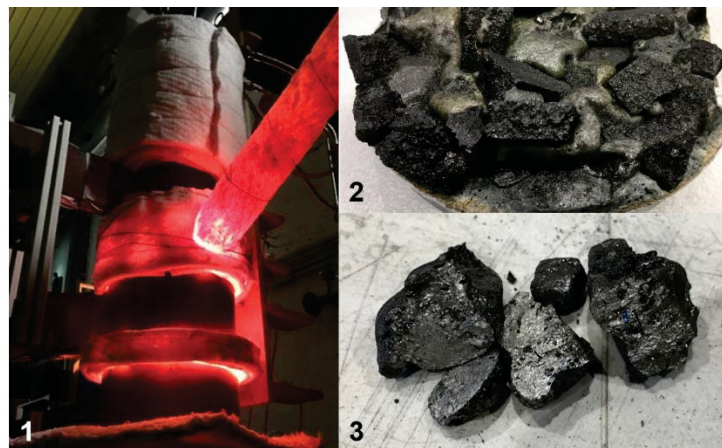


Figure 40: InduRed reactor in operation and slag/metal products from the first continuous experiment (1: reactor in operation, 2: graphite cubes and slag, 3: metal pieces)

- product slag quality regarding slag stability: If phosphorus is removed from the slag completely, $\beta\text{-C}_2\text{S}$ can transform into $\gamma\text{-C}_2\text{S}$, causing a high increase in volume and the disintegration of the slag (s. chapter 2.1.2). A powder is formed and the flowability of the slags is inhibited. Temperature control, therefore, is highly crucial as well as the slag composition. The phenomenon occurred once in the second continuous experimental trial. The product can be seen in **Figure 41**. Experiments with synthetic slags and literature research have shown that this is only a matter of slag cooling velocities and do not occur if the plant is operated as proposed.



Figure 41: Powder found in the InduRed reactor after the second continuous experimental campaign

- product slag quality regarding utility and applicability: The slags produced by the proposed process do not contain significant amounts of phosphorus, iron or chromium. They could, hence, be used in road construction. However, by further decreasing the basicity and adding additional network-forming oxides, a slag with a high glass content can be produced that has the potential to possess properties similar to granulated BFS used in the cement industry. An experiment has been conducted as described above in cooperation with Felix Breuer (Chair of Thermal Processing Technology), setting a basicity value of 1.1 and an Al_2O_3 content after reduction of roughly 12 m.-%. The product was wet granulated and developed a high glass content (>75%). Further experiments as well as mortar tests (regarding strength) are necessary to extensively evaluate the utility potential of the product slag.
- exhaust gas utilisation: The exhaust gas is post-combusted and led into a scrubber in order to produce H_3PO_4 . By combusting CO and P_2 , high amounts of heat are produced and shall be utilised in the future.
- feed of liquid slag and additives: If additives are added to the liquid BOFS and the mixture is fed in its liquid state, the smelting step does not have to be conducted in an additional process unit. At the same time, the energy for smelting does not have to be provided by induction in the reactor.
- metal-slag separation: The products can be collected and separated by density using a skimmer, similar to the tapping and product separation of a BF.
- metal quality: The improvement of the metal quality can either be achieved by optimising the reactor structurally (especially focusing on the gas suction) or, as proposed in this thesis, by altering the whole process route. This approach is presented in the following chapter.

- processing of Cr-rich slags from stainless steel production: Preliminary experiments with slags from stainless steel production containing roughly 4 m.-% of chromium (analysed as the element) were conducted. The produced slag after reduction at temperatures of up to >2273.15 K contained 0.11 m.-% Cr and the metal product consisted of 0.18 m.-% P. The P-content of the input slag was 0.15 m.-%.

3.3 Improvement of the metal quality

By using the results from the preliminary experiments and by drafting simplified mass balances for the implementation of the InduRed process into integrated iron and steel works, it could be shown that the phosphorus gasification degree potentially allows for the internal recycling along the BF-BOF steelmaking route. However, a gasification degree of 85% or higher in an industrial scale process cannot yet be guaranteed. The effect of a carbon-rich hot metal substitute (that also contains Mn, Cr, Si, P and Ti) on the energy balance in the BOF is not yet fully determined and the separate production of manganese, chromium and iron is ultimately desired. Therefore, in the course of the research related to this thesis, the carbon uptake and possible options for constructional changes made to the reactor and especially to the gas suction have been evaluated and will be further investigated and carried out during the scale-up stage.

On a theoretical level and by carrying out preliminary experiments to support respective calculations, an alteration of the currently suggested slag treatment process has been investigated. Its aim is to separate a phosphorus-rich phase – that is also carrying most of the chromium – from an iron- and manganese-rich phase. It requires an additional refining step that is also currently being studied. In this chapter, the process is presented and the assumptions made in order to set up mass balances are explained.

3.3.1 Process alteration

It is well known and reported in respective literature that the FeO content of BOFS is the main limiting factor for the gasification of phosphorus during the reduction of the slags. In order to improve the metal quality, the process shown in **Figure 42** is proposed.

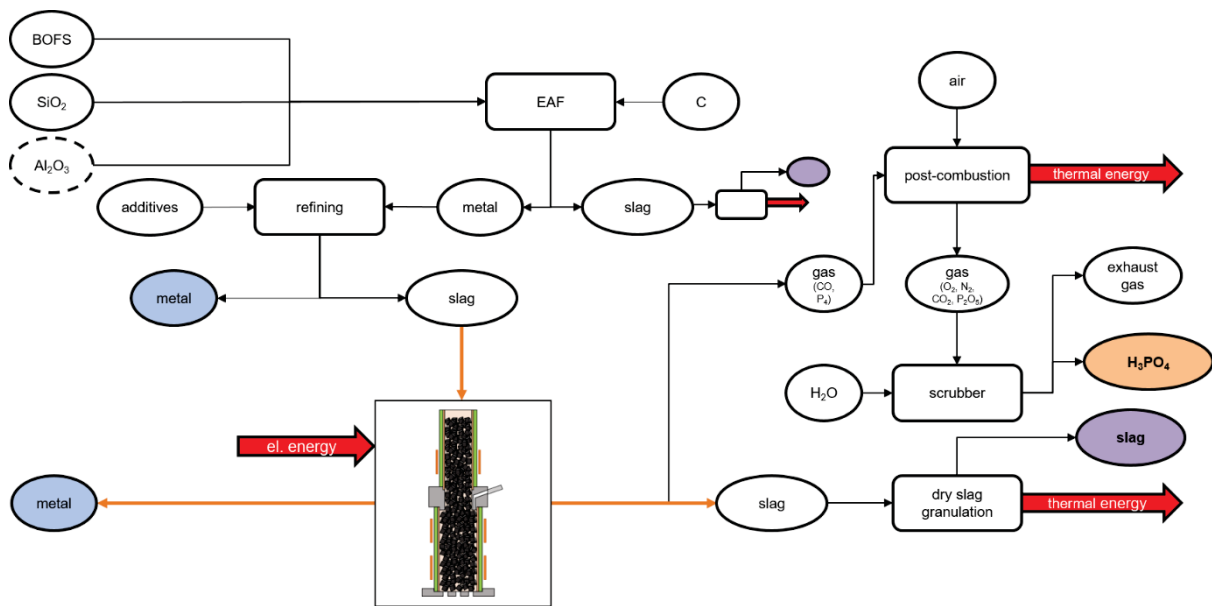


Figure 42: Proposed alteration of the basic oxygen furnace slag treatment process

The reduction of BOFS is done completely in a well-known unit, for example in an EAF. The metal product is then refined using a lime source, a magnesia source and, potentially, an iron source in order to bind refining products into a slag matrix. Preferably, the slag takes up mostly chromium and phosphorus while accumulating low amounts of iron oxide and manganese oxide. It is desired to be similar to calcium phosphate slags discussed in chapter 2.1.6. The metal product shall be free from Cr and P and consist mostly of Fe and Mn.

In a next step, the produced slag shall be treated in the InduRed plant as described above. If the slag contains low amounts of iron (desirably < 15 m.-%), phosphorus is expected to be almost completely gasified.

Currently, the refining process is the research subject of a project related to the work conducted in the course of this thesis. No slag from an industrial scale process is available for experiments at this point. Therefore, synthetic slags are used to investigate the potential of the treatment of chromium- and phosphorus-rich slags.

3.3.2 Determination of a potential phosphate slag composition

If BOFS is reduced as completely as possible and the total amount of phosphorus is taken up by the metal produced, the composition of this metal phase can be estimated. The estimation used as a basis for further calculations and experiment planning in this thesis is shown in **Table 11**.

Table 11: Estimated metal composition after reduction of basic oxygen furnace slag in an EAF

element	content in metal from EAF [m.-%]
Fe	87
Cr	1
Mn	5
P	2
Si	1
C	4
total	100

A subsequent refining step has to oxidise phosphorus and bind it within a slag matrix as quickly as possible. The following **Table 12** shows the assumptions made to define the required refining step. If 100 g of metal from the EAF are refined, the shown amount of slag is formed. The CaO amount was determined by assuming that 90% of the phosphorus can be bound as C_3P and 100% of the Si can be bound as C_2S , adding 20% excess CaO (**). The desired iron content lies between 10 m.-% and 20 m.-% as FeO and is assumed to be 15 m.-% in this calculation (*).

Table 12: Estimated slag composition after refining the metal product from EAF reduction

species after refining	amount after refining 100 g of metal [g]	assumed amount of metal oxidised [%]
FeO	3.85	*
Cr ₂ O ₃	1.02	70
MnO	3.87	60
P ₂ O ₅	4.12	90
SiO ₂	2.14	100
CaO	10.65	**
total	25.66	-

Since pure CaO will not be used for the refining step, MgO and Al₂O₃ are added to the composition resulting from the theoretical refining step. Additionally, the SiO₂ amount is altered so that the basicity B_2 is set at 1.5. The desired, resulting slag composition that is also used in the experiments described in the following chapter is shown in **Table 13**.

Table 13: Desired slag composition for the reduction experiments on Cr- and P-rich slags

species	desired content in synthetic slag [m.-%]
FeO	11.56
Cr ₂ O ₃	3.07
MnO	11.63
P ₂ O ₅	12.38
SiO ₂	21.38
CaO	31.98
Al ₂ O ₃	3.00
MgO	5.00
total	100.00

Figure 43 shows this composition in the respective phase diagram.

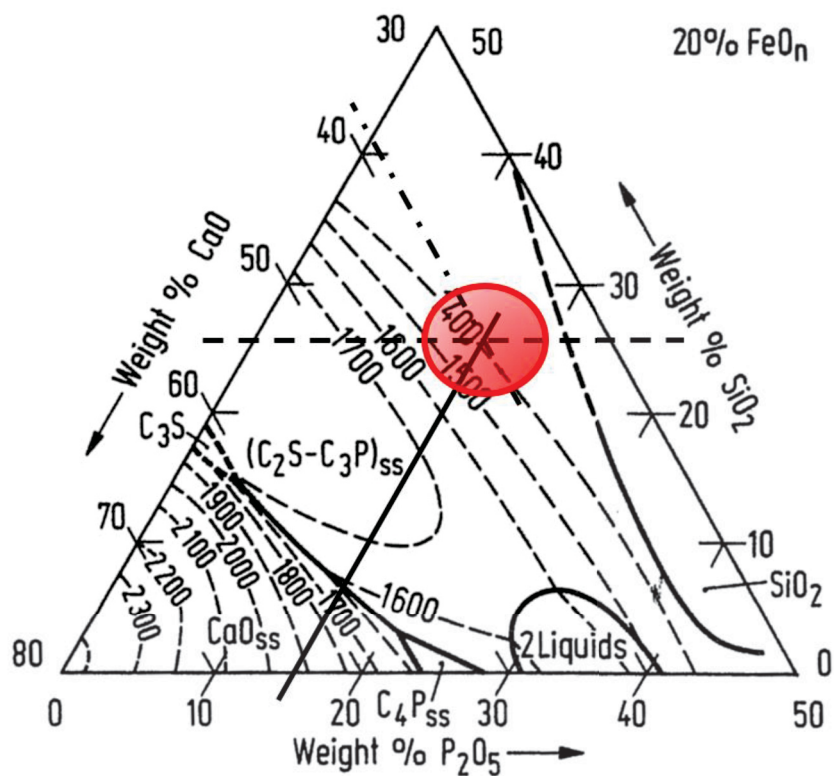


Figure 43: Potential calcium phosphate slag composition after pre-treatment for the reduction in the InduRed plant [23]

FeO, Cr₂O₃ and MnO are added up and represent the FeO_n value of 20% in the diagram. Al₂O₃, being a network forming oxide, was added to SiO₂. MgO was added to CaO.

3.4 Treatment of chromium- and phosphorus-rich slags

As presented in chapter 3.3, the alteration of the BOFS treatment route leads to the formation of phosphate slags that are rich in chromium, phosphorus and manganese. A current research project related to the work presented in this thesis focuses on the production of such slags. Until they are available, an estimated slag composition is calculated and chemicals are used to produce synthetic slags in a smelting step. The resulting slag mixtures are reduced with carbon powder. Preliminary experiments were conducted in an MgO crucible holding roughly 35 g of sample. Experiments were also conducted in the InduMelt plant in order to support the assumptions made regarding the advantages of using the presented reactor concept.

3.4.1 Objectives

As explained above, the objective of the experiments presented in this chapter is to investigate the possibility of phosphorus gasification from chromium- and phosphorus-rich slags. The FeO content is low and the iron phosphide formation shall therefore be limited. The composition of the resulting metal phase shall be analysed and a comparison between standard carbo-thermal reduction and the use of the inductively heated graphite bed shall be determined. It shall be evaluated if the formation of chromium or manganese phosphides is indicated to play a role in the proposed treatment process.

3.4.2 Methodology

The preliminary experiments were conducted at the lab of Prof. Morita (森田先生), part of the Department of Materials Engineering at the Bunkyo campus of the University of Tokyo (UTokyo, 東京大学) in the course of an outgoing research stay. The equipment used consisted of a furnace using heating elements, MgO crucibles and the required chemicals. The smelting and reduction processes were, again, separated into two individual experiments.

The furnace itself has a simple setup. A power supply unit with a control panel allows for the programming of heating and cooling rates as well as phases in which the temperature is held constant. Heating elements are positioned inside the furnace which is lined with refractory materials. An Al₂O₃-pipe reaches through the reactor. It is heated by the heating elements and the temperature of its outer surface is measured by a thermocouple. A plug at the top and the bottom of the pipe seals the reactor atmosphere from the ambient air. Using thin aluminium

oxide pipes, the reactor can be purged with argon. The furnace is able to reach a temperature of roughly 1873 K. The thermocouple measures the temperature at the outside of the reactor pipe. A crucible can be positioned within the pipe using porous refractory materials that fit into it. One after another they are put into the reactor from the bottom until the middle of the crucible reaches the middle of the pipe, which is also where the thermocouple is placed. Frequent measurements have shown that a temperature difference of roughly 20 K originates between the set temperature and the actual temperature of the sample. The heating elements' conjunctions on the top of the furnace were cooled by a fan. MgO crucibles were chosen because of their expected minor interference with the basic slags that also contain low amounts of the oxide. The setup of the furnace is shown in **Figure 44**.

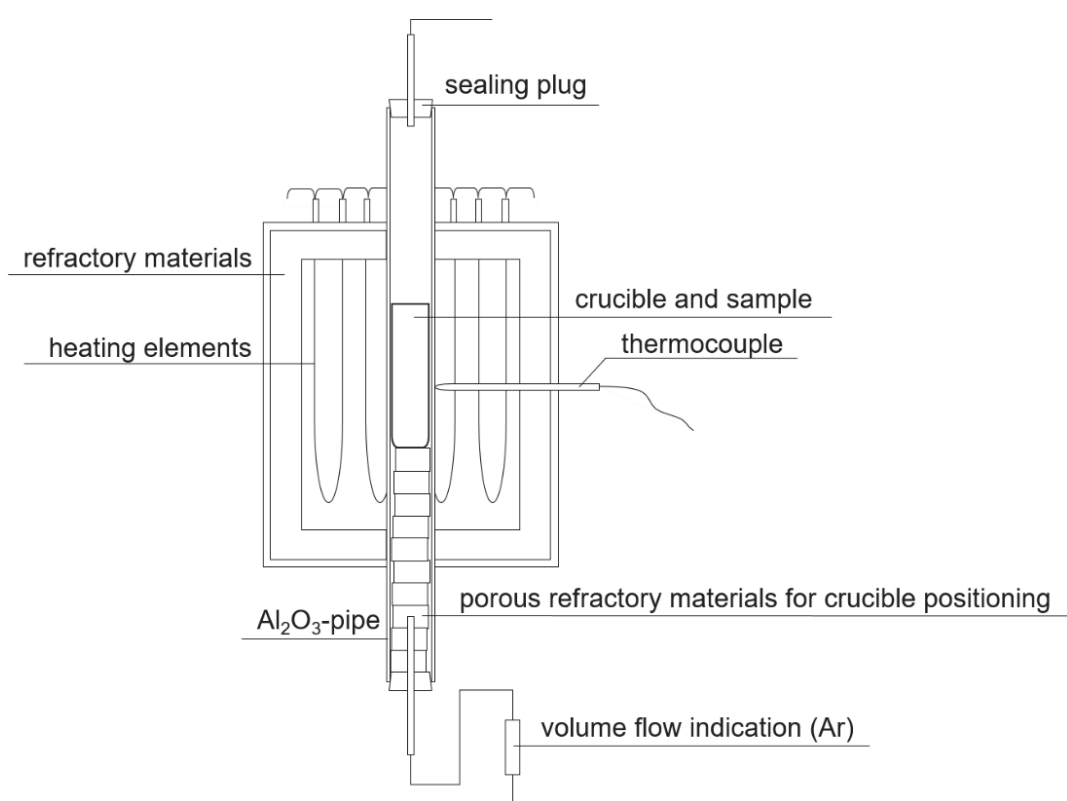


Figure 44: Furnace setup used for preliminary experiments on Cr- and P-rich slags at UTokyo

The determination of the composition chosen for preliminary experiments on the reduction of Cr- and P-rich slags is described in 3.3.2. Based on these assumptions, the mixtures were prepared using pure chemicals (purity > 95.0-99.5%). However, FeO, P₂O₅, CaO and MnO were not available as such. Fe₃O₄, C₃P (containing CaO itself), CaCO₃ and MnO₂ were used. The respective equivalents regarding the content of FeO, P, CaO and Mn were calculated. An argon flow of 200 mlmin⁻¹ was used to avoid false air influences.

In order to protect the MgO crucible, a heating rate and cooling rate of 200 Kh^{-1} was chosen. The set temperature of 1793.15 K (smelting) was held for an hour. This is true for the smelting step as well as the reduction step. The reduction temperature was set at 1893.15 K.

The sampling procedure was quite straightforward due to the small sample size. A saw was used to slice the crucible and the slag. Using a centre punch, the crucible was removed from the slag, which was crushed and powdered using a hammer and, subsequently, a combination of mortar and pestle. After the reduction step, metal had to be removed from the slag. The metal particle size was extremely small, which is why fine exposure was required. The evaluation method used is described in chapter 3.2.2. In this case, however, only ICP-MS was used as an analysis method.

The reference experiments in the InduMelt plant were conducted as described in chapter 3.2.2. The main difference was the maximum reaction temperature, which was 1873.15 K (instead of 1923.15 K used in the preliminary experiments described in chapter 3.2.3) due to the desired comparison with the experiments conducted at UTokyo. Another difference was the omitted tapping in both the smelting and the reduction steps.

3.4.3 Experiment execution

- smelting of synthetic slag for standard carbo-thermal reduction: The furnace described above was programmed so that a heating rate and a cooling rate of 200 Kh^{-1} were defined. The set temperature of 1893.15 K was held for an hour and leads to a temperature of 1873.15 K in the sample. The reactor was purged with Ar. The composition of the compound mixture is shown in **Table 14**. A total of 35.5 g was prepared. The resulting mixture composition was shown in chapter 3.3.2.

Table 14: Reagent mixture composition for the production of synthetic slags

reagent	reagent content [m.-%]
Fe_3O_4	22.13
Cr_2O_3	2.26
MnO_2	10.46
C_3P	19.84
SiO_2	15.65
CaCO_3	22.73
Al_2O_3	2.60
MgO	4.33
total	100.00

Figure 45 shows the full equipment used.



Figure 45: Furnace including equipment used for preliminary experiments with Cr- and P-rich slags at UTokyo (1: power supply and control unit, 2: furnace, 3: ceramics pipe holding the crucible, 4: Ar supply)

- reduction of synthetic slags by standard carbo-thermal reduction: After heating, the temperature was held for an hour in the reactor that was purged with Ar and then cooled. 13.97 g of the slag were powdered and mixed with 1.25 g of carbon powder. The reduction temperature was 1873.15 K.
- smelting of synthetic slag for the reduction in the InduMelt plant: The execution of this experiment is different from the preliminary experiments described in chapter 3.2.3 only in the points mentioned in chapter 3.4.2 (maximum temperature, tapping). The composition of the reagent mixture as well as the chemicals used are the same as in the preliminary smelting experiments (and similar in purity). 945 g were used in the smelting step. The smelting temperature was set at 1823.15 K, overshooting slightly during heat-up.
- reduction of synthetic slags in the InduMelt plant: After crushing, 348 g of the smelting product were mixed with 52.5 g of carbon powder and used in the reduction experiment and reduced between 1873.15 K and 1923.15 K.

3.4.4 Results

In order to reliably evaluate the results from the reduction experiments, the slag composition after the smelting step has to be analysed. The slag produced for the standard carbo-thermal

reduction can be seen in **Figure 46**. **Table 15** shows the calculated slag composition in comparison with the one calculated from the analysis. A good correlation can be seen, except for the enrichment of MgO in the slag matrix – presumably from the crucible. Since the accumulation of MgO does not influence the total amounts of input Fe, P, Mn and Cr used for the further evaluation, the calculated results are further used.

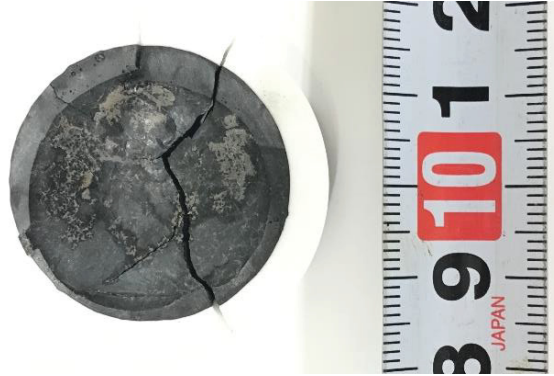


Figure 46: Synthetic, Cr- and P-rich slag for standard carbo-thermal reduction

Table 15: Desired and analysed composition of the synthetic slag produced for standard reduction experiments

species	desired content in SS_{prel} [m.-%]	SS_{prel} composition calculated from analysis [m.-%]
FeO	11.56	9.21
Cr ₂ O ₃	3.07	1.26
MnO	11.63	9.46
P ₂ O ₅	12.38	10.28
SiO ₂	21.38	18.92
CaO	31.98	31.50
Al ₂ O ₃	3.00	-
MgO	5.00	9.92
total	100.00	100.00

ICP-MS analysis was also used for the determination of the element contents in the metal and slag products after reduction. The analysis results are shown in **Table 16**.

Table 16: ICP-MS analysis results after carbo-thermal reduction of Cr- and P-rich slags

species	content in slag after reduction [m.-%]	content in metal after reduction [m.-%]
Fe	2.62	32.30
Cr	0.27	7.66
Mn	2.46	32.40
P	1.27	17.70
Si	12.00	0.00
Ca	30.80	0.39
Mg	7.88	-

Based on these results, the reduction degrees as well as the phosphorus distribution achieved were calculated. They can be seen in **Table 17** and **Table 18**. **Table 19** shows the product stream masses. A comparison with the results from the InduMelt plant is shown in the following paragraphs. The product slag and metal retrieved are depicted in **Figure 47**.

Table 17: Reduction degrees achieved by standard carbo-thermal reduction of Cr- and P-rich slag

element	reduction degree [%]
Fe	80.63
Mn	81.85
Cr	91.56
P	84.38

Table 18: Phosphorus distribution after standard carbo-thermal reduction of Cr- and P-rich slag

P source/destination	P amount [g]	P amount [%]
P input	0.75	100.00
P in metal	0.55	73.49
P in slag	0.12	15.62
P to gas	0.08	10.89

Table 19: Product stream masses after standard carbo-thermal reduction of Cr- and P-rich slag

product stream	amount [m.-%]
slag	66.47
metal	22.44
gas	11.09



Figure 47: Metal and slag product phases after standard carbo-thermal reduction of Cr- and P-rich slag

Figure 48 shows the phosphorus balance for the proposed process when the results from the preliminary experiments are used as a basis.

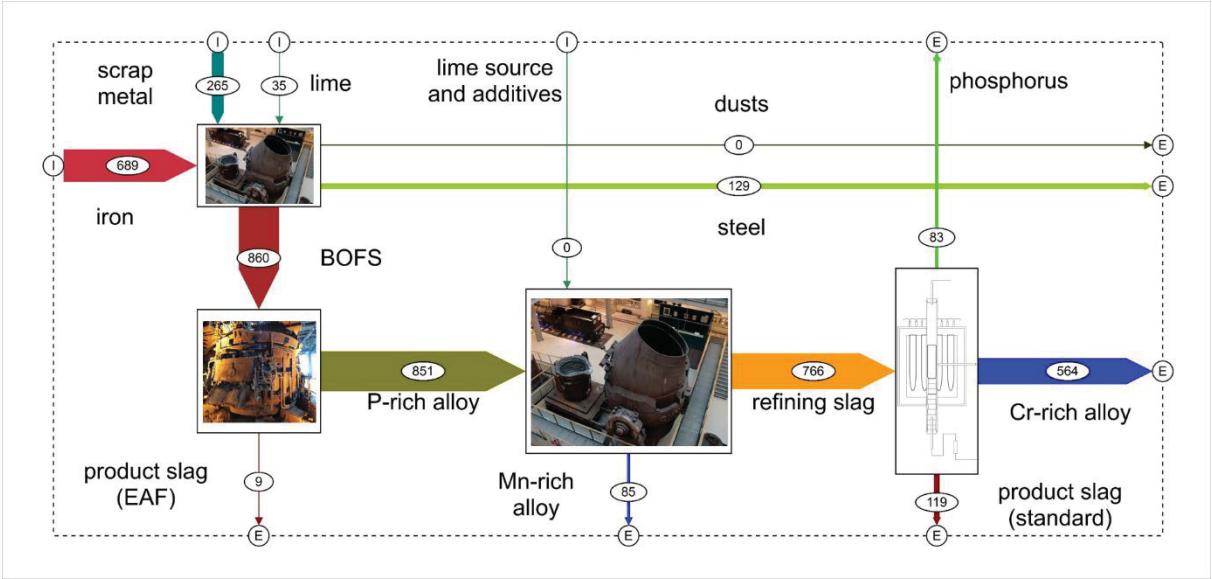


Figure 48: Phosphorus balance using results from the preliminary experiments (standard carbo-thermal reduction of Cr- and P-rich slag)

The experiments in the InduMelt plant were conducted as described above. **Figure 49** shows the prepared slag mixture and the slag product after the smelting step.



Figure 49: Synthetic slag mixture (left) and product after smelting (right) for reduction in the InduMelt plant

The desired slag composition is compared with the composition calculated from ICP-MS analysis results. The ratio of all oxides (calculated from their element content) is highly similar to the desired composition. However, due to the use of Al_2O_3 refractory materials, the enrichment of Al is high and a dilution of the slag occurs. Changes in flowability and activities might influence the reduction and P gasification behaviour. The absolute element input for Fe, Cr, Mn and P does not change, however, and due to the full reduction (Cr-, P- and Fe-free slag), the reduction degree and P distribution calculation is not influenced.

The reduction products metal and slag were analysed and the results are presented in **Table 20**.

Table 20: ICP-MS analysis results after reduction in the InduMelt plant

species	content in slag after reduction		content in metal after reduction	
	[m.-%]		[m.-%]	
Fe	0.43		39.80	
Cr	0.02		8.63	
Mn	0.57		21.20	
P	0.01		14.33	
Si	8.30		0.30	
Ca	9.71		0.39	

Figure 50 depicts the product after cooling. The slag, metal spheres and graphite cubes can be seen. **Table 21** shows the reduction degrees achieved in the experiment and **Table 22** gives an overview of the phosphorus distribution among the product phases. **Table 23** shows the product stream masses used for the balancing.

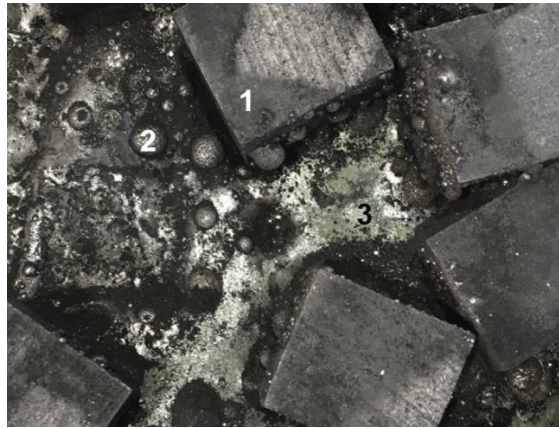


Figure 50: Graphite cubes (1) with metal spheres (2) and slag (3) after reduction of synthetic slag in the InduMelt plant

Table 21: Reduction degrees achieved by reduction of synthetic, Cr- and P-rich slag in the InduMelt plant

element	reduction degree [%]
Fe	96.98
Mn	96.00
Cr	99.43
P	99.85

Table 22: Phosphorus distribution after reduction of synthetic, Cr- and P-rich slag in the InduMelt plant

P source/destination	P amount [g]	P amount [%]
P input	18.81	100.00
P in metal	10.92	58.09
P in slag	0.03	0.15
P to gas	7.85	41.76

Table 23: Product stream masses after reduction of synthetic, Cr- and P-rich slag in the InduMelt plant

product stream	amount [m.-%]
slag	63.37
metal	21.90
gas	14.73

If the results achieved by using the InduMelt plant for reduction are used to calculate the P balance of the proposed process, promising first results can be achieved, as shown in **Figure 51**.

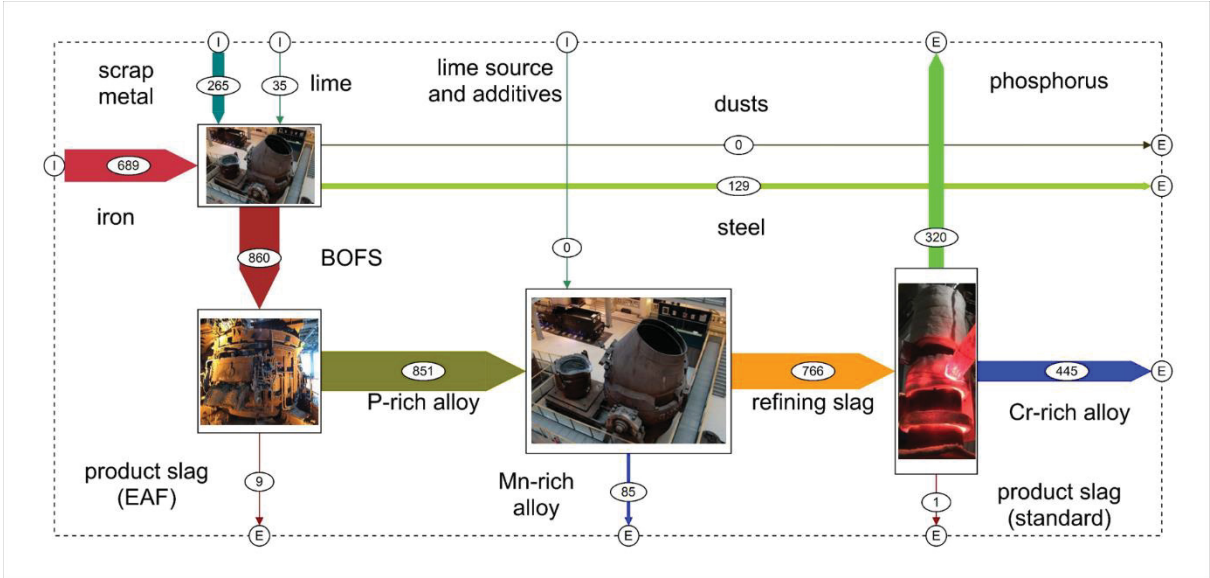


Figure 51: Phosphorus balance using results from the InduMelt reduction experiments with Cr- and P-rich slag

In order to illustrate the mass streams of the products in comparison to steel production, the goods balance is also shown (**Figure 52**).

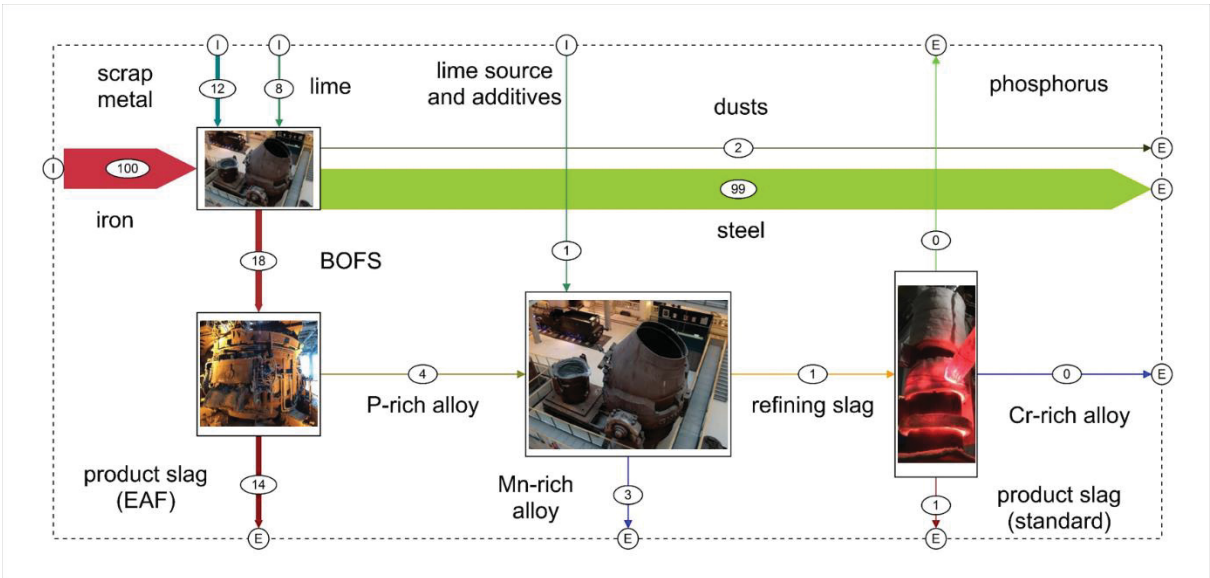


Figure 52: Goods balance using results from the InduMelt reduction experiments with Cr- and P-rich slag

These first results in this specific field of research are highly promising and will be verified in future experiments. The achieved reduction degrees and phosphorus distributions (carbo-thermal reduction as well as reduction in the InduMelt plant) are compared to highlight the potential advantage of the applied reactor concept over standard carbo-thermal reduction (**Figure 53** and **Figure 54**).

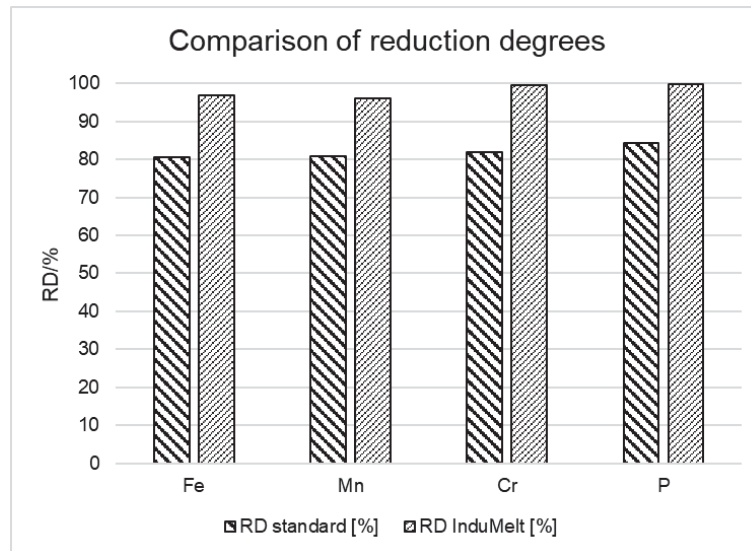


Figure 53: Comparison of reduction degrees achieved by standard reduction and reduction in the InduMelt plant

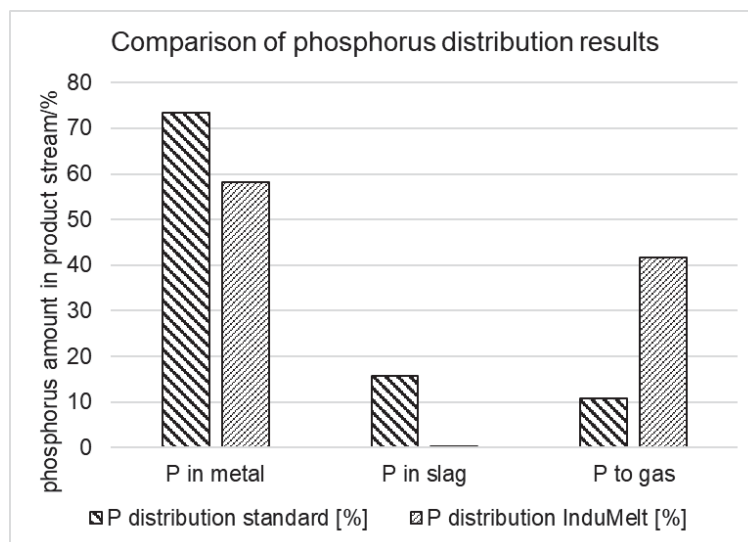


Figure 54: Comparison of phosphorus distribution achieved by standard reduction and reduction in the InduMelt plant

Figure 55 and **Figure 56** show the slag composition in the respective phase diagrams. The illustrations are based on the results achieved by applying the novel reactor concept described in this thesis.

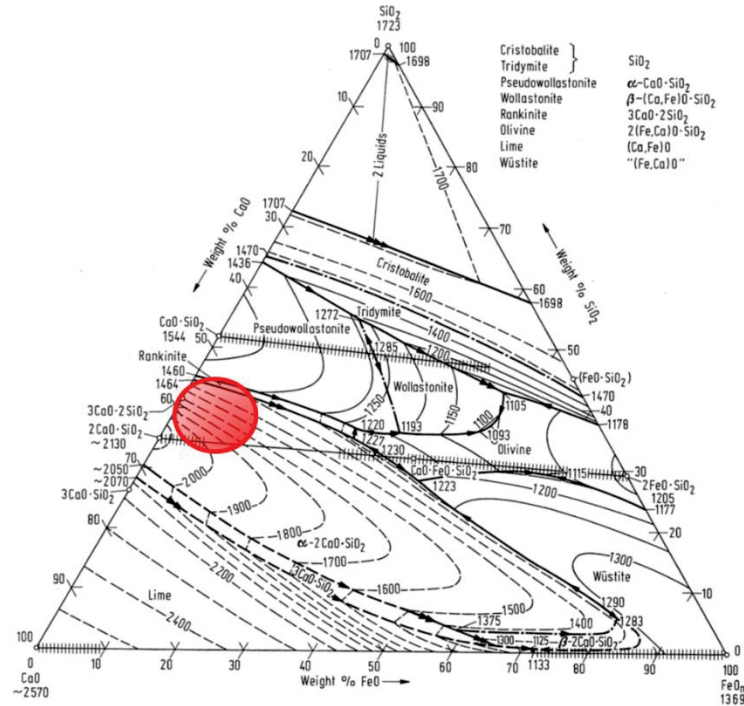


Figure 55: Calcium phosphate slag composition after reduction of Cr- and P-rich slags [23]

The metal-free slag (neglecting Al- and Mg-oxide contents), naturally, is located in the same area as the product slag from the preliminary experiments without the additional refining step (BOFS reduction) due to the complete reduction that can be achieved.

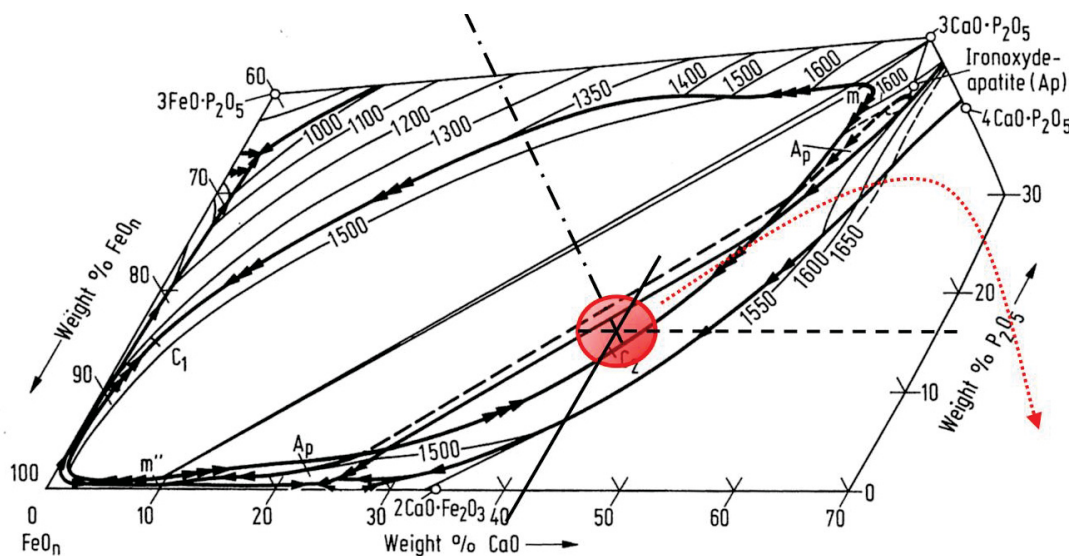


Figure 56: Path of the calcium phosphate slag during reduction [23]

Not taking into account other metal oxides or network-forming slag components, the path of the calcium phosphate slags in the reduction process can be depicted. It can be assumed, based on thermodynamic data, that the iron oxide is reduced before the phosphorus compounds.

The potential formation of chromium phosphides and the influence of the high manganese amounts with regard to phosphide formation might be a reason for lower gasification rates than expected. In order to produce reliable data, repetitions with different compositions have to be conducted. Additionally, Cr-rich and Mn-free slags as well as Mn-rich and Cr-free slags containing similar P amounts shall be reduced and investigated in future research activities.

3.4.5 Research prospects

The preliminary experiments conducted with regard to phosphorus gasification from Cr- and P-rich slags were highly promising. The proposed reactor concept enables high gasification rates and the experiments' results go beyond the current state of knowledge.

However, in order to ensure better comparability, the experimental setup for the InduMelt plant will be adapted. MgO crucibles will be used and an argon purge system will be installed. The replacement of Al_2O_3 is supposed to inhibit the effect of slag dilution observed in the experiments conducted.

The number of experiments will be increased in order to verify the results presented in this thesis. This is true for the investigation of the alternative process route as well as for the direct reduction of BOFS in the InduRed reactor.

As soon as slags from actual industrial- or semi-industrial-scale are available, they will also be investigated. In particular, the chromium, iron and phosphorus contents will be altered.

Most importantly, the influence of high Cr and Mn contents must be investigated separately. The possibility of both Mn and Cr phosphide formation makes it impossible at this point to further interpret the gasification rate results.

Improvement strategies for the reduction of slags in the InduMelt reactor include:

- use of MgO crucibles
- implementation of an Ar purge system
- installation of an exhaust gas suction for the lab-scale plant

4 Conclusions

A number of theoretical and practical tasks were conducted and described in the course of this thesis. Therefore, before concluding the thesis with regard to the hypotheses verbalised in chapter 1.2, a short summary is provided.

Subsequently, the hypotheses are commented on individually and a final conclusion is drawn at the end of this chapter.

4.1 Summary

The state of knowledge with respect to the reduction of BOFS with simultaneous removal of phosphorus via the gas phase described in chapter 2.1.3 suggests that this gasification is feasible in principle. However, the accumulation of phosphorus in the metal product of reduction poses a significant limitation to this treatment approach.

The influence of the FeO content of BOFS was extensively investigated. Only at FeO contents of roughly 2 m.-% and a slag basicity of 1.0, 55% of the input phosphorus could be gasified at 1673 K (state of knowledge, s. chapter 2.1). The slags processed in the course of this thesis had an FeO content of roughly 22 m.-% and the most promising operating temperature was determined to be 1923.15 K. The lowest basicity tested was 1.5.

The carbon demand as well as the determination of suitable reduction temperatures was based on the theoretical work using a Richardson-Ellingham diagram, a Baur-Glaessner diagram and a Rist diagram. The carbon addition proved sufficient and the temperature dependency as well as its influence on P reduction degrees paralleled expectations. The

reaction schematics were not contradicted. Higher SiO_2 activity (lower basicity) and higher reduction temperatures both increased the gasification rate.

As presented in chapter 2.1.4, there are considerable advantages of the InduRed reactor. The application of the reactor concept proved successful in exceeding the state of knowledge and in enabling the phosphorus gasification at high rates. The advantages comprise the graphite bed's large surface area, direct heat input, continuous gas removal, high CO partial pressures, the non-existence of a molten iron bath and the reduction of the influence of transport limitations.

Processes producing Cr- and P-rich slags, like the LD-AC process, were used to derive a potentially producible slag composition after implementing an alternate process route, including a second refining step following a standard reduction unit in which P is fully accumulated in liquid Fe.

Such slags were synthetically produced and reduced by both standard carbo-thermal reduction and the InduRed reactor. High gasification rates were achieved. However, the influence of high Mn and Cr contents cannot be neglected.

4.2 Assessment of hypotheses and results

The main hypothesis verbalised as a basis of this thesis is stated again as follows:

By carbo-thermal reduction of basic oxygen furnace slags in an inductively heated bed of graphite pieces, high phosphorus gasification rates can be achieved.

In order to corroborate or refute this hypothesis, the following assumptions were stated and are commented with regard to the research objective:

1. A modification of BOFS is required in order to retain flowability and to thermodynamically support the phosphorus gasification.

The necessity of such a modification step was highlighted in the theoretical work of this thesis and can be derived from literature research results. Experimental work in this regard supported the hypothesis in terms of both flowability and gasification rates. A slag basicity lower than 1.5 is suggested in order to achieve high gasification rates.

2. The most important modification is the addition of a silica source.

This statement proved accurate by conducting both theoretical and experimental work. Other additives, such as Al_2O_3 , influence the slag quality and are to be investigated more closely in the future. However, for general feasibility, SiO_2 addition is crucial.

3. BFS is a suitable silica source for the modification step.

P gasification results with BF addition were highly successful. It can be stated that the silica source BF is suitable as an additive, even though better results could be achieved using pure SiO_2 .

4. High temperatures are required to achieve high phosphorus gasification rates.

This assumption proved accurate with respect to two individual effects: Firstly, high temperatures increase the reduction degree of P and secondly, increasing temperatures inhibit the formation of iron phosphides, which are crucial to the gasification mechanism.

5. The iron oxide content of BOFS poses the most influential limitation to the gasification process.

Hypothesis number five was supported in the area of BOFS reduction. This finding of literature research could be affirmed in slags with low Cr and Mn contents. However, experiments with Cr-rich synthetic slags suggest a more complicated situation.

6. Altering the process route in order to produce and treat Cr- and P-rich slags in the presented reactor concept leads to even higher gasification rates.

The synthetic slags produced showed low FeO and high Cr and P contents. Nevertheless, preliminary experiments showed that even though the iron content was low, the gasification rates were much lower than those achieved during BOFS treatment.

7. Chromium and manganese phosphide formation does not limit the gasification rates.

This hypothesis cannot be corroborated. Lower gasification rates were achieved in experiments with slags containing less FeO than BOFS. The nature of this effect cannot be fully described at this point. Cr as well as Mn can form phosphides and overlaying influence probabilities do not yet allow further interpretation.

8. The applied reactor concept benefits the phosphorus gasification substantially.

This assumption can be fully corroborated. Standard carbo-thermal reduction by carbon addition to synthetic, Cr- and P-rich slags and heating led to significantly lower gasification rates by a factor of 4-5. During the treatment of BOFS, extremely high gasification rates of roughly 83% were achieved.

In conclusion, the main hypothesis can be rigorously supported. The novel approach contributed to exceeding the state of knowledge in the field of BOFS treatment as well as the application of the InduRed reactor concept.

5 Research prospects

In the course of the experiments conducted for this thesis, highly promising results could be obtained. However, many aspects of the proposed treatment processes are still unclear and require additional investigations. Regarding high Cr and Mn contents in slags processed in the InduRed reactor, completely new challenges were detected. Known as well as new aspects of the addressed area of interest need further research attention in the future.

5.1 Slag quality

The most important aspect of the product slag quality is its utilisation versatility. Ideally, latent hydraulic activity can be achieved by using suitable amounts of additives, especially SiO_2 and Al_2O_3 . Dry slag granulation might serve as a quick cooling approach that simultaneously increases energy efficiency.

5.2 Metal quality

The metal quality needs to be further improved. Two approaches will be investigated:

1. Plant modifications, the use of different refractory materials as well as the implementation of an Ar purge shall further increase the phosphorus gasification rates achieved during carbo-thermal BOFS reduction in the InduRed plant. If P contents in the metal product approach 0.1 m.-%, a direct recycling in the BOF is conceivable.

2. The alternate process route using a second refining step might provide a possibility to improve the metal quality. The reduction of Cr-, P- and Mn-rich slags has shown that gasification rates are not yet sufficiently high. If the influence of either Cr or Mn can be neglected, the requirements for the refining step can be derived.

Both approaches require a number of experiments in order to verify the results obtained so far. As soon as slags from actual semi-industrial-scale experiments are available, their treatment will be investigated as well.

5.3 Process and scale-up

Plant- and process related, further continuous experimental campaigns based on the findings in this thesis are needed. Based on these campaigns, the feasibility of a scale-up by a factor of 10 (i.e. 20-40 kg h^{-1}) shall be determined. In the next scale, the gas utilisation and the phosphoric acid production as well as the slag-metal separation shall be investigated.

In conclusion, the work conducted in the course of this thesis has led to a number of prospective tasks that allow for the design of further experiments. A proof of principle was successful and the state of knowledge could be exceeded.

6 Bibliography

- [1] Wirtschaftsvereinigung Stahl and Stahlinstitut VDEh, World crude steel production by region, <https://en.stahl-online.de/wp-content/uploads/2019/03/Folie2-2.png>, last accessed 26. August 2019.
- [2] Androsch, F., 2019, How megatrends drive innovation. In Steel Institute VDEh (Ed.): 4th European Steel Technology and Application Days. Düsseldorf: Steel Institute VDEh.
- [3] Suarez, F. F., Battles for technological dominance: an integrative framework, *Research Policy* 33 (2004), 2, 271–286.
- [4] World Steel Association, World Steel in Figures 2019, <https://www.worldsteel.org/en/dam/jcr:96d7a585-e6b2-4d63-b943-4cd9ab621a91/World%2520Steel%2520in%2520Figures%25202019.pdf>, last accessed 26. August 2019.
- [5] Schmid, H., 2016, BOFS and BF composition, email to Christoph Ponak, Linz.
- [6] European Commission, 2017, Mitteilung der Kommission an das Europäische Parlament, den Rat, den Europäischen Wirtschafts- und Sozialausschuss und den Ausschuss der Regionen über die Liste kritischer Rohstoffe für die EU 2017. Edited by European Commission, Brussels.
- [7] Roos, E. and K. Maile, *Werkstoffkunde für Ingenieure*, Springer-Verlag, Berlin Heidelberg, 2015.
- [8] Urban, W., M. Weinberg and J. Cappel, De-Phosphorization Strategies and Modelling in Oxygen Steelmaking, *Iron and Steel Technology* 134 (2014), 8, 27–39.

- [9] World Steel Association, World Crude Steel Production - Summary, <https://www.worldsteel.org/en/dam/jcr:dcd93336-2756-486e-aa7f-64f6be8e6b1e/2018%2520global%2520crude%2520steel%2520production.pdf>, last accessed 20. August 2019.
- [10] Schmid, H., L. Cattini, W. Martinelli and J. Rieger, 2016, Aktueller Entwicklungsstand der Metallrückgewinnung und Chromabtrennung aus LD-Schlacken. In Max Aicher Unternehmensgruppe (Ed.): Schlacken-Symposium 2016. Kreislaufwirtschaft stabil weiterentwickeln. Freilassing, 89–102.
- [11] Neuhold, S., D. Höllen, J. G. Raith, M. Berger, S. Schüler and D. Mudersbach, 2018, Auslaugverhalten von Stahlwerksschlacken und natürlichen Gesteinskörnungen - ein Vergleich. In Max Aicher Unternehmensgruppe (Ed.): Schlacken-Symposium 2018. Ressourcenschonung durch Nutzung von Sekundärrohstoffen: Wann wird politische Forderung zur Realität? Freilassing, 179–189.
- [12] Somnath Basu, Studies on dephosphorisation during steelmaking, dissertation, Royal Institute of Technology, Stockholm, 2007.
- [13] Federal Ministry for Sustainability and Tourism Austria and International Organizing Committee for the World Mining Congresses, 2019, World Mining Data 2019, Wien.
- [14] Wirtschaftsvereinigung Stahl and Stahlinstitut VDEh, Hot metal and crude steel production, https://en.stahl-online.de/wp-content/uploads/2013/10/Bild-24_eng.jpg, last accessed 26. August 2019.
- [15] World Steel Association, Steel industry co-products, https://www.worldsteel.org/en/dam/jcr:2941f748-b906-4952-8b11-03ffee835b39/Co-products_position_paper_vfinal.pdf, last accessed 26. August 2019.
- [16] World steel prices, 2019, Sheffield, UK. Available online at <https://worldsteelprices.com/>, checked on 26.08.2019.
- [17] Biswas, A. K., Principles of blast furnace ironmaking, Cootha Publ. House, Brisbane, 1981.
- [18] Csiro, L. L., S. Devasahayam and V. Sahajwalla, 2013, Evaluation of coal for metallurgical applications. In Dave Osborne (Ed.): The Coal Handbook. Towards Cleaner Production. Sawston, UK: Woodhead Publishing Ltd., 352–386.
- [19] Miller, T. W., J. Jimenez, A. Sharan and D. A. Goldstein, 1998, Oxygen Steelmaking Processes. In R. J. Fruchan (Ed.): The Making, Shaping and Treating of Steel.

- Steelmaking and Refining Volume. 11th ed. Pittsburgh, PA, USA: The AISE Steel Foundation, 475–524.
- [20] Shamsuddin, M., *Physical Chemistry of Metallurgical Processes*, John Wiley & Sons, Inc., Hoboken, New Jersey, USA, 2016.
- [21] Maxl, E., H. Hiebler, H. Presslinger and K. Antlinger, *Microanalytical Investigations of Oxidizing Slags with Special Consideration of Phosphorus- and Sulphur-containing Phases*, *ISIJ International* 33 (1993), 1, 88–97.
- [22] Müller, M., S. Seebold, G. Wu, E. Yazhenskikh, T. Jantzen and K. Hack, 2017, *Experimental investigation and modelling of the viscosity of oxide slag systems*. In Annelies Malfliet (Ed.): *Proceedings of the 5th International Slag Valorisation Symposium*. Leuven, 37–51. Available online at <http://slag-valorisation-symposium.eu/2017/wp-content/uploads/downloads/Session%201/Michael%20M%C3%BCller%20-%20Paper%20-%20Experimental%20investigation%20and%20modelling%20of%20the%20viscosity%20of%20oxide%20slag%20systems%20-%20SVS2017.pdf>.
- [23] Allibert, M., *Slag atlas*, Verlag Stahleisen GmbH, Düsseldorf, 1995.
- [24] Waligora, J., D. Bulteel, P. Degrugilliers, D. Damidot, J. L. Potdevin and M. Measson, *Chemical and mineralogical characterizations of LD converter steel slags: A multi-analytical techniques approach*, *Materials Characterization* 61 (2010), 39–48.
- [25] Isawa, T., 2013, *Update of iron and steel slag in Japan and current developments for valorisation*. In Annelies Malfliet, et.al. (Eds.): *Proceedings of the 3rd International Slag Valorisation Symposium*. Leuven, 87–98.
- [26] Horii, K., Y. Kitano, N. Tsutsumi and T. Kato, 2013, *Processing and Reusing Technologies for Steelmaking Slag*. Edited by Nippon Steel, Tokyo (Nippon Steel Technical Report, 104).
- [27] Ludwig, H. M., H. Wulfert, W. Ruhkamp and B. Möser, 2018, *Mobilisierung von hydraulisch aktiven Phasen in LD-Schlacken durch Herstellung von ultrafeinem Material*. In Max Aicher Unternehmensgruppe (Ed.): *Schlacken-Symposium 2018. Ressourcenschonung durch Nutzung von Sekundärrohstoffen: Wann wird politische Forderung zur Realität?* Freilassing, 231–247.
- [28] Arlt, K.-J. and N. Wolsfeld, 2018, *Einsatz von Stahlwerksschlacken im Deponiebau*. In Max Aicher Unternehmensgruppe (Ed.): *Schlacken-Symposium 2018*.

- Ressourcenschonung durch Nutzung von Sekundärrohstoffen: Wann wird politische Forderung zur Realität? Freilassing, 99–114.
- [29] Ferreira Neto, J. B., J. O.G. Faria, C. Fredericci, F. F. Chotoli, A. N. L. Silva, B. B. Ferraro et al., 2015, Modification of molten steelmaking slag for cement application. In Annelies Malfliet, Yiannis Pontikes (Eds.): Proceedings of the 4th International Slag Valorisation Symposium. Leuven, 77–83.
- [30] Liu, C., M. Guo, B. Blanpain and S. Huang, 2017, Effect of Al₂O₃ addition on the crystallisation of a high basicity BOF slag: Perspective of glass forming ability for slag valorisation. In Annelies Malfliet (Ed.): Proceedings of the 5th International Slag Valorisation Symposium. Leuven, 121–124.
- [31] Hsieh, W. and Y.-H. Tseng, 2015, Dry slag granulation of modified BOF slag. In Annelies Malfliet, Yiannis Pontikes (Eds.): Proceedings of the 4th International Slag Valorisation Symposium. Leuven, 101–105.
- [32] Li, G., H. Zhang, H. Ni and M. Guo, 2013, Current development of slag valorisation in China. In Annelies Malfliet, et.al. (Eds.): Proceedings of the 3rd International Slag Valorisation Symposium. Leuven, 57–68.
- [33] Weinberg, M., J. Adam, G. Harp, T. Merkel and H. Tabani, 2005, Entwicklung und Erprobung eines neuartigen, umweltentlastenden Granulationsverfahrens zur Herstellung von Granulaten aus LD-Schlacken für qualitativ hochwertige Einsatzgebiete. Edited by Betriebsforschungsinstitut, VDEh-Institut für Angewandte Forschung GmbH, Düsseldorf/Duisburg.
- [34] Schraut, K., B. Adamczyk, S. Simon, J. von Werder, B. Meng, D. Stephan and C. Adam, 2018, Zementklinker durch Nachbehandlung von Stahlwerksschlacken. In Max Aicher Unternehmensgruppe (Ed.): Schlacken-Symposium 2018. Ressourcenschonung durch Nutzung von Sekundärrohstoffen: Wann wird politische Forderung zur Realität? Freilassing, 219–229.
- [35] Tossavainen, M., F. Engstrom, Q. Yang, N. Menad, M. Lidstrom Larsson and B. Bjorkman, Characteristics of steel slag under different cooling conditions, Waste Management 27 (2007), 1335–1344.
- [36] Liu, C., S. Huang, P. Wollants, B. Blanpain and M. Guo, Valorization of BOF Steel Slag by Reduction and Phase Modification: Metal Recovery and Slag Valorization, Metallurgical and Materials Transactions B 48B (2017), 3, 1602–1612.
- [37] Locher, F. W., Zement, Verlag Bau+Technik GmbH, Düsseldorf, 2000.

- [38] Harada, T., H. Hirata, T. Arai, T. Toh and C. Shuto, Optimization of Slag Reduction Process with Molten Slag Charging (Development of the Molten Slag Reduction Process - 2), *ISIJ International* 189 (2018), advance publication by J-STAGE.
- [39] Nakase, K., A. Matsui, N. Kikuchi, Y. Kishimoto and Y. Miki, 2013, Method for recovering iron and phosphorus from steelmaking slag. Patent no. JP 2013044029 A.
- [40] Matsui, A., K. Nakase, N. Kikuchi and Y. Kishimoto, 2012, Method for recovering iron and phosphorus from steelmaking slag. Patent no. JP 2012219298 A.
- [41] Shin, D. J., X. Gao, S. Ueda and S.-y. Kitamura, 2019, Separation of phosphorus and manganese from steelmaking slag by selective reduction. In Annelies Malfliet, et.al. (Eds.): *Proceedings of the 6th International Slag Valorisation Symposium*. Mechelen, 197–200.
- [42] Chaudhary, P. N. and J. Pal, 2002, An overview of treatment of steel-making slag for recovery of lime and phosphorus values, Jamshedpur.
- [43] Liu, C., M. Guo, L. Pandelaers, B. Blanpain, S. Huang and P. Wollants, Metal Recovery from BOF Steel Slag by Carbo-thermic Reduction, *BHM* 162 (2017), 7, 258–262.
- [44] Morita, K., M. Guo, N. Oka and N. Sano, Resurrection of the iron and phosphorus resource in steel-making slag, *Journal of Material Cycles and Waste Management* 4 (2002), 2, 93–101.
- [45] Matinde, E., Y. Sasaki and M. Hino, Phosphorus Gasification from Sewage Sludge during Carbothermic Reduction, *ISIJ International* 48 (2008), 7, 912–917.
- [46] Nakase, K., A. Matsui, N. Kikuchi, Y. Miki, Y. Kishimoto, I. Goto and T. Nagasaka, Fundamental Research on a Rational Steelmaking Slag Recycling System by Phosphorus Separation and Collection, *Journal for Manufacturing Science & Production* 13 (2013), 1-2, 39–45.
- [47] Nakase, K., A. Matsui, N. Kikuchi and Y. Miki, Effect of Slag Composition on Phosphorus Separation from Steelmaking Slag by Reduction, *ISIJ International* 57 (2017), 7, 1197–1204.
- [48] Nagata, K., Final Report of the Working Group on Foundation and Application of Steelmaking Slag, *ISIJ International* (1997).
- [49] Ponak, C., S. Windisch, V. Mally and H. Raupenstrauch, 2019, Recovery of Manganese, Chromium, Iron and Phosphorus from Basic Oxygen Furnace Slags. In GDMB (Ed.): *European Metallurgical Conference 2019*. Optimum utilization of

- resources and recycling for a sustainable solution, vol. 3. Clausthal-Zellerfeld: GDMB Verlag GmbH, 1311–1319.
- [50] Pierson, H. O., Handbook of carbon, graphite, diamond and fullerenes, Noyes Publications, Park Ridge, New Jersey, 1993.
- [51] Schönberg, A., K. Samiei, H. Kern and H. Raupenstrauch, Der RecoPhos-Prozess - Rückgewinnung von Phosphor aus Klärschlammasche, Österreichische Wasser- und Abfallwirtschaft 66 (2014), 11-12, 403–407.
- [52] Samiei, K. and A. Schönberg, 2014 (unpublished), Basic Design of the InduCarb Reactor power input for a homogeneous temperature distribution, Chair of Thermal Processing Technology (Montanuniversitaet Leoben), Leoben.
- [53] Edlinger, A., 2010, Verfahren zum Aufbereiten von festen oder schmelzflüssigen Stoffen. Patent no. AT 507262 A1.
- [54] Edlinger, A., 2006, Method for reducing metal oxide slags or glasses and/or for degassing mineral melts and device for carrying out said method. Patent no. WO 2006079132 A1.
- [55] Wirtschaftsvereinigung Stahl and Stahlinstitut VDEh, Hot metal production in blast furnaces, https://en.stahl-online.de/wp-content/uploads/2013/10/Bild-31_eng.jpg, last accessed 26. August 2019.
- [56] Wartmann, R., 1982, Mathematisches Modell des Hochofenprozesses. In F. Oeters, R. Steffen (Eds.): Metallurgie Teil I - Eisenerzeugung, vol. 1. Düsseldorf: Verlag Stahleisen GmbH, 274ff.
- [57] Pelton, A. D., 2013, Thermodynamics and Phase Diagrams of Materials. In R. W. Cahn, P. Haasen, E. J. Kramer (Eds.): Materials Science and Technology: John Wiley & Sons, Inc., 1–73.
- [58] Atkins, P. and J. de Paula, Atkins' Physical Chemistry, W. H. Freeman and Company, USA, 2010.
- [59] Schürmann, E., 1982, Thermodynamik der Eisenerzreduktion. In F. Oeters, R. Steffen (Eds.): Metallurgie Teil I - Eisenerzeugung, vol. 1. Düsseldorf: Verlag Stahleisen GmbH, 41–72.
- [60] Babich, A., Ironmaking, RWTH Univ. Dep. of Ferrous Metallurgy, Aachen, 2008.
- [61] Dorn, F. W. and H. Harnisch, Zur Reduktion von Calciumphosphat bei der Phosphor-Herstellung, Chemie-Ingenieur-Technik 42 (1970), 19, 1209–1215.

- [62] Sohn, H.-S., Z.-P. Chen and W.-G. Jung, Reduction kinetics of manganese oxide in basic oxygen furnace type slag, *Steel Research International* 71 (2000), 5, 145–152.
- [63] Wu, T., J. Gao, Y. Zhang and F. Yuan, 2017, Thermodynamic prediction of chromium reduction behaviour from slag. In Annelies Malfliet (Ed.): *Proceedings of the 5th International Slag Valorisation Symposium*. Leuven, 165–168.
- [64] Breil, G., *Elektrothermische Erzeugung von Phosphor*, *Chemie-Ingenieur-Technik* 35 (1963), 8, 549–608.
- [65] Outotec Research Center (Roine, Antti), 2019, *HSC Chemistry 7*, Outotec Research Center (Outotec Oyj), Espoo, Finland.
- [66] Schlesinger, M. E., *The Thermodynamic Properties of Phosphorus and Solid Binary Phosphides*, *Chemical Reviews* 102 (2002), 11, 4267–4301.
- [67] Basu, S., A. K. Lahiri and S. Seetharaman, A Model for Activity Coefficient of P₂O₅ in BOF Slag and Phosphorus Distribution between Liquid Steel and Slag, *ISIJ International* 47 (2007), 8, 1236–1238.
- [68] Kikuchi, N., A. Matsui, K. Takahashi, H. Tobo and Y. Kishimoto, 2011, Method for reclaiming iron and phosphorus from steelmaking slag. Patent no. EP 2383352 A1.
- [69] Perlow, N. I. and M. P. Kwitko, *Die Stahlerzeugung in Sauerstoffkonvertern*, VEB Deutscher Verlag für Grundstoffindustrie, Leipzig, 1967.
- [70] Broll, S. and W. Jeitschko, The chromium phosphide carbide Cr₈P₆C, *Journal of Alloys and Compounds* 229 (1995), 2, 233–237.
- [71] Zaitsev, A. I., N. E. Shelkova, A. D. Litvina, B. M. Mogutnov and Z. V. Dobrokhotova, Thermodynamic Properties and Phase Equilibria in the Cr-P System, *Journal of Phase Equilibria* 19 (1998), 3, 191–199.
- [72] HENSCHKE GmbH, 2017, graphite electrode specification, Fürth. Available online at https://henschkegmbh.de/index.php?option=com_content&view=article&id=55&Itemid=63&lang=en, last accessed 29. August 2019.